THE EFFECTS OF COPPER DEPLETION ON INTRACEREBRAL ANGIOGENESIS AND GROWTH OF EXPERIMENTAL BRAIN TUMORS

by

David Zagzag, B.Sc., M.D.

A thesis submitted to the Faculty of Graduate Studies and Research, McGill University, in partial fulfillment of the requirements for the degree of Doctor of Philosophy

Department of Neurology and Neurosurgery
McGill University
Montreal, Canada

ABSTRACT

A crucial requirement for the stepwise, continued growth of a brain tumor is the acquisition of a blood supply from the host, i.e. angiogenesis. The mechanisms of copper activity linked to neovascular and neoplastic growth are largely unknown. Copper ion was shown to be a cofactor for angiogenesis.

We tested the effect of copper depletion achieved by a low copper diet and a copper chelator D-penicillamine, on the intracerebral growth of two experimental brain tumors. We developed an *in vivo* brain tumor model using the VX2 carcinoma. Implantation of 5×10^5 VX2 carcinoma cells into the parietal lobe of normocupremic rabbits consistently yielded large hemorrhagic, necrotic, vascularized tumors. The cortical surface revealed numerous, hypertrophied, tortuous new vessels with feeding arteries and draining veins similar to the angioarchitecture of malignant human brain tumors. We report here that copper depletion prevents tumor neovascularization and restricts tumor growth of the VX2 carcinoma in the rabbit brain. Low copper diet and penicillamine are both necessary to achieve angiogenic inhibition. We also tested the effect of copper depletion on the 9L gliosarcoma. We observed that invasive growth of the tumor was blocked in rats depleted of copper. Electron microscopy revealed the absence of cytoplasmic extensions, including pseudopodia, by contrast, in normocupremic controls, cytoplasmic extensions, typical of mobile cells, invaded the surrounding neuropil. Our findings link the activity of copper in vascular and neoplastic growth.

We found an increase in the peritumoral brain water content in the copper depleted animals and that copper depletion by itself in non tumor implanted animal has no effect on brain water content.

Because of the ability to pharmacologically suppress capillary growth induced by the VX2 carcinoma, we could test the relative contribution of breakdown of the blood-brain barrier compared with that of angiogenesis in the appearance of contrast enhancement in computed tomographic examinations. We conclude from our data that tumor neovascularization, in our brain tumor model, is the key determinant for the appearance of contrast enhancement.

The same protocol used in the brain failed to prevent tumor neovascularization and growth of the VX2 carcinoma in the muscle of the rabbit thigh indicating the crucial role played by the milieu (muscle versus brain) for the growth of malignant tumor. In the same manner, lung metastases were not prevented.

RESUME

La croissance progressive et continue des tumeurs malignes du cerveau necessite l'acquisition d'un apport vasculaire ou: angiogenèse. Les mechanismes d'action du cuivre liés à la croissance vasculaire et néoplasique sont inconnus. L'implication du cuivre dans l'angiogenèse a clairement été demontreé.

Nous avons testé l'effet d'une dépletion cuprique, obtenue par une diète pauvre en cuivre et une chelation par la D-Penicillamine, sur la croissance intracerebrale de deux tumeurs experimentales. Nous avons developpé un modèle tumoral cérébral en utilisant les cellules de la lignée carcinomateuse VX2. L'implantation de 5×10^5 cellules dans le lobe parietal de lapins normocupremiques entraine des tumeurs volumineuses, hemorrhagiques, necrotiques et vascularisées. La surface corticale a montré de nombreux néovaisseaux, hypertrophiés, tortueux avec des artères nourricières et veines de drainage semblables à ceux composant l'architecture vasculaire des tumeurs malignes cerebrales humaines. La dépletion cuprique empêche la néovascularisation tumorale et arrête la croissance tumorale du carcinome VX2 dans le cerveau du lapin. Une diète pauvre en cuivre d'une part et la penicillamine d'autre part sont toutes deux necessaires pour obtenir une inhibition de l'angiogenèse. La dépletion cuprique bloque la croissance invasive du Gliosarcome 9L chez le rat. Chez le rat hypocupremique la microscopie electronique révéle l'absence de prolongements cytoplasmiques observés chez le rat normocupremique, prolongements cytoplasmiques typiques de cellules en mouvement envahissant le neuropil avoisinant. L'ion cuivre est donc lié aux croissance vasculaire et néoplasique.

La dépletion cuprique entraine une augmentation du contenu en eau péritumoral. La dépletion cuprique chez des animaux sans tumeur cérébrale n'a aucun effet sur le contenu cérébral en eau.

Grace à la possibilité pharmacologique de supprimer la croissance capillaire produite par le carcinome VX2, nous avons pu etudier le rôle respectif de la rupture de la barrière hemato-encephalique d'une part et de l'angiogenèse tumorale d'autre part dans l'apparition du renforcement de contraste au cours des examens tomodensitometriques. Nous concluons à partir de nos données que l'angiogenèse tumorale est, dans notre modèle tumoral cerebral, l'élément clé, determinant l'apparition du renforcement de contraste.

Le même protocole experimental utilisé au niveau cérébral n'a pas réussi à prevenir l'angiogenèse et la croissance tumorales du carcinome VX2 au niveau du muscle de la cuisse du lapin indiquant le role crucial joué par le milieu dans lequel une tumeur maligne se develope. De façon similaire les metastases pulmonaires n'ont pas été empechées par ce même protocole.

To Tania, Jonathan and Anna

To my parents, family and friends

PREFACE

This thesis is written in the form of publications, except for the references which are cited in the final section (Bibliography) of this manuscript. Chapters 2-7 are joined by linking pages (écrites en français) to give continuity. This option is provided by Section 7 of the Guidelines Concerning Thesis Preperation.

Au chapitre I, une introduction générale décrit l'aspect historique du domaine et les travaux anterieurs reliés à la presente recherche. Les points importants et les principales conclusions sont degagés et regroupés ensemble dans une conclusion au Chapitre VIII.

Publications:

*Zagzag D, Brem S, Robert F: Neovascularization and tumor growth in the rabbit brain: A model for experimental studies of angiogenesis and blood brain barrier. Am J Pathol. 1988, 131:361-372

*Zagzag D, Brem S: Control of neoplastic development in the brain: Copper depletion prevents neovascularization and tumor growth. Surg Forum 1986, 37:506-509.

*Zagzag D, Goldenberg M, Brem S: Angiogenesis and breakdown of the blood-brain barrier modulate the computerized tomography contrast enhancement of a rabbit brain tumor. A.J.N.R. In press

The EM observations described in Chapter IV have been made by Dr. A.M.C. Tsanaclis.

REMERCIEMENTS

J'aimerais d'abord sincerement remercier mon directeur de thèse, le Dr. Steven S Brem. Steven a travaillé avec acharnement depuis déjà plusieurs années sur les mechanismes impliqués dans l'angiogenèse tumorale. Sa recherche a fourni une importante contribution dans ce domaine. Je le remercie pour m'avoir laissé beaucoup de liberte dans la poursuite de mon travail, me permettant ainsi d'apprendre comment orienter et organiser un projet de recherche. Je le remercie aussi pour son enthousiasme, son support et ses critiques constructives tout du long de mon sejour dans son laboratoire.

Dr. Françoise Robert gave unstintingly of her time in reviewing the pathological material and instructing the author in understanding and appreciating pathology and neuropathology. To her, because of her constant encouragement and supervision during the course of this work.

My appreciation and gratitude is hereby extended to Dr. Ana Maria Tsanaclis for her collaboration.

Acknowledgements to Dr. David Langleben and Dr. Marvin Goldenberg, their many helpful suggestions were deeply appreciated.

This experimental work was performed in the neurosurgical laboratory at the Lady Davis Institute for Medical Research. The author wishes to express his particular gratitude to its director Dr. Norman Kalant for his cooperation and to Mrs. Therese Davila and all her team for their help and kindness.

We thank Dr. Y Tanaka and Mr. J Gabor for determinations of serum copper levels; Lynn Miller, Marguerite Wotoczek, Edouard Depestre, Betty Stein, Marie Pierre Koubi, Phyllis Bresler, Sylvano Ordonselli

for excellent technical assistance: Jennifer Morrison and Christine Lalonde for the art work and diagrams; David Saxe, Wendy Zubis. Suzanne Wiiçman for photography. To all I extend thanks and my everlasting gratitude for the success of this work. Personal thanks to Ann-Marie Crosby for typing this thesis.

We thank Dr. VT Marchesi, Editor-in-Chief of the American Journal of Pathology for giving us the permission to use the accepted manuscript as the Chapter II of this thesis. I express indebtedness to the Cancer Research Society for their personal fellowship grant for the last two years.

Surtout et enfin j'adresse à ma femme Tania le plus grand des remerciements pour son amour, soutien, et abnegation dont elle a fait preuve au cours de notre sejour à Montreal.

TABLE OF CONTENTS

LIST OF FIGURES

Chapter IV

LIST OF TABLES

Chapter VII

CHAPTER I

Angiogenesis, Tumor Growth and Copper Ion

Angiogenesis, the development of a new microvasculature is an event common to a variety of physiological and pathological conditions. It is a key step in the formation of embryonic (1) hyperplastic (2) and neoplastic tissues (3). Neovascularization furthermore is a hallmark of several human diseases, e.g. diabetic retinopathy (4) and atherosclerosis (5) collectively described as "angiogenic diseases" (6). The interrelationof capillary endothelial proliferation and tumor growth has been demonstrated in numerous experiments and clinical observations. It has long been observed that tumor growth is accompanied by the growth of new blood vessels from the host (7,8). In the last two decades it has been demonstrated that angiogenesis and tumor growth are interdependent (9-13). Tumors depend upon obtaining a blood supply for their continued growth; two phases exist in tumor growth: 1) **Avascular Phase** lacking blood supply, tumors exist as small population of cells, generally less than 3mm in diameter; growth is limited by diffusion gradients of local nutrients. These slow growing tumors have the potential to grow rapidly if they acquire a blood supply (13-16). 2) **Vascular Phase** where rapid exponential growth follows the acquisition of a blood supply leading to a prominent vascularized tumor (17-20). Tumors can be separated physically or sequentially from avascular to vascular phase (11). Tumors remain dormant surviving as tiny avascular nodules when artificially deprived of a blood supply (11). In experimental models, e.g. by placing it in the vitreous tumor of the eye, once the tumor nodule comes into contact with the retinal blood vessels, angiogenesis occurs, associated with explosive growth into a large vascularized tumor (15). Studies of the sequential growth of

experimental gliomas, showed these tumors also pass through two distinct periods (17,21,22). Without new blood vessels, gliomas do not exceed a critical diameter of approximately 2mm (21).

Currently malignant brain tumors have a poor prognosis

The current treatment of malignant brain tumors is disappointing (23). The one-and-five year survival rates, respectively, are only 45% and 8% (26); malignant tumors respond poorly to aggressive surgical extirpation, radiotherapy and chemotherapy (25). In malignant gliomas chemotherapy has an 30 to 40% response rate (26) and one can expect an additional time of about 3 months of survival on the average (26). New therapeutic approaches are obviously needed.

Angiogenic inhibition as a therapeutic strategy

Anti-angiogenesis as a new concept for therapy of solid tumors was first introduced in 1971 (10,13,27). The possibility of achieving this goal was made plausible by the demonstration of angiogenic inhibitors in avascular tissues such as the vitreous (28) and cartilage (29). Protamine (30) and heparin-cortisone combination (31) were also found to be angiogenic inhibitors and even able to cause regression of experimental solid tumors. It was then suggested that antiangiogenesis could represent a powerful new therapeutic tool for brain tumors (15).

Brain tumors: A target for angiogenic inhibition

What is the evidence suggesting that angiogenic inhibition would be a good therapeutic approach for brain tumors?

1) Brain tumors, of all solid tumors, show the highest degree of capillary proliferation (32) and the vascular endothelial component represent as much as 40-50% of the volume of certain gliomas and meningiomas (32). 2) Kinetic studies show the capillary endothelium in brain tumors have a high labelling index approximately 20% (17) contrasted to 0.04% for normal brains and twice as high in any other tumor (33) 3) Neural tumors are potential sources of growth factors (34,35) 4) For human astrocytomas the degree of capillary proliferation correlates with the biological aggressiveness of the tumor as well as clinical recurrence (15,36). 5) The abnormal microvasculature may be responsible for intratumoral hemorrhages(37) and the occasional transformation to an endothelial sarcoma(38). 6) Infiltration of malignant tumors occurs preferentially along vascular channels (30,40).

Copper is a key cofactor for angiogenesis

Copper ion plays a central role in the growth of new capillaries. What is the evidence for copper's role in angiogenesis and what was the rationale for our experiments? Copper ion was shown to augment endothelial locomotion in vitro (41) Zn,Ca,Mn,Cr,Fe,Al,Sb,Mo were not active (41). Cellular shape is a crucial parameter for locomotion and migration (42). The tripeptide glycylhistidyllysine (GHL) when bound to copper is able to cause a change in the cell shape from round to flat and induces adhesion (43). Cellular flattening and adhesion are two key factors for cellular migration to occur (44). An increase in local copper preceeds the penetration of capillaries in the cornea after angiogenic stimulation (45). No change was observed in the levels of

Ca,Fe,Mg,Zn,P and K in the cornea during angiogenesis (45). Copper sulfate induce neovascularization in the standard corneal assay (46,47). Ceruloplasmin, heparin, the tripeptide GHL are angiogenic only when bound to copper (48). Hypocupremic rabbits are unable to mount an angiogenic response in the cornea after stimulation by PGE1 (45). In our laboratory it was shown that in 50% of hypocupremic rabbits there was no angiogenesis induced by a variety of human brain tumors as opposed to 26% in the control (49). All these facts clearly indicate the crucial role played by copper ion in angiogenesis and that was the rationale for our experiments. Our working hypothesis was that angiogenic inhibition achieved by copper depletion could result in abortion of tumor growth and after the previous work done in our laboratory in the cornea, the major issue was to test the effect of copper depletion on tumor growth in the brain. Our challenge was to achieve angiogenic inhibition in the brain and therefore abortion of tumor growth.

Copper and malignancies

It has been known for years that the level of serum copper reflects the clinical activity of many tumors. Growing tumors have substantially increased serum ceruloplasmin levels. Serum copper levels (SCL) are significantly increased in patients with malignant lymphomas and Hodgkin's disease (50-57) with a positive correlation between SCL and the activity of the lymphoma (50,51,53-56). The same findings exist in patients with sarcomas (58). The SCL are found to be extremely high in patients with bronchial carcinoma (58), malignancies

of the large bowel, stomach, urinary bladder and female reproductive system (60). Ceruloplasmin is significantly increased above the normal before treatment in patients with lung cancer (61). The degree of elevation correlated with the TNM international classification (ie, T: extent of primary tumor, N: condition of lymph nodes, M: absence or presence of metastases).

SCL were used as an index to therapy response (62,63) Furthermore it was suggested that the antineoplastic effect of chemotherapeutic aspects could be related to the chelation of copper ion in some coenzyme involved in tumor growth (64).

Copper and malignancies in the CNS

There have been very few studies of copper ion concentration in brain tumors. A 2-4 times greater concentration of copper ion was found in the tumor tissues of 29 necropsy specimens of malignant brain tumors (9 astrocytomas, 10 glioblastomas multiforme and 10 medulloblastomas) as compared to control brain tissue at distance from the tumor (65). SCL and ceruloplasmin levels are increased in patients with primary brain tumors as compared to patients with other neurological diseases or healthy subjects (66). Peritumoral tissue of glioblastoma contains more copper than the tumor itself conversly low grade astrocytomas have more copper in the tumor than around (67) predicting a role for copper ion in invasiveness. Copper content of the cerebrospinal fluid is also elevated in patients with cerebral neoplasms (68). A positive correlation between copper levels and the degree of malignancy of the tumor exists (68).

In summary, in a wide range of malignant tumors inside and outside the CNS the level of serum ceruloplasmin and copper correlates with tumor progression. The elevation occurs early and rises in proportion to tumor volume, returns to normal after removal, and rises again with extension and regrowth (69,70). Primary brain tumors sequester copper and induce an elevation of the levels of serum copper (66).

CHAPTER II

Neovascularization and Tumor Growth in the Rabbit Brain: A Model for Experimental Studies of Angiogenesis and Blood-Brain Barrier

Abstract

A model for the study of tumor angiogenesis within the rabbit brain is presented. Implantation of the VX2 carcinoma provides a reproducible tumor accompanied by angiogenesis. We report the sequential growth, histology, tumor neovascularization and vascular permeability of the tumor following its intracerebral implantation. Tumor angiogenesis correlates with the rapid and logarithmic intracerebral tumor growth. The proliferation of blood vessels in the tumor and the organization of tumor cells around tumor vessels are described. Breakdown of the blood-brain barrier (detected by Evans blue leakage) starts in the early stages of tumor development and becomes prominent as the tumor vasculature and size increase. This model is useful for experimental studies of angiogenesis.

During the past fifteen years the field of angiogenesis research has relied mainly on three models for the in vivo study of capillary proliferation the rabbit (1) and rodent (2,3) cornea micropocket, the chorioallantoic membrane of the chick embryo (4) and the hamster cheek pouch. The VX2 carcinoma is an anaplastic squamous cell tumor that results from a malignant change of a Shope-virus induced skin papilloma of the domestic rabbit (6). To induce intracerebral oncogenesis and neovascularization, we selected the rabbit VX2 carcinoma because previous experiments demonstrated 1) its angiogenic capacities when implanted in the cornea (1) and 2) its high rate of successful implantation, short induction time, reproducibility and stable histology when transplanted to the brain (7-10). Using this tumor, we have developed a model for the study of tumor angiogenesis within the brain and its relationship with tumor growth and breakdown of the blood-brain barrier (BBB).

Materials and Methods

VX2 Tumor Preparation

The VX2 carcinoma was maintained by intramuscular injection of 5 x 10^5 viable cells in the lateral thigh of the New Zealand White (NZW) rabbit with serial passage every three weeks when tumor masses measured 2cm in diameter (Figures 1A,1B). For intracerebral implantation, the tumor was removed from the thigh, freed of necrotic tissue, and placed in Hanks' balanced salt solution (HBSS) (Flow Laboratories Inc., McLean, VA). We cut $2mm^3$ fragments that were passed through a Cellector tissue sieve mounted with a series of meshes from 520μ to 190 μ opening size (Bellco Glass Inc., Vineland, NJ). The suspension, centrifuged at

Figure 1 Tumor transfer. A - The removal of the tumor from the thigh of the rabbit. B - The processing of the tumor with the use of a cellector tissue sieve.


A

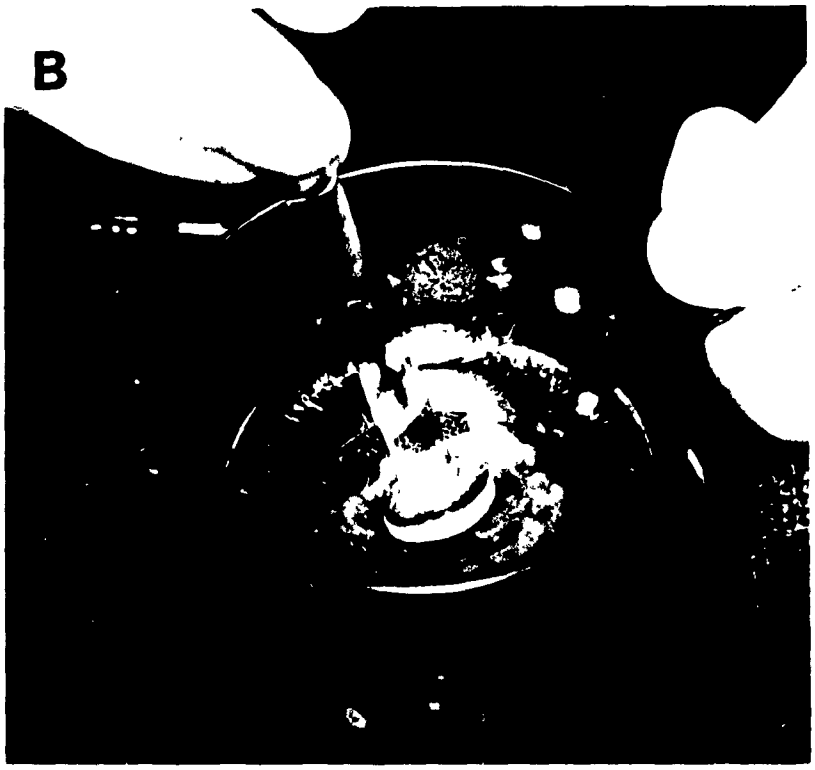
B

1500 rpm for 3 minutes, formed pellets that were resuspended in HBSS to give a final concentration of 1 x 10^7 cells/ml. Viable cells were counted by trypan blue exclusion (70-80%)

Tumor Implantation

Sixty adult male NZW rabbits weighing 2.5-3 kg, were anesthetized by intramuscular injection of 6 mg/kg acepromazine maleate (Atravet, Ayerst Laboratory, Montreal, Quebec), and 25 mg/kg ketamine hydrochloride (Rogarsetic, Rogar/STB Inc., Montreal, Quebec) supplemented by subcutaneous anesthesia of 1% lidocaine for the scalp. We made a 3 cm incision along the midline, reflected the periosteum, and placed a 1mm burr hole with a surgical drill (Teledyne Emesco, George Tieman and Co., Plainview, NY) 5 mm to the right of the sagittal suture and 5 mm posterior to the coronal suture, (Figures 2A and 3A) care being taken not to perforate the dura. The inner table of the skull was kept intact, (Figure 3B) except for a central hole allowing the insertion of a 26-gauge needle attached to a microsyringe (Figures 2B and 3C). Fifty microliters of HBSS containing 5 X 10^5 viable cells were slowly injected into the right parietal lobe (Figure 2C) at a depth of 2mm corresponding to the location of the centrum semiovale (11).

After removal of the needle, the burr hole was sealed with bone wax (Ethicon, Peterborough, Ontario) to prevent reflux. The scalp was then closed with surgical staples and the rabbit was returned to its cage. All procedures were performed aseptically. After recovery from anesthesia, each animal was examined to be certain that there was no neurological injury after the injection. Each animal was examined daily for weight, level of consciousness, and motor activity.

Figure 2 The cells are injected 5mm lateral to the midline and 5mm posterior to the coronal suture (A) at an intracerebral depth of 2mm (B and C)

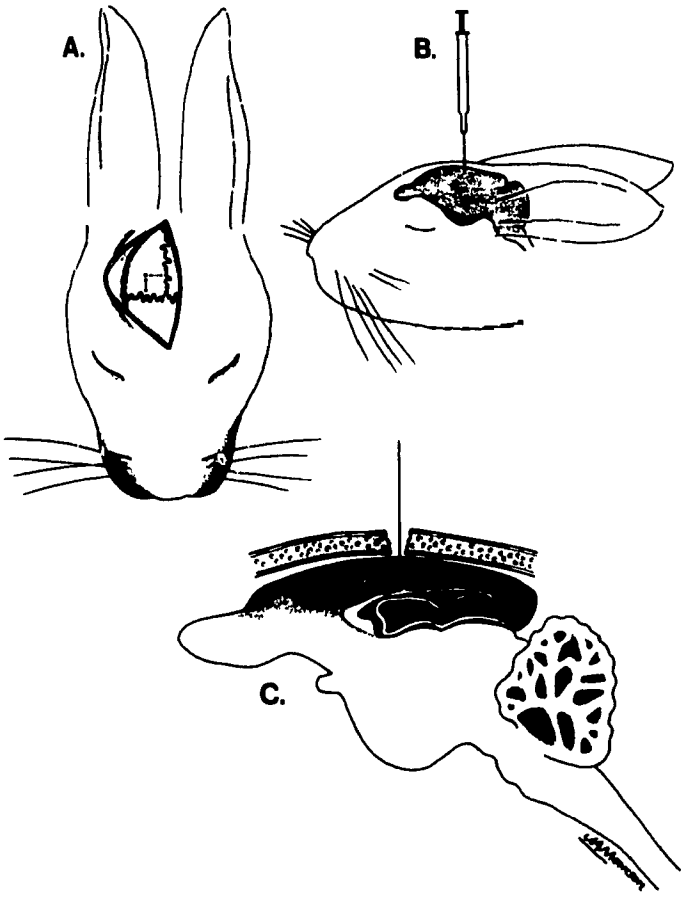
A.
B.
C.

Figure 3 The surgical field (A) coronal suture (arrow), sagittal suture (arrowhead). The tabla interna is kept intact except for a central hole (B) allowing the insertion of 26-gauge needle(C)

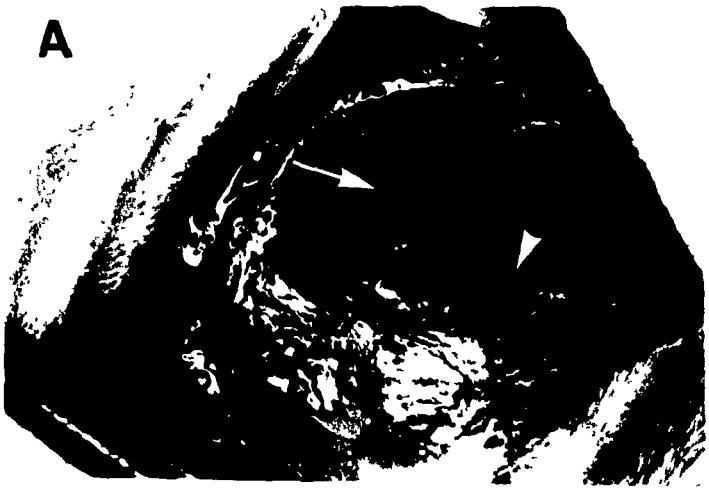
A


B


C

Experimental Protocol

The 60 rabbits implanted with viable tumor cells were divided into two groups: Group A: we determined the natural history of the VX2 carcinoma implanted in the brain of 20 rabbits. These animals were sacrificed when neurological deterioration occured (loss of appetite, gait disturbances,weakness of the extremities, left hemiparesis or hemiplegia, decreased level of consciousness). Time from implantation to sacrifice, tumor volume and tumor histology were determined.Group B: we studied the growth of the tumor and the sequential development of tumor angiogenesis and breakdown of the BBB in 40 rabbits. After implantation of tumor cells, eight animals were sacrificed on days 6, 10, 14, 18 and 22. On each of these days, three rabbits were given 2% Evans blue, (JT Baker Chemical Co., Phillisburg, NJ) dissolved in 0.9% NaCl at a dosage of 2cc/kg intravenously, one hour prior to sacrifice to detect breakdown of the BBB (12). Another three rabbits received 3cc of ink (Labink, K.S.C. Inc., Medford, MA) into the right common carotid artery, one minute before sacrifice in order to delineate abnormal vessels. The remaining two animals were sacrificed without injection of dye.

Control group: 15 additional rabbits were implanted with heat-killed cells as a control for trauma and breakdown of the BBB due to the injection. These rabbits received Evans blue and were sacrificed according to the same schedule as Group B.

The rabbits were sacrificed with 120mg/kg of intravenous sodium pentobarbital (Euthanyl, MTC Pharmaceuticals, Mississauga, Ontario). After removal of the skull and the dura the cortical surface was

examined for the presence of the tumor, the degree of neovascularization, and the amount of brain swelling or shift of the midline. Cortical neovascularization was scored as follows: 0= no new blood vessels; 1+= minimal vascular ramifications; 2+= many new tortuous blood vessels; 3+= many new tortuous blood vessels with hemorrhages. A semiquantitative scale regarding the leakage of Evans blue in group B was established: 0=none; + = slight (barely visible blue coloration); ++= moderate (easily detectable coloration); +++=severe (intense blue staining). The brains were then removed and fixed in 10% phosphate buffered formalin for 6 days. The specimens were then serially sectioned at 1.5mm intervals in the coronal plane. The maximal diameters of the tumor were measured in three planes: coronal (d1), sagittal (d2), and transverse (d3) and the tumor volume was calculated with the formula $\underline{d1xd2xd3x\pi/6}$ (13). In the early stages of the tumor development (days 6 and 10) a calibrated stereoscopic microscope was used to measure tumor diameters. The presence of necrosis and hemorrhage was noted, midline shift to the left measured, brain stem compression recorded and Evans blue leakage assessed in group B. The brain slices were embedded in paraffin , sectioned and stained with hematoxylin and eosin.

Histologically angiogenesis was scored using the vasoproliferative component of the MAGS (microscopic angiogenesis grading system) scale (14) used to quantify angiogenesis in a variety of tumors. The microvessels were counted at a magnification of 200X. At this magnification the field examined encompassed an area of 2.54mm^2. The histologic slides were first scanned at low magnification and the area of maximum

vascular density was selected for grading. This area was usually at the tumor periphery. We defined the vascular density (VD) as the highest number of vascular lumens per field (X200) encountered in the tumors. Each lumen lined with endothelial cells was considered an individual blood vessel. Although a tortuous vessel might reappear in the same field, each discontinuous vascular lumen was counted as a separate vessel. Ten different fields in the most vascular area of the tumor were counted and only the one having the highest vascular density was used for analysis. Care was taken not to count interstitial hemorrhages or to confuse leukocytes or tumor cells with endothelial cells.

Statistical analysis was performed using standard linear regression and correlation (15). A p value <0.05 was the chosen level for significance.

Results

Group A:

Tumor Growth

One animal was excluded from the study because it died from unknown cause within 48 hours after tumor implantation. Tumors developed in 18 of the 19 remaining rabbits. Of these 18 rabbits seven animals died between days 16 and 22 and eleven were sacrificed when neurological deterioration appeared between days 16 and 24. The survival time was 19.9 $\pm$ 2.3 days (mean $\pm$ standard deviation) for all 18 animals.

Gross Pathology

After removal of the skull and the dura the tumor was evident as a pale mass in ten animals. In two of these ten cases the dura was

invaded by the tumor (Figure 4A). In all 18 animals the cortical surface (Figure 4A and 4B) revealed multiple hypertrophied, tortuous new vessels (2+ in 13 animals and 3+ in 5). Brain swelling and midline shift was evident in 17 animals.

Coronal sections revealed that all 18 tumors were localized to the right cerebral hemisphere, above the ventricle. Eight tumors reached the cortical surface. Central necrosis was evident in seven animals. Intratumoral hemorrhages were seen in five animals. There was no tumor spread to the contralateral side even though severe midline shift (2 to 5mm) and compression of the ventricular system and brain stem were observed in 17 tumors (Figure 5). The tumor volume was 582.6 ± 126mm^3 (mean ± standard deviation). Complete autopsies of all the 18 animals failed to reveal extracerebral growth of the tumor.

Tumor Histology

The tumors were undifferentiated with large polygonal cells, amphophitic cytoplasm, and vesicular and pleomorphic nuclei with prominent nucleoli. Tumor cells were organized around blood vessels both within the tumor (Figure 6A) and at the margins of the tumor (Figure 6B). Mitotic figures were frequent. On the basis of the vasculature three different zones were recognized within the tumor: an outer zone of high vascular density (VD=17.6 ± 3.4), an intermediate zone (VD=9 ± 2.4) and an inner zone of hemorragic necrosis (Figure 7). Hyperplastic endothelial cells with primitive cytological features were not seen. The interface between tumor and surrounding brain was obvious. Few perivascular mononuclear infiltrates were present, mainly adjacent to

Figure 4 Cortical neovascularization. A - the invaded dura (D) is reflected revealing the underlying tumor which reaches the cortex. Feeding arteries directed toward the tumor, large draining veins and cortical hemorrhages (arrowhead) can be seen. B - the tumor is not apparent, however, neovascularization is evident. Note the intracerebral hemorrhage (arrowhead)


A
D


B

Figure 5 The tumor induces a severe midline shift. The tumor margins are evident (arrowheads)

Figure 6 Perivascular organization of tumor cells. A- within the tumor (H & E, X400). B. - Invasive spread of tumor cells along microvessels (arrows) at the margin of the tumor (H & E, X150).

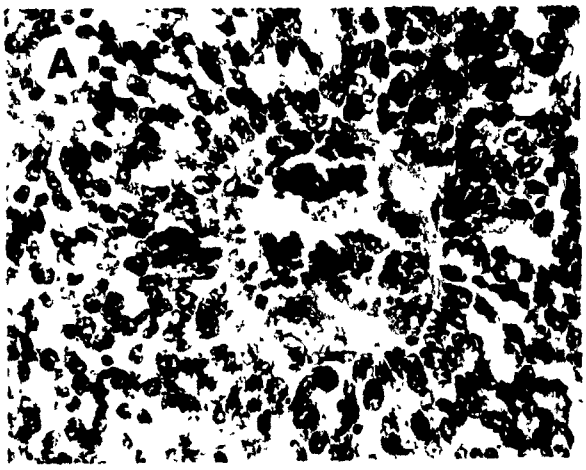
A

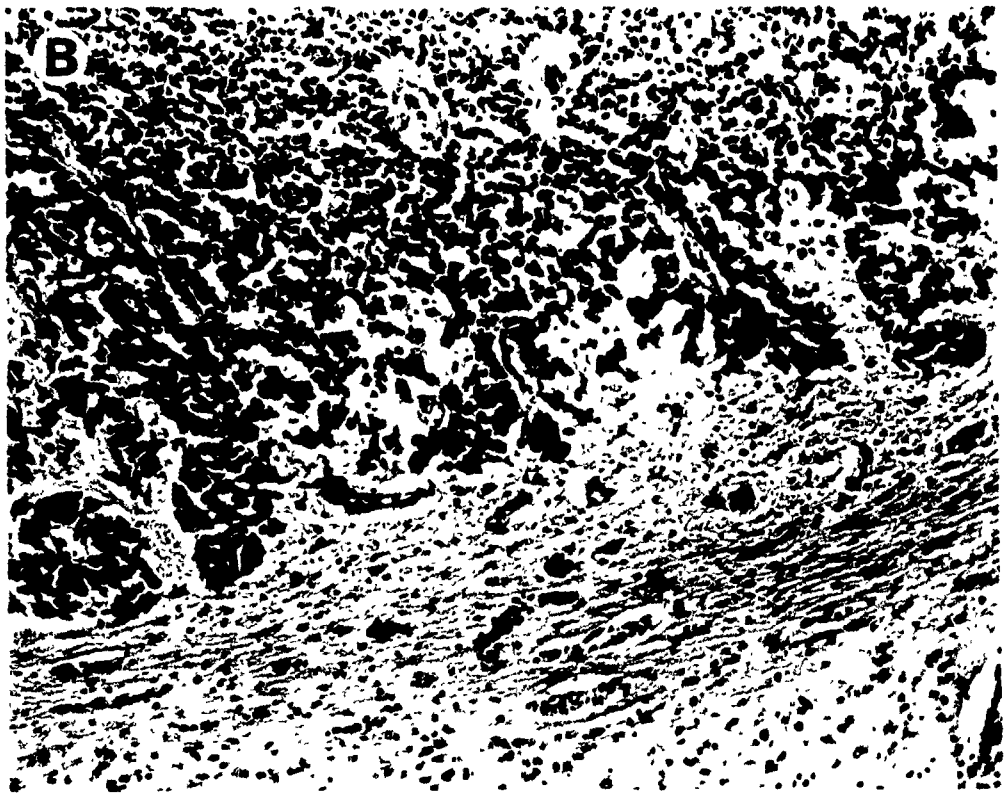
B

Figure 7 Interface between the central necrosis (N) and the intermediate zone (H & E, X300)

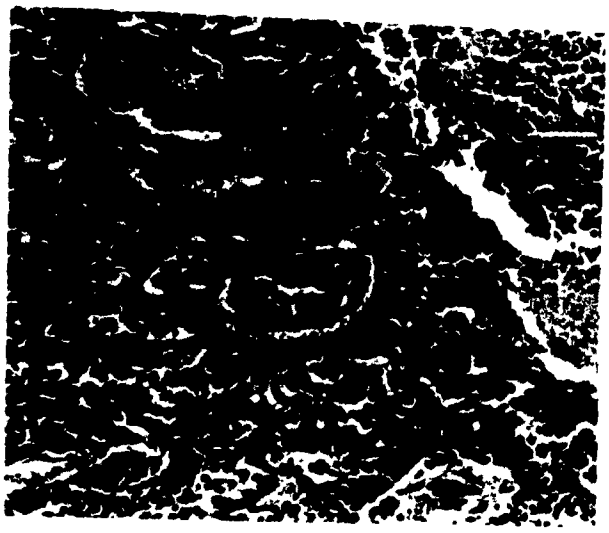

the tumor. The white matter surrounding the tumor was vacuolated and spongy in appearance representing peritumoral edema (16,17).

Group B:

Tumor Growth

All 40 animals developed tumors. Three animals died before sacrifice (two on day 17 and one on day 19) so only seven animals were studied on day 18 and six on day 22.

Gross Pathology

On external examination of the brains, moderate cortical neovascularization was first observed on day 14, (0 in two animals and 1+ in 6). It was more marked on day 18 (1+ in 3 animals and 2+ in 4) and it became severe by day 22 (2+ in 2 animals and 3+ in 4). With intra-arterial injection of ink prior to sacrifice, the abnormal cortical vascular network could be further delineated (Figure 8A and B). Midline shift to the left was first noted on day 18 in six out of seven animals. On day 22 the tumor was first apparent at the cortical surface in three out of six animals; in one of these the dura was invaded by the tumor. Brain swelling as well as midline shift was obvious in the six animals studied.

In coronal sections, on day 6 (Figure 9A) the tumors appeared as tiny, pale, barely visible plaques of 0.3 to 1.5mm in diameter. On day 10 (Figure 9B) they remained pale and their diameter varied between 0.5 and 2.5mm. On day 14 (Figure 9C) the tumors showed a brown coloration, their diameter ranged between 2 and 4mm. On day 18 (Figure 9D) the diameters varied between 3.5 and 7.5mm, with evident midline shift (1 to 3mm). Finally, by day 22 (Figure 10A and B) tumor diameters ranged

Figure 8 Intracarotid injection of ink further delineates the abnormal cortical vascular network. A - The tumor is located beneath the cortical surface but induces neovascularization. B - The tumor appears on the cortical surface and displays proliferating and stained microvessels

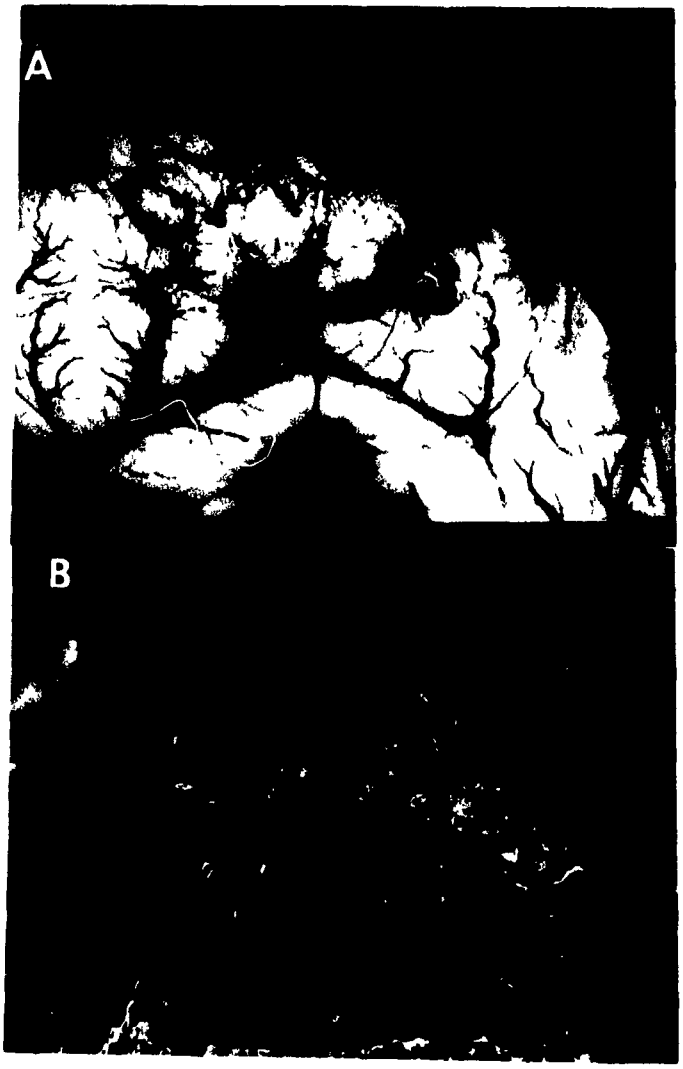
A
B

Figure 9 Coronal sections reveal the sequential growth of the VX2 carcinoma. A - day 6: the tumor (arrowhead) is located in the centrum semiovale. B - day 10. C - day 14. D - day 18. (H & E, X3)

A

B

C

D

Figure 10 Coronal sections on day 22. A - The tumor is located beneath the cortical surface. B - The tumor reaches the cortical surface (H) & E, X3)

A

B

between 7 and 13mm. In four animals the tumor reached the cortical surface (Figure 10B). Central intratumoral necrosis was evident in two out of six animals. An intratumoral hemorrhage was observed in one animal. Severe contralateral midline shift (3 to 6mm), compression of the right ventricular system and distortion of the brain stem were noted in all six animals. Tumor volume (Table 1) increased in a logarithmic fashion (Figure 11).

Evans Blue extravasation (Table 1) appeared within the tumor on day 6 and around the tumor on day 14. On day 18, Evans blue extravasation was marked in the tumor and slight around the tumor. On day 22 we observed severe Evans blue extravasation on the cortical surface of the tumor (Figure 12A). The necrotic center was unstained (Figure 12B). Evans blue extravasation was present to a lesser extent around the tumor. No dye extravasation was observed elsewhere in the brain. In control animals focal staining was detected only near the injection site on day 6, increased on day 10 and disappeared by day 14.

Tumor Histology

Tumor neovascularization (Table 1 and Figure 13) was first observed on day 6 (VD=5.4 $\pm$ 1). By day 10 (VD=9.5 $\pm$ 1.2) the vessels diameters appeared to be increased by comparison with those of day 6. The vascular density increased progressively until day 14 (VD=16.1 $\pm$ 1.1) (Figure 14). The vascular density on day 18 (13.1 $\pm$ 1.3) was less, due to the displacement of the capillaries by the proliferating pool of tumor cells. When there was tumor infiltration of the cortex, on day 22, a secondary burst of neovascularization was observed (Figure 15). As in group A, at the same stage of tumor growth, 3 different zones

Table 1 - Tumor Volume, Vascular density and Breakdown of the Blood-Brain Barrier in Group B

Day of Sacrifice	No. of Rabbits	Tumor Volume (mm^3)	Tumor Vascular Density*	Breakdown of the BBB† Tumor	B.A.T.‡
6	8	0.2 ± 0.1	5.4 ± 1.0	-	0
10	8	0.6 ± 0.3	9.5 ± 1.2	+	0
14	8	12.6 ± 3.5	16.1 ± 1.1	—	-
18	7§	69.4 ± 14.8	13.1 ± 1.3	—	—
22	6‖	523.5 ± 116.7	19.5 ± 1.0¶ 11.8 ± 1.5**	——	—

All data expressed represent mean ± standard deviation

* Vascular Density defined as the maximum number of vascular lumens per field (X200) encountered in a tumor

† Breakdown of the blood-brain barrier (BBB) detected by extravasation of Evans blue: 0 = none; + = slight; ++ = moderate; +++ = severe. Three animals were studied on each day of sacrifice.

‡ B.A.T. = Brain adjacent to tumor

§ One rabbit died from tumor growth prior to scheduled day of sacrifice

‖ Two rabbits died from tumor growth prior to scheduled day of sacrifice

¶ Outer zone

** Intermediate zone

Figure 11 Tumor growth is logarithmic. The log transformed plots of tumor volume approximate a straight line with a correlation coefficient: $r = 0.99$ ($p<0.01$; $y = 0.22 x - 2.16$)

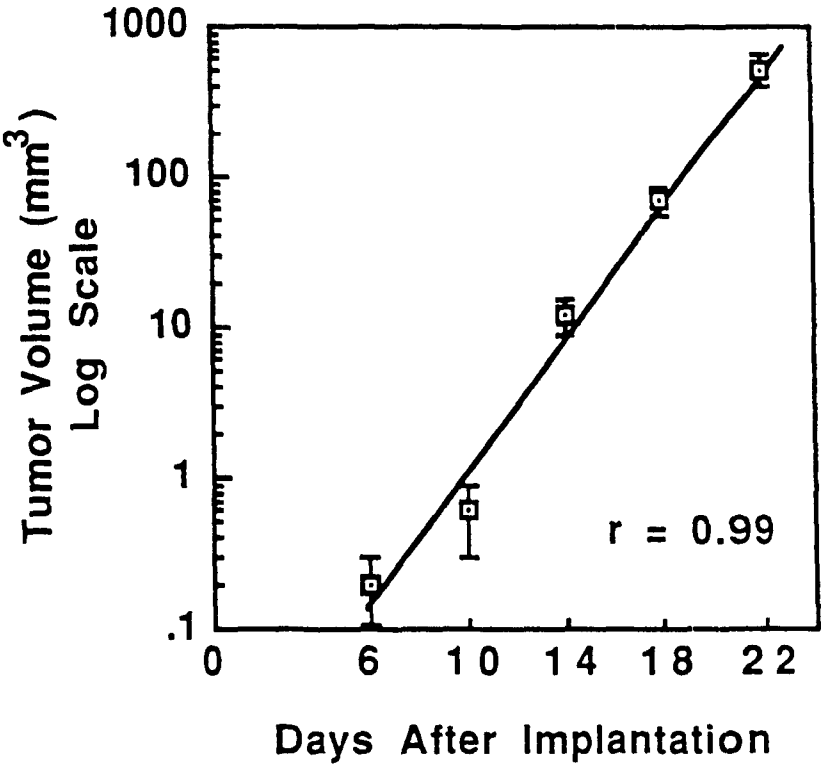
1000
100
10
1
.1
Tumor Volume (mm^3)
Log Scale
r = 0.99
0
6
10
14
18
22
Days After Implantation

Figure 12 Extravasation of Evans blue as seen on Day 22. A - Cortical surface. B - Coronal section: Evans blue extravasation is mainly located at the tumor periphery. Tumor margins are evident (white arrowheads) as well as the limits of the blue staining (black arrowheads)

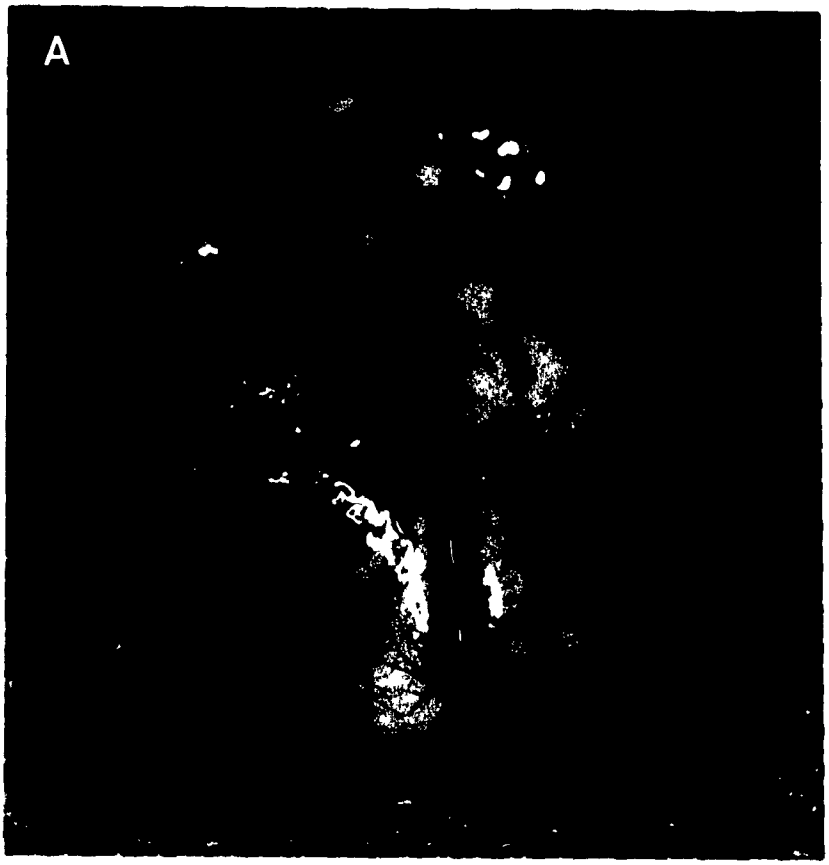
A

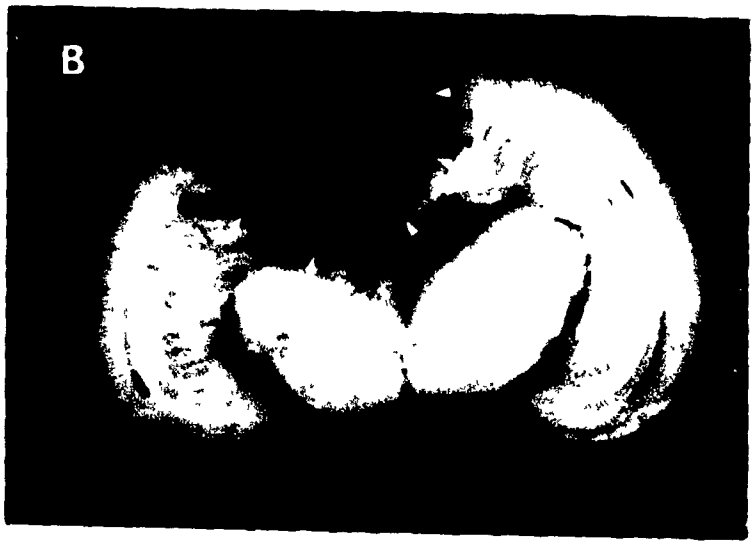
B

Figure 13 Sequential progression of tumor angiogenesis. On day 22, two zones appear: A peripheral zone (— — —) with the highest degree of angiogenesis and an intermediate zone (.....) with moderate neovascularization

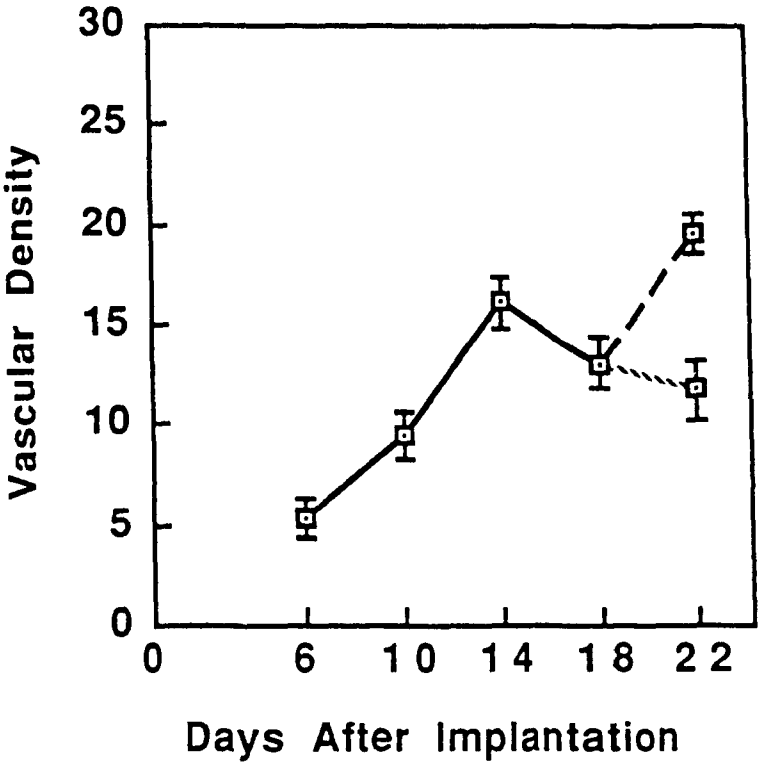
30
25
20
15
10
5
0
Vascular Density
0
6
10
14
18
22
Days After Implantation

Figure 14 Highly vascularized tumor on day 14 (H & E, X60)

Figure 15 Vascular proliferation is observed after tumor infiltration of the cortex on day 22 (H & E, X150)

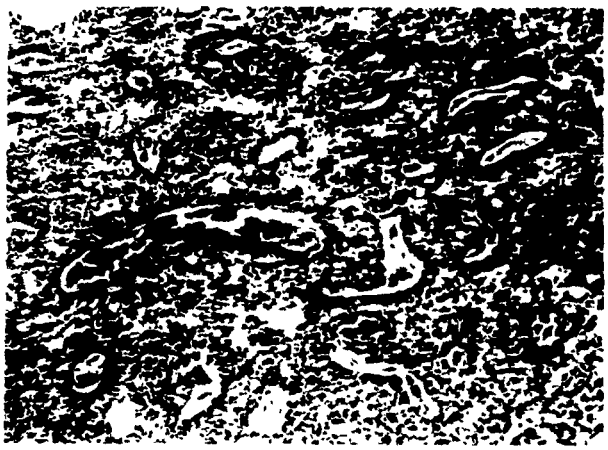

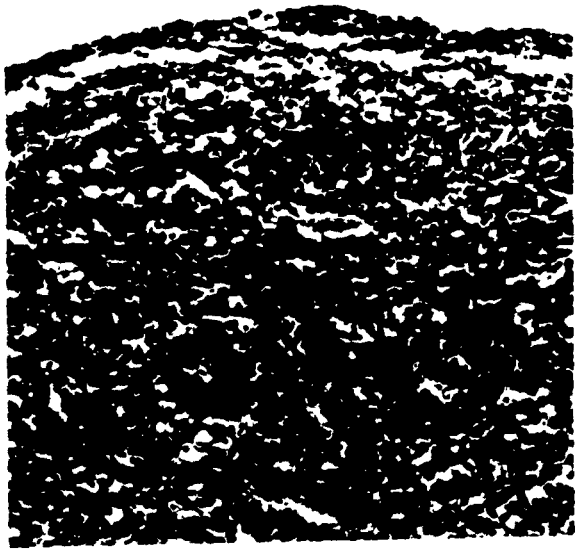

were noted: an avascular center with large necrotic foci, an intermediate zone with a relative decrease in the vascular density (VD=11.8 ± 1.5), and a peripheral zone with numerous capillaries (VD=19.5 ± 1). At any of these five stages endothelial cell hyperplasia was not observed. We found a significant positive correlation between tumor volume and tumor vascular density ($r=0.92$; $p<0.01$) (Figure 16). The perivascular organization of tumor cells was observed as early as day 6 and throughout the experiment. Scattered foci of petechial hemorrhages of various size were first noted on day 14. By day 22 they were mainly located in the central necrotic area. Tiny areas of tumor necrosis were first seen on day 14. Their coalescence by day 18 gave rise to massive central necrosis by day 22. In all tumors, mononuclear infiltrates appeared on day 10, mainly arcund the tumor and persisted for the remainder of the study.

Cerebral peritumoral edema first observed on day 6, became progressively more prominent and associated with vacuolation, and loosening of the neuropil, resulting in a spongy appearance (Figure 17).

Discussion

This reproducible model allows the experimental study of tumor angiogenesis within the rabbit brain. The VX2 carcinoma has been previously used for the study of angiogenesis (1,18) and its inhibition (19). The growth of VX2 carcinoma in the brain has also served as a model for tumor growth (7) and neuroimaging (8-10) but, to our knowledge, not for the study of the interrelationship between tumor growth and angiogenesis within the rabbit brain.

Figure 16 There is a strong positive correlation between tumor volume and tumor vascular density ($r = 0.92$; $y = 0.24x-2.05$)

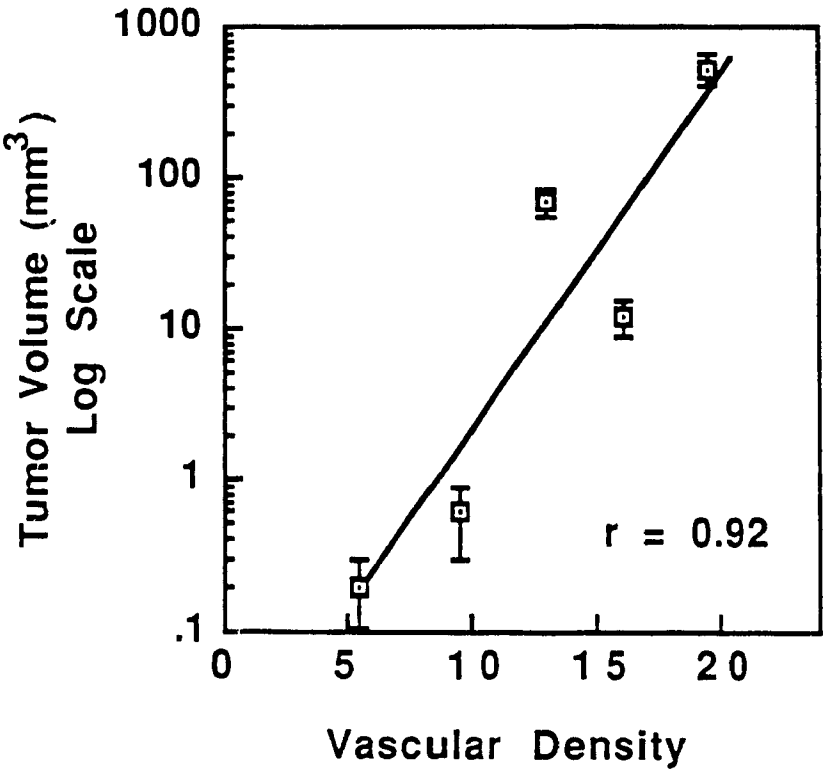
1000
100
10
1
.1
Tumor Volume (mm^3)
Log Scale
r = 0.92
0
5
10
15
20
Vascular Density

Figure 17 Vacuolation and loosening of the neuropil around the tumor on day 14, corresponding to peritumoral edema (E). The tumor is located outside the ventricle (V) (H & E, X150)

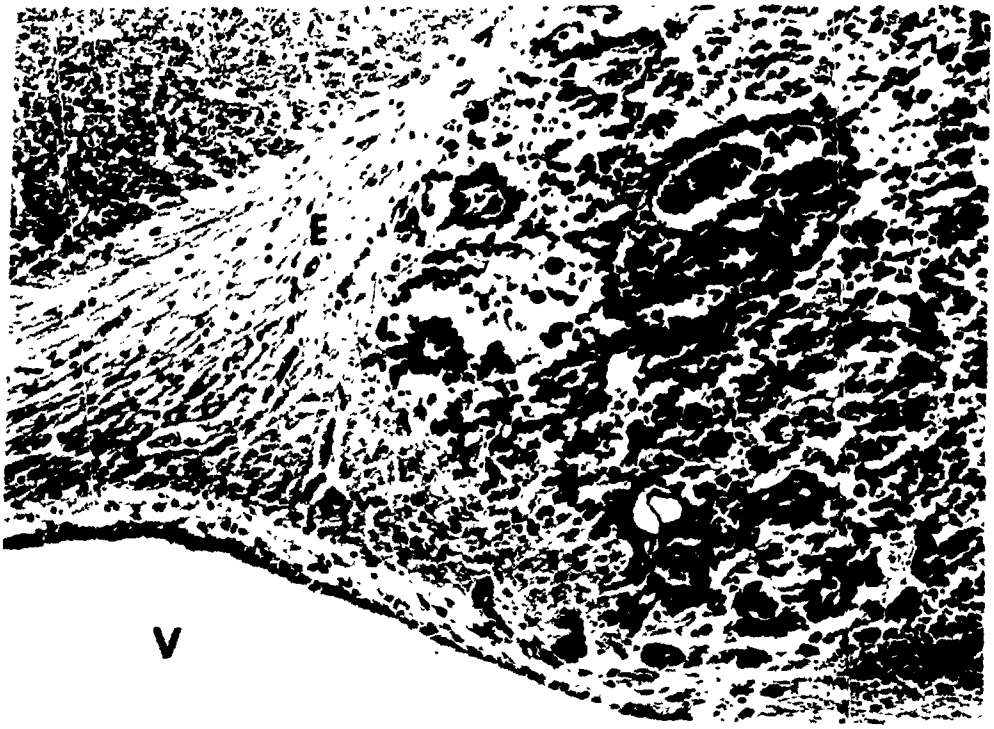
E
V

The described model is valuable for several reasons: 1) The predictable tumor type and location are associated with a stereotypic and well defined sequence of vascular changes. 2) When compared to other tissues, the normal adult brain is characterized by a capillary endothelium population that is quiescent and non proliferative (14,20). Angiogenesis is observed in the adult brain in pathological states, particularly that of malignancy, and the contrast with quiescent normal vessels made angiogenesis easily detectable. 3) The model allows the measurement of angiogenesis on both macroscopic (5) (cortical neovascularization), and microscopic scales (14). We observed cortical vascular changes that mimic those of human brain malignancies (11). Because cortical neovascularization might not be observed if VX2 carcinoma cells were implanted at a depth of 6 to 12mm within the brain (7-10), we chose an implantation site of 2mm into the brain close to the cortical surface. The short distance between the angiogenic source and the cortical blood vessels allowed for the angiogenic response, as has previously been described in the corneal assay (1).

On the basis of the vasculature, we observed 3 different tumor zones on day 22. These 3 zones have also been observed in experimental gliomas (22). A second flare of neovascularization was also seen by day 22 after tumor implantation, when the tumor reached the cortex. This could be related to the higher capillary density normally found in the cortex (23).

A specific feature of tumor angiogenesis in the brain is the breakdown of the BBB, associated with capillary proliferation (24). Leakage of Evans blue was mainly observed at the tumor periphery where

the highest degree of neovascularization appears. The permeability of blood capillary sprouts and newly formed blood capillaries compared to older blood capillaries is increased (25). Blood vessels of experimental (26) and human (27) brain tumors are structurally altered with abnormal vascular permeability. This model could be useful in further studies of the breakdown of the BBB induced by experimental brain tumors.

We noted a perivascular organization of tumor cells that could be related to favorable nutritional and oxygenation gradients. A solid tumor cannot grow beyond a few millimeters in size until an adequate vascular system is acquired (28) partially because diffusion of oxygen constitutes a limiting factor (29). Previous studies showed that both labeling and mitotic indices of mouse mammary carcinoma cells decrease with increasing distance from the nearest capillary (29,30). The attachment of tumor cells to blood vessels is also observed in vitro in the absence of a microcirculation (31) suggesting that tumor infiltration preferentially occurs along vascular paths (32).

These experiments support the concept that tumor growth in the brain, as in other sites (1,18,28), is a function of angiogenesis.

Notre modèle de tumeur cérébrale entrainant une angiogenèse évidente tend à démontrer qu'au niveau du système nerveux central aussi, la croissance tumorale est étroitement liée au phenomene d'angiogenèse tumorale. Une fois le modèle de tumeur cérébrale developpe, nous nous sommes attachés a tester l'effet de la depletion cuprique sur le development et la croissance du carcinome VX2. On avait deja demontre que la dépletion cuprique etait capable d'inhiber la néovascularisation tumorale au niveau de la cornée du lapin. Notre but était donc de savoir si la dépletion cuprique pouvait prevenir l'angiogenèse tumorale et de ce fait la croissance tumorale in vivo dans le cerveau.

CHAPTER III

Angiogenesis Inhibition by Copper Depletion Prevents the Growth of the VX2 Carcinoma in the Rabbit Brain

Abstract

We implanted 5 x 10^5 VX2 carcinoma cells into the parietal lobe of 140 New Zealand white rabbits. In the first experiment we implanted 36 rabbits divided into four groups; 1) Control, 2) pair fed, 3) acute copper depletion and 4) chronic copper depletion. Copper depletion is achieved by a low copper diet and penicillamine, the last group consisting of hypocupremic animals revealed tiny avascular tumors as opposed to the three other normocupremic groups that displayed large vascularized tumors. Injections of Evans blue revealed a localized breakdown of the BBB in the normocupremic groups, by contrast the hypocupremic animals showed a diffuse breakdown of the BBB. In the second experiment, we operated on 90 rabbits that received viable VX2 carcinoma cells and 10 sham animals that received heat-killed cells. In this experiment the results of the first experiment were confirmed. Penicillamine alone has an effect on tumor growth without an angiogenic inhibitory effect. In the third experiment, we operated on 14 animals in order to test the effect of a low copper diet alone. We found a decrease in tumor size but no angiogenic inhibition. In all of these three experiments there was no increase in survival time in any of the experimental groups. These experiments represent the first angiogenic inhibition in the brain. We observed that both a low copper diet and penicillamine are necessary to achieve a significant decrease in tumor size and an angiogenic inhibition.

Copper ion is a cofactor of angiogenesis (1-5), furthermore hypocupremic rabbits are unable to mount an angiogenic response in the cornea (2,5). We tested the effect of copper depletion on intracerebral growth and angiogenesis of the VX2 carcinoma.

Materials and Methods

First Experiment

Using the previous described brain tumor model. We implanted 40 rabbits divided in four groups: 1) Control: rabbits on a normal diet (5301, Ralston Purina Canada Inc., Longeuil, Quebec). 2) Acute copper chelation and penicillamine therapy: (Acute CDPT): low copper diet (LCD) (Ralston Purina #5890C-1, Richmond, IN) and D-penicillamine (#4875, Sigma Chemical Co., St. Louis, Mo) 60mg a day per os started after tumor implantation up until sacrifice. 3) Pair fed: rabbits on a normal (#4875) but volume restricted diet to match the weight of the rabbits on a LCD (Figure 1). (Caloric restriction effects tumor growth (7 & 8)) 4) Chronic CDPT: LCD started 6 weeks before the tumor implantation and up until sacrifice and D-Penicillamine 6 days before and after tumor implantation, at the same dosage as in group 2.

In each group, three animals were given Evans blue and two received ink by techniques described in Chapter II.

Second Experiment

We implanted 70 rabbits divided in 7 groups of 10 each. Four groups were similar to the first set of experiments 1) control 2) acute CDPT 3) pair fed 4) Dexamethasone 0.75mg/day started day of surgery, intramuscularly, with a normal diet. 5) Penicillamine starting day of surgery, 60 mg/day per os with a normal diet. 6)Chronic CDPT

Figure 1 In early experiments (6) animals that were fed a low copper diet failed to gain weight

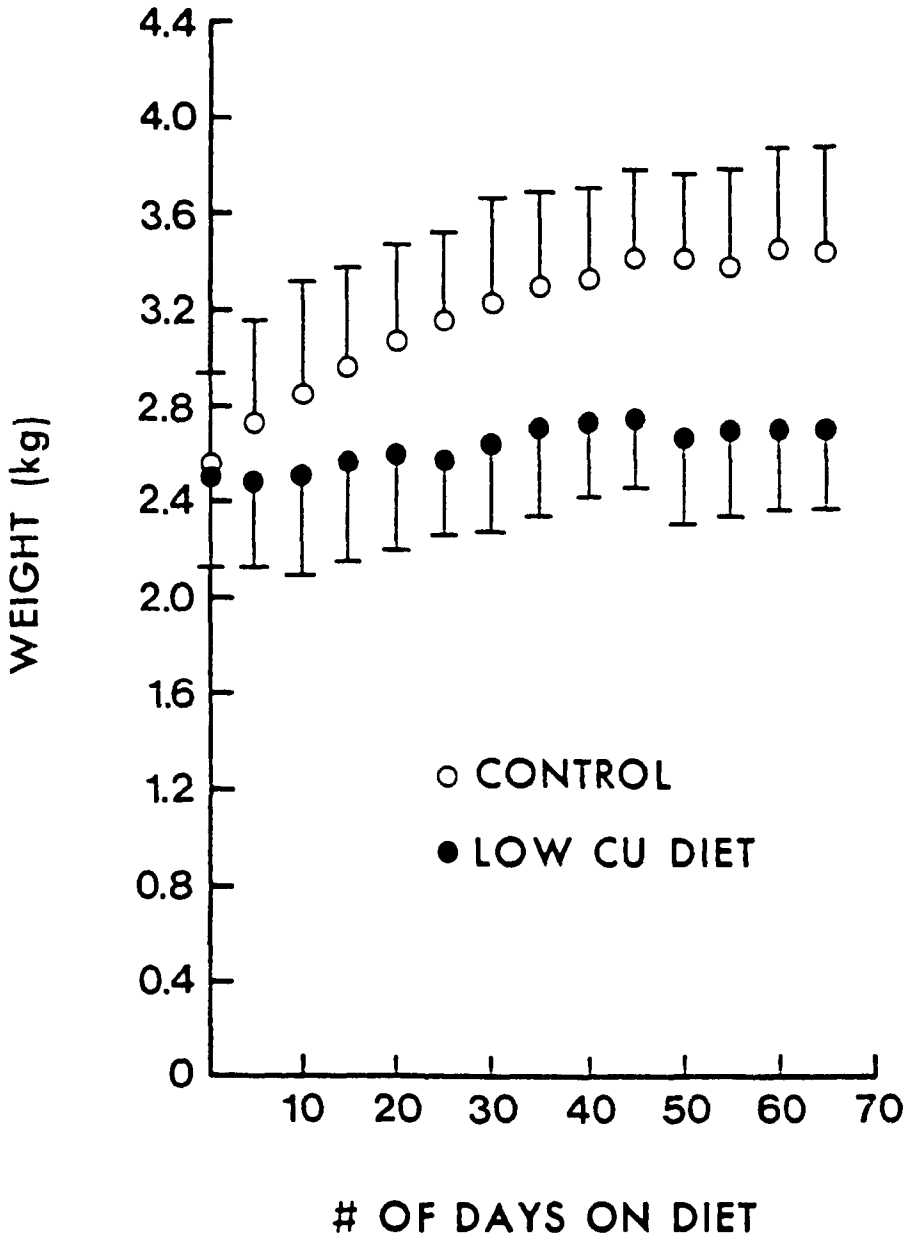
4.4
4.0
3.6
3.2
2.8
2.4
2.0
1.6
1.2
0.8
0.4
0
WEIGHT (kg)
10
20
30
40
50
60
70
OF DAYS ON DIET
CONTROL
LOW CU DIET

7) CDPT plus dexamethasone at the same dosage as group 4 but started on day 14. Ten additional sham rabbits received 5 x 10 heat-killed carcinoma cells, to test the non specific effect of cerebral injury in hypocupremic rabbits. Five additional rabbits to group 1,2,3,6 were implanted for Evans blue and ink injections.

Third Experiment

We then implanted 14 more NZW rabbits to test the effect of LCD alone on the intracerebral growth of the VX2 carcinoma. We divided the 14 animals into two groups of seven: Control and LCD.

In each experiment after tumor implantation the same follow-up was performed as described in Chapter II. When the animals developed neurological signs they were sacrificed, the brains were removed; the assessment of cortical findings, brain sections, measurements of tumor volumes, specimens preparation for histology and determination of capillary density were performed in the same manner as described in Chapter II.

At the beginning of each experiment, the day of tumor cells implantation, and the completion of each experiment, the serum copper levels were measured by atomic absorption spectrophotometry (9). Care was taken to avoid copper contamination (10) by the use of special plastics containers.

Statistical analysis was performed by analysis of variance and Tukey test or modified student t test (11),a p value less than 0.05 was the chosen level for significance.

Results

First Experiment

The results are summarized in Table I. Copper levels of the different groups are shown in the Table I and Figure 2. Groups 1,2,3 remain normocupremic (NC) throughout the experiment whereas Group 4 was hypocupremic (HC) at the time of implantation. Less than 50% of baseline was established to induce angiogenesis inhibition (2).

The survival curves of all four groups overlapped (Figure 3).

In the NC group the cortical surface revealed numerous, tortuous, prominent vessels surrounding a prominent tumor similar to day 22 (Figure 4). By contrast, the cortical surface of hypocupremic rabbits was relatively pale with obvious swelling (Figure 5), free of tumor with a normal vascular network. The control animals revealed large vascularized tumors (Table 1, Figures 6 and 7). No significant difference was observed in the two other normocupremic groups (acute copper depletion and pair fed). Pale laminar plaques were found in the HC group with a 96% reduction ($p < 0.01$) as compared to control (Table 1, Figures 6 and 7).

In both NC and HC tumors, we found marked midline shift and distortion of the brain stem (Figure 6). Capillary density in the HC group was significantly ($p<0.05$) decreased compared to other three groups (Table 1, Figures 8,9,10). In NC animals we found an extravasation of Evans blue mainly confined to the tumor area (Figure 11). By contrast broad areas of Evans blue extravasation were observed in HC rabbits (Figure 12). In summary (Figure 13) angiogenesis resulted in large vascularized tumors whereas its inhibition or "angiosuppression" led to

TABLE 1: Copper Depletion Results in Suppression of Intracerebral Oncogenesis and Angiogenesis

Experimental Group (n)	Diet	Penicillamine (mg/d)	Serum $\bar{X}$ Copper (μg/dL)			Tumor Vascularity ($\bar{X}$ cappillary density, No./HPF)	Tumor Size ($\bar{X}$ volume-mm^3)
			Initial	Implantation	Death		
Control (9)	Normal	0	62	63.5	61	15.4 ± 3.9	537 ± 397
CDPT Acute (9)	Normal, then low copper	60	59	63	57	11.5 ± 5.5	632 ± 262
Pair-fed (9)	Restricted	0	57	60	55	12 ± 4.8	708 ± 374
CDPT Chronic (8)	Low copper	60	63	12	9	3.3 ± 1	27 ± 30

Figure 2 Reduction of serum copper level by low copper diet and chelation. The chronic CDPT group (◆) was hypocupremic at time of tumor cells implantation and at time of sacrifice. The three other groups remain normocupremic throughout the experiment

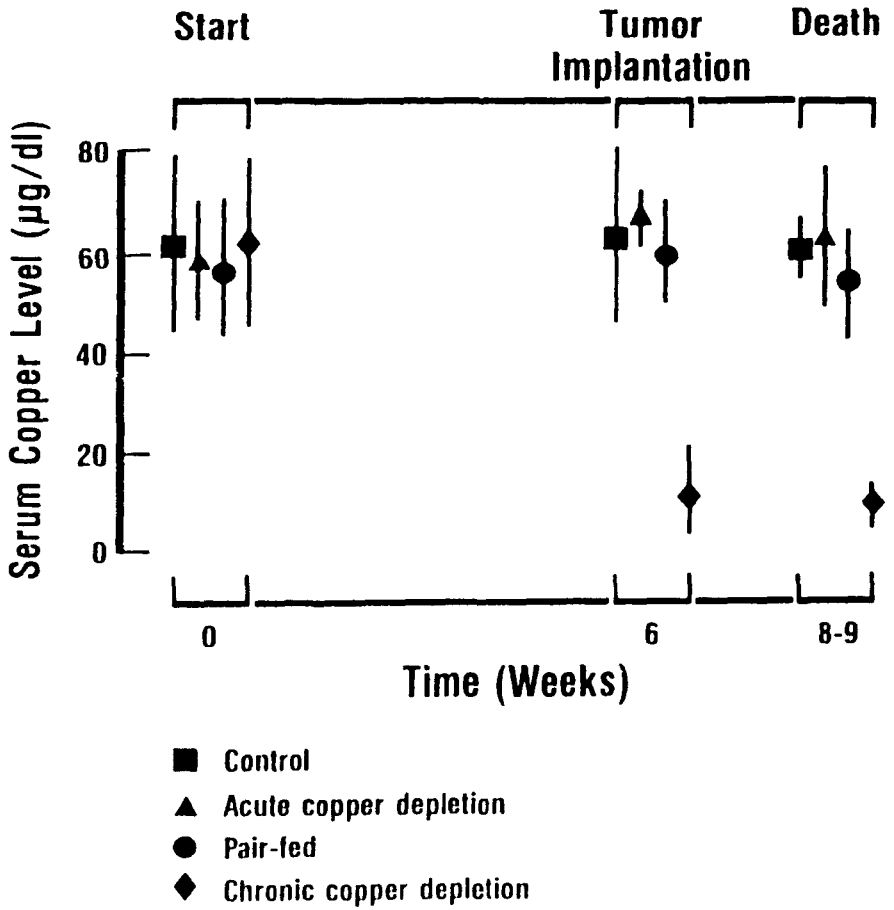
Start
Tumor Implantation
Death
Serum Copper Level (µg/dl)
80
60
40
20
0
0
6
8-9
Time (Weeks)
Control
Acute copper depletion
Pair-fed
Chronic copper depletion

Figure 3 The survival curves of the four groups overlaped without statistically significant difference

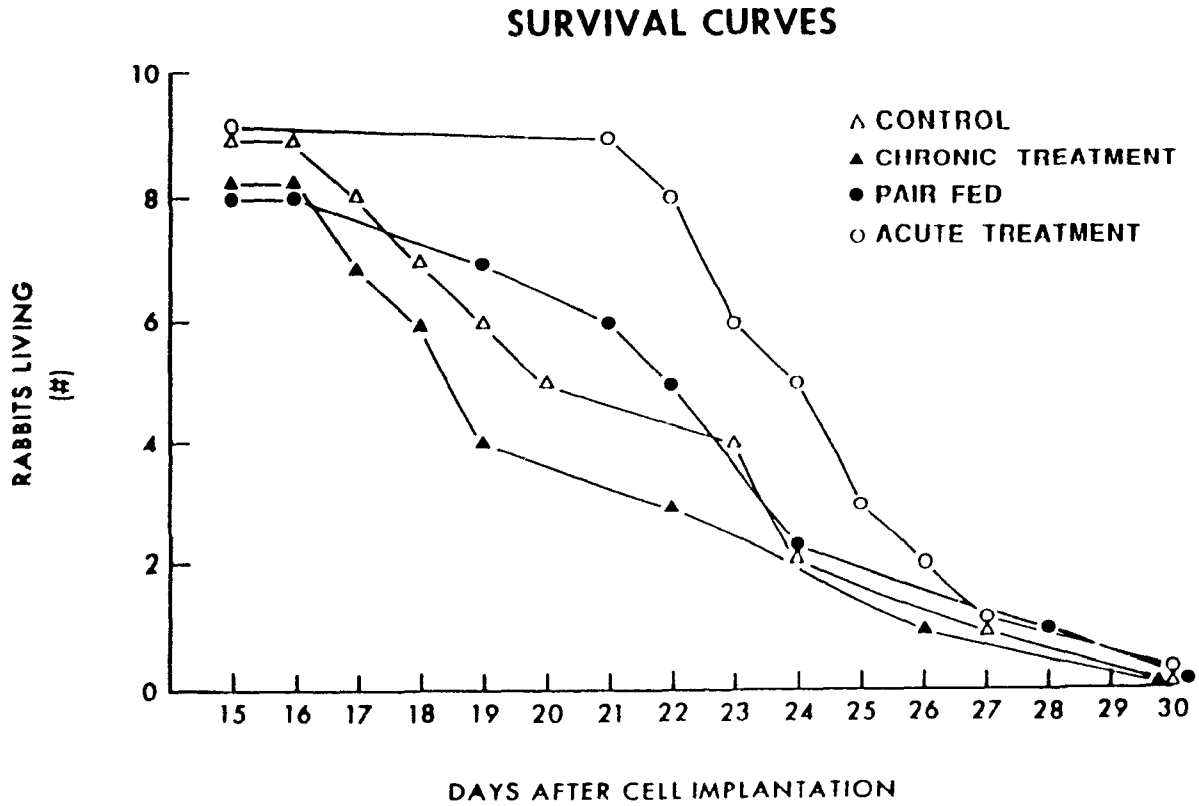
SURVIVAL CURVES
RABBITS LIVING (#)
10
8
6
4
2
0
15 16 17 18 19 20 21 22 23 24 25 26 27 28 29 30
DAYS AFTER CELL IMPLANTATION
△ CONTROL
▲ CHRONIC TREATMENT
● PAIR FED
○ ACUTE TREATMENT

Figure 4 The cortical surface of a normocupremic animal reveals multiple, hypertrophied, tortuous new vessels. Note the presence of the tumor

Figure 5 Cortical surface in a rabbit injected with ink, under chronic CDPT. Note the normal cortical vascular network and the brain swelling

Figure 6 Inhibition of tumor growth by copper depletion in the rabbit brain: The three normocupremic groups displayed large, vascularized tumors with necrotic centers and hemorrhages: A: Control, B: Pair-fed, C: Acute copper depletion and chelation. The chronic CDPT tumor (D) grew "en plaque" resulting in a tiny laminar nodule (arrow). Note the distortion of the brain stem also present around the tiny tumor (arrowheads)

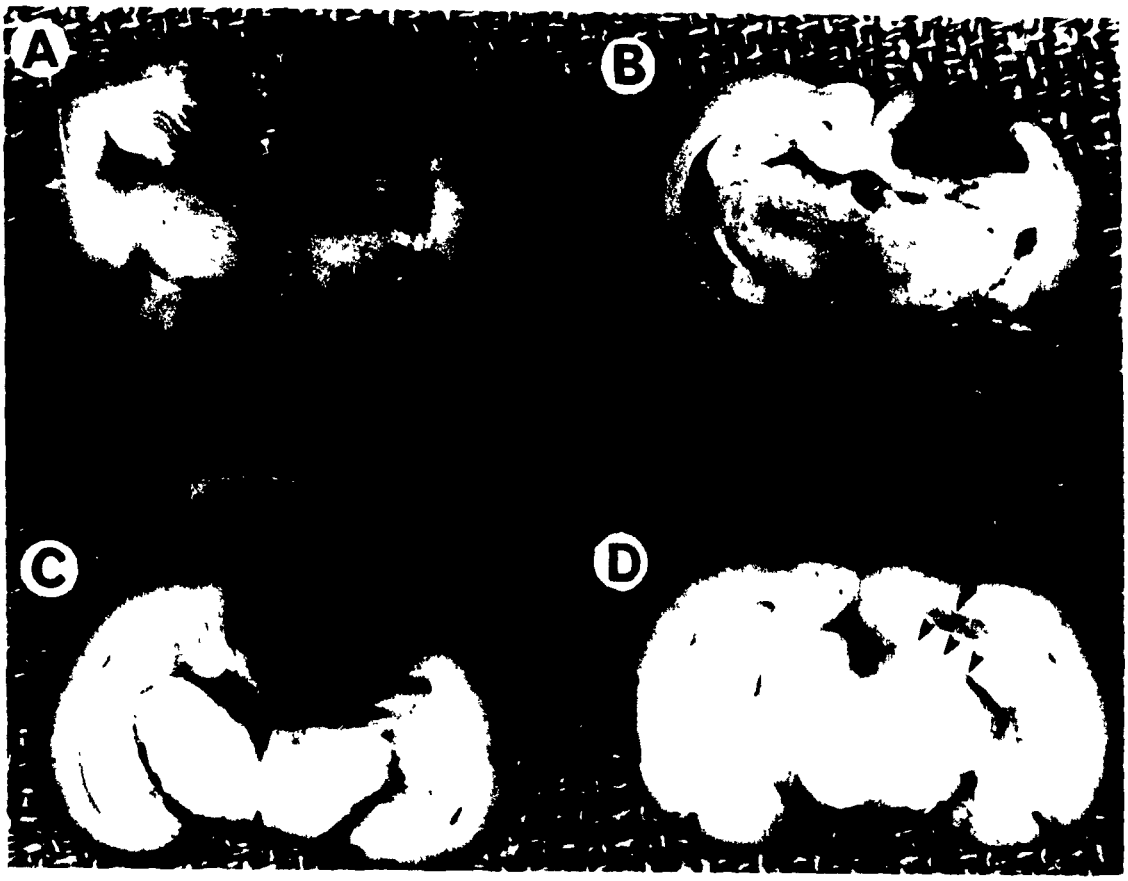
A
B
C
D

Figure 7 Reduction of tumor volume by angiogenic inhibition. Histogram showing statistically significant decreased tumor volume in the tumors of the chronic CDPT animals ($p<0.01$)

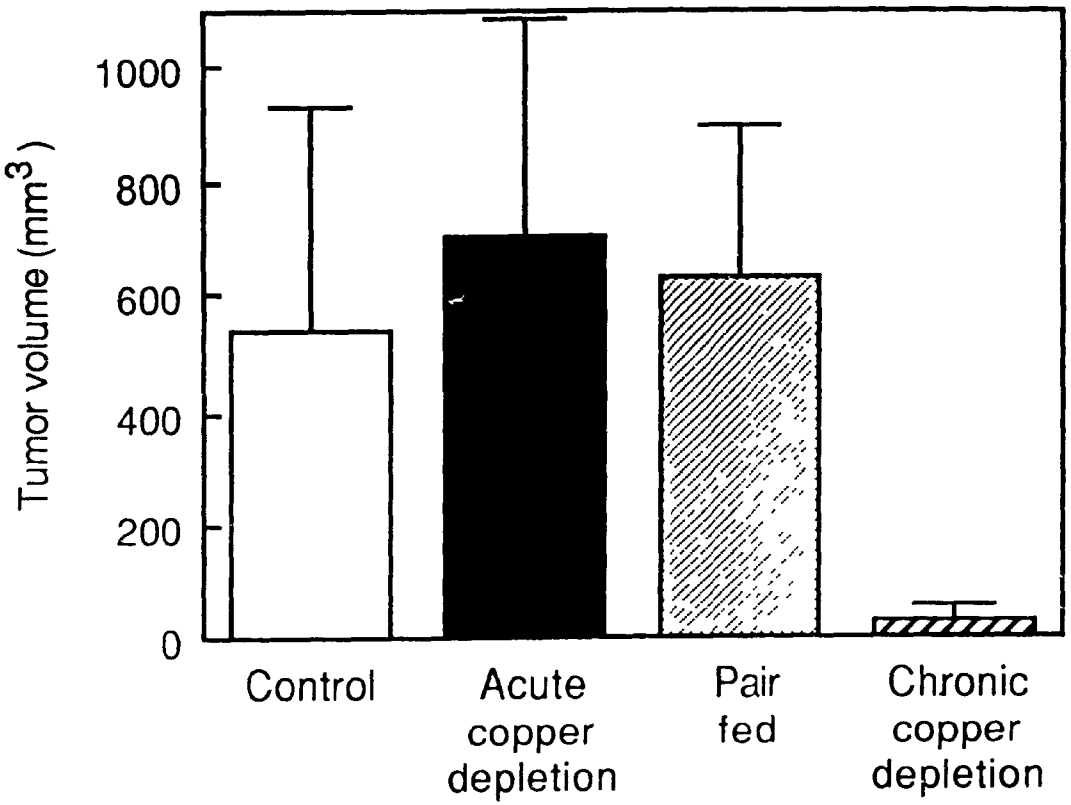
Tumor volume (mm^3)
1000
800
600
400
200
0
Control
Acute copper depletion
Pair fed
Chronic copper depletion

Figure 8 Quantitative studies of vascular density indicate a three-to-four fold increase in the NC tumors as compared to those treated by copper depletion and Penicillamine

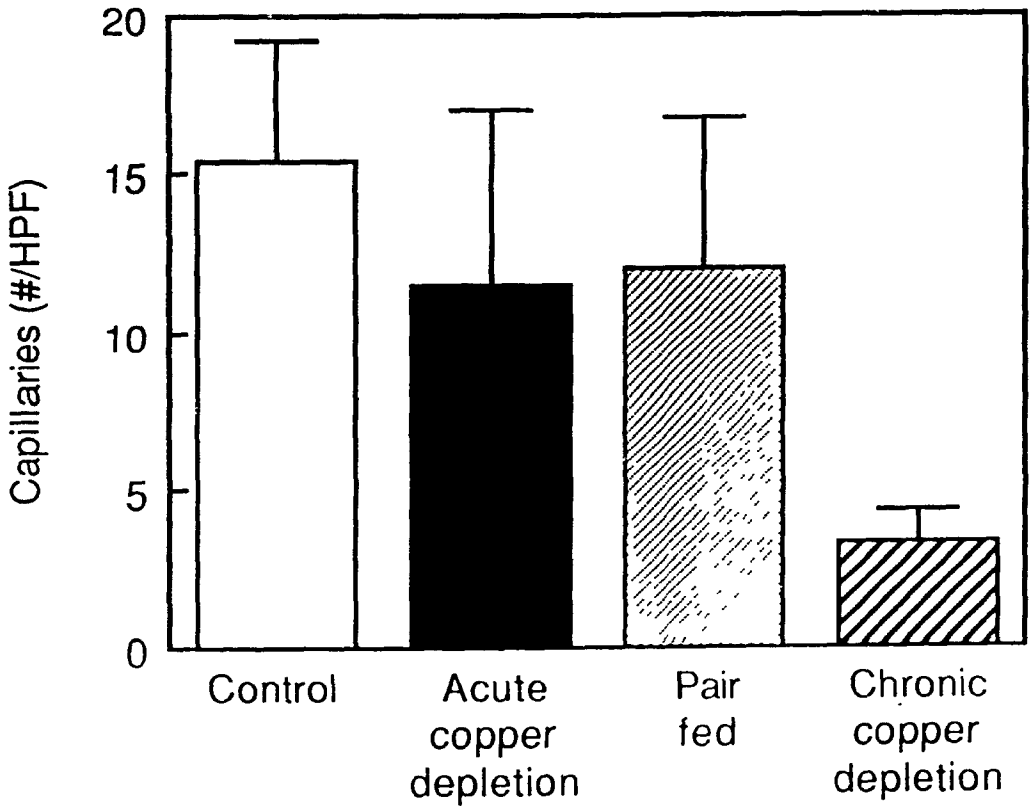
Capillaries (#/HPF)
20
15
10
5
0
Control
Acute copper depletion
Pair fed
Chronic copper depletion

Figure 9 Prominent vascular proliferation in a NC tumor (H & E, X150).

Figure 10 Histologic appearance of a treated tumor: angiogenesis is suppressed (H & E, X450)

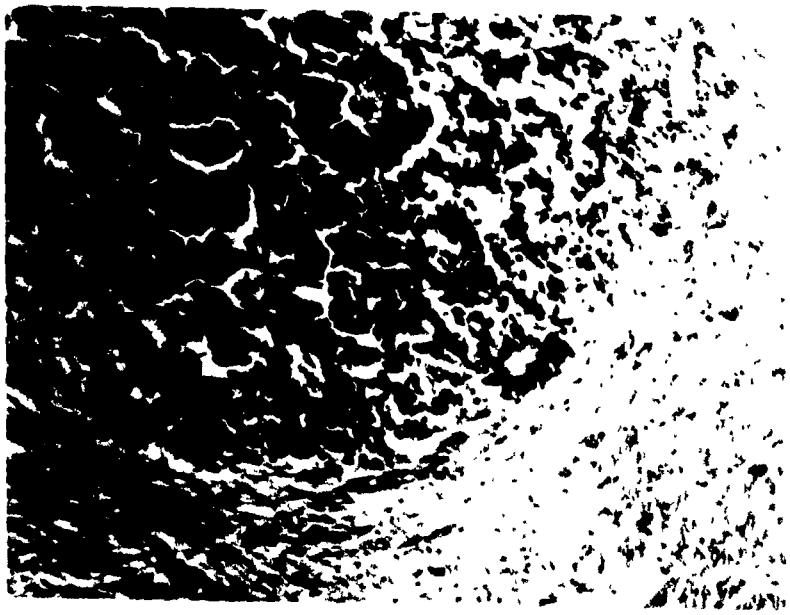

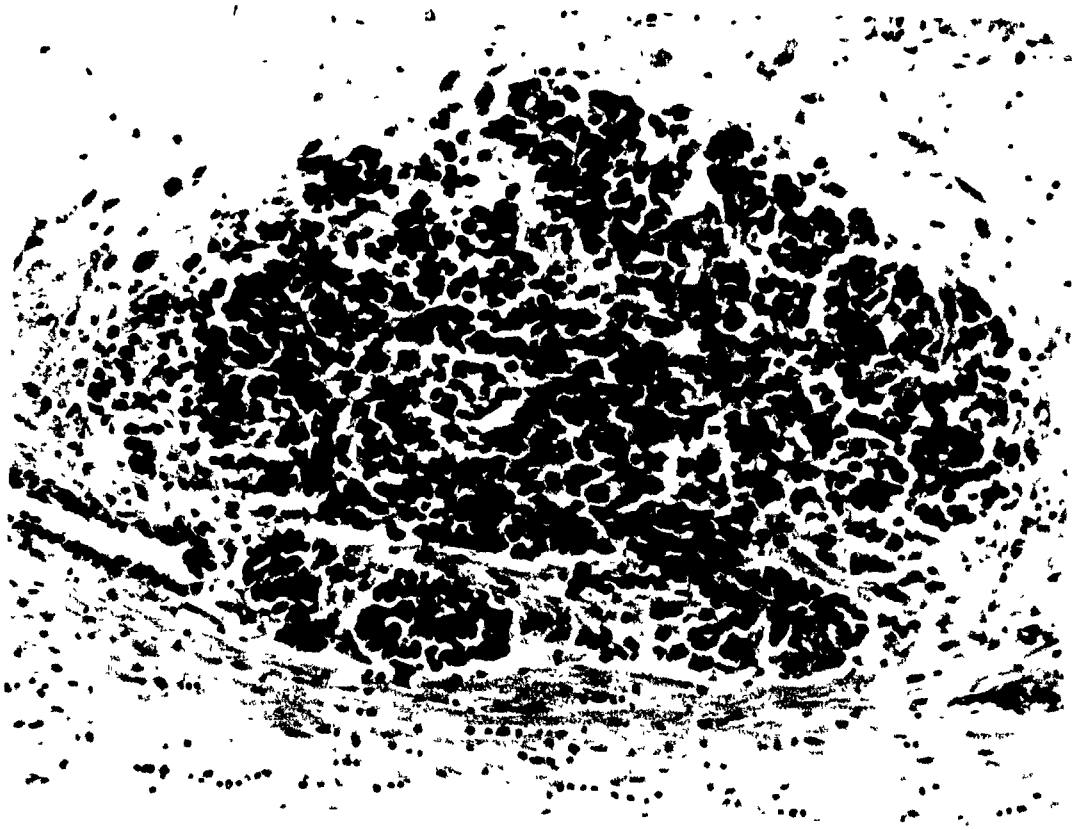

Figure 11 The Evans blue extravasation mainly located to the tumor area in a NC tumor

Figure 12 Broad areas of Evans blue extravasation observed in a hypocupremic tumor

Figure 13 Angiogenesis results in a hypervascularized tumor. By contrast the cortical vascular network is normal after "Angiosuppression" achieved by copper depletion and Penicillamine that also results in a marked brain swelling

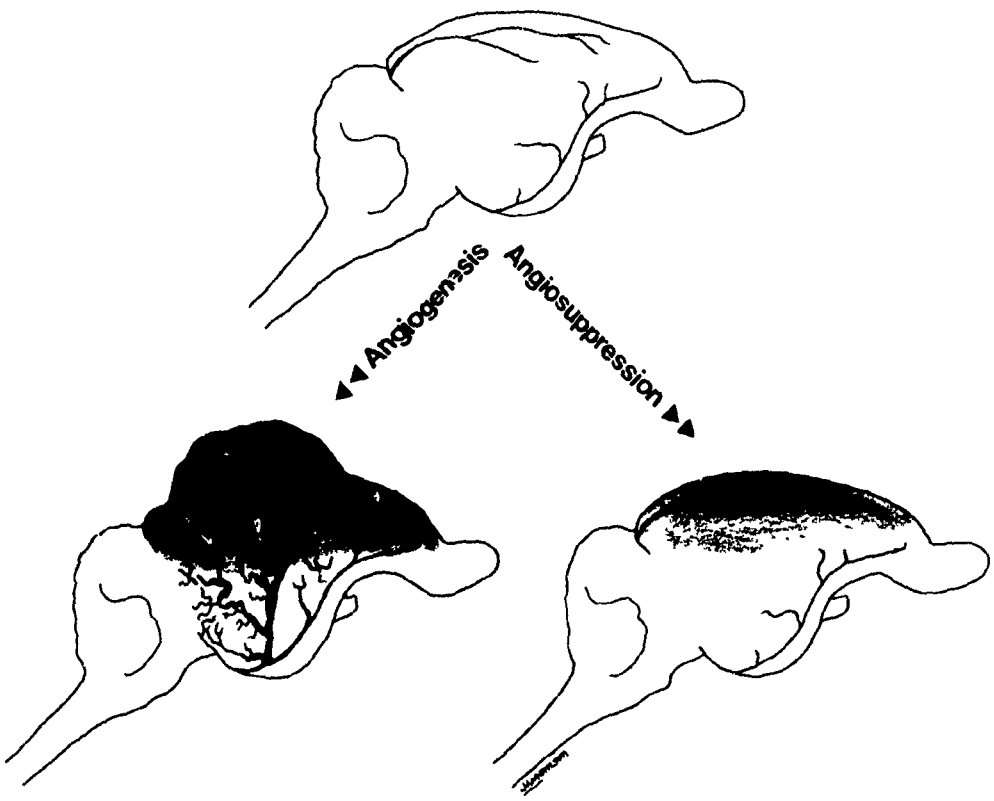
Angiogenesis
Angiosuppression

tiny avascular tumors with a great deal of peritumoral swelling.

Second Experiment

The results are summarized in Table 2.

All the groups remained NC throughout the experiment except for those (Groups 6 and 7) on chronic CDPT (Table 3 and Figure 14).

Once again, the survival curves (Figures 15 and 16) of the different groups were similar except for the group after sham surgery that received heat-killed cells.

In this sham group except for two animals that died because of respiratory problems the other 8 animals of the group remained alive and were sacrificed four months after the surgical procedure.

Similarly as in the previous experiment control, acute CDPT and pair-fed animals developed large tumors. The two HC groups compared to control revealed tiny tumors, $p < 0.01$ (Table 2 and Figure 17). Dexamethasone and penicillamine started on day of surgery had an effect on tumor size, compared to control, $p < 0.05$.

All of the five NC groups (control, acute CDPT pair fed, dexamethasone and penicillamine revealed similar vascular densities (Table 2, Figure 18). Vascular density was markedly decreased in the HC groups 6 and 7, ($p < 0.05$). Evans blue studies showed extravasation similar to the first set of experiments (Figures 19 and 20).

Third Experiment

The evolution of copper levels are presented in Table 4.

The mean survival time was similar in both groups (Table 4). Tumor volume (Figure 21) was significantly smaller ($p<0.01$).

Capillary density was similar in both groups (Table 4).

TABLE 2: Copper Depletion Results in Suppression of Intracerebral Oncogenesis and angiogenesis of the VX2 Carcinoma

Experimental Group	N	Diet	Penicillamine (mg/day)	Survival Days ($\bar{X} \pm SD$)	Tumor Vascularity Vascular Density ($\bar{X} \pm SD$, No./HPF)	Tumor Size Volume ($\bar{X} \pm SD, mm^3$)
1) Control	14	Normal	0	16.8 ± 1.3	15.9 ± 3.6	506 ± 344
2) CDPT, acute post-implantation	13	Normal, then low copper	60	20.5 ± 4.5	12.3 ± 5.6	696 ± 395
3) Pair-fed	13	Restricted	0	18.2 ± 2.8	11.8 ± 4.3	611 ± 318
4) Dexamethasone .75mg/kg/day	9	Normal	0	18.8 ± 4.0	9.0 ± 1.0	185 ± 153
5) Penicillamine	9	Normal	60	16.8 ± 4.3	13.3 ± 1.2	112 ± 95
6) CDPT, chronic	12	Low copper	60	18.3 ± 5.4	3.2 ± 1.2	26 ± 25
7) CDPT, chronic Dexamethasone .75mg/kg/day	10	Low copper	60	20.2 ± 2.3	4.1 ± 0.9	29 ± 18

TABLE 3: Serum Copper Levels ($\bar{X} \pm SD$, μg/dl)

Group	Intial	Implantation	Death
1) Control	62.0 ± 17.4	63.5 ± 17.0	61.0 ± 6.3
2) Acute CDPT	59.0 ± 12.6	66.0 ± 5.1	63.3 ± 13.2
3) Pair-fed	57.4 ± 13.3	60.0 ± 10.1	54.0 ± 11.2
4) Dexamethasone	73.0 ± 19.4	59.0 ± 17.6	64.4 ± 8.4
5) Penicillamine	74.5 ± 20.6	65.2 ± 14.0	66.0 ± 13.0
6) Chronic CDPT	62.0 ± 17.2	12.2 ± 9.0	9.0 ± 5.3
7) Chronic CDPT + dexamthasone	75.1 ± 15.0	6.9 ± 3.0	6.8 ± 2.9

Figure 14 A low copper diet six weeks before tumor implantation is necessary to achieve hypocupremia as observed in chronic CDPT group (◆) and in the chronic CDPT and dexamethasone group (○). The other give groups remained normocupremic throughout the experiment

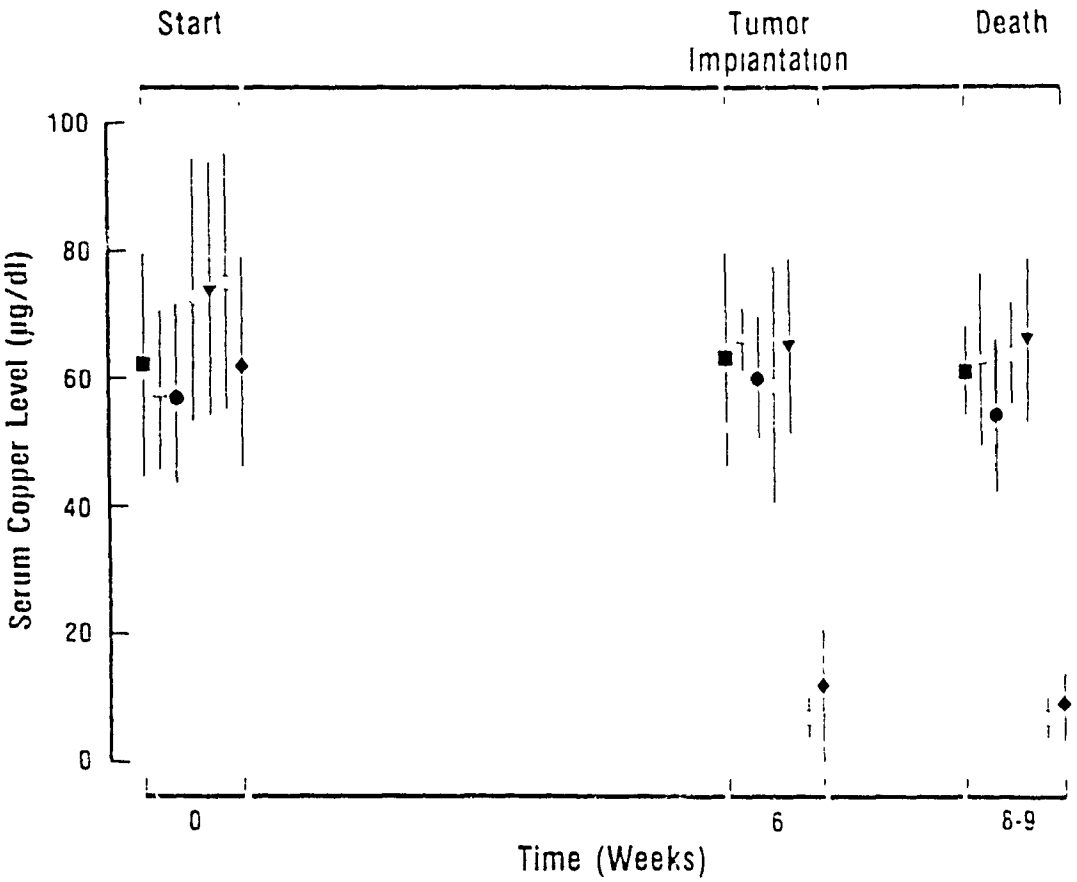

- ■ Control
- ▲ Acute copper depletion
- ● Pair fed
- ◇ Steroids after cell implantation
- ▼ Penicillamine after cell implantation
- ○ Chronic copper depletion + steroids starting 14 days after implantation
- ◆ Chronic copper depletion

Figure 15 There is no increase in survival time by addition of dexamethasone to chronic CDPT; Dexamethasone alone; of Penicillamine alone. The sham implanted animals demonstrate chronic CDPT by itself is not able to cause the death of the animals

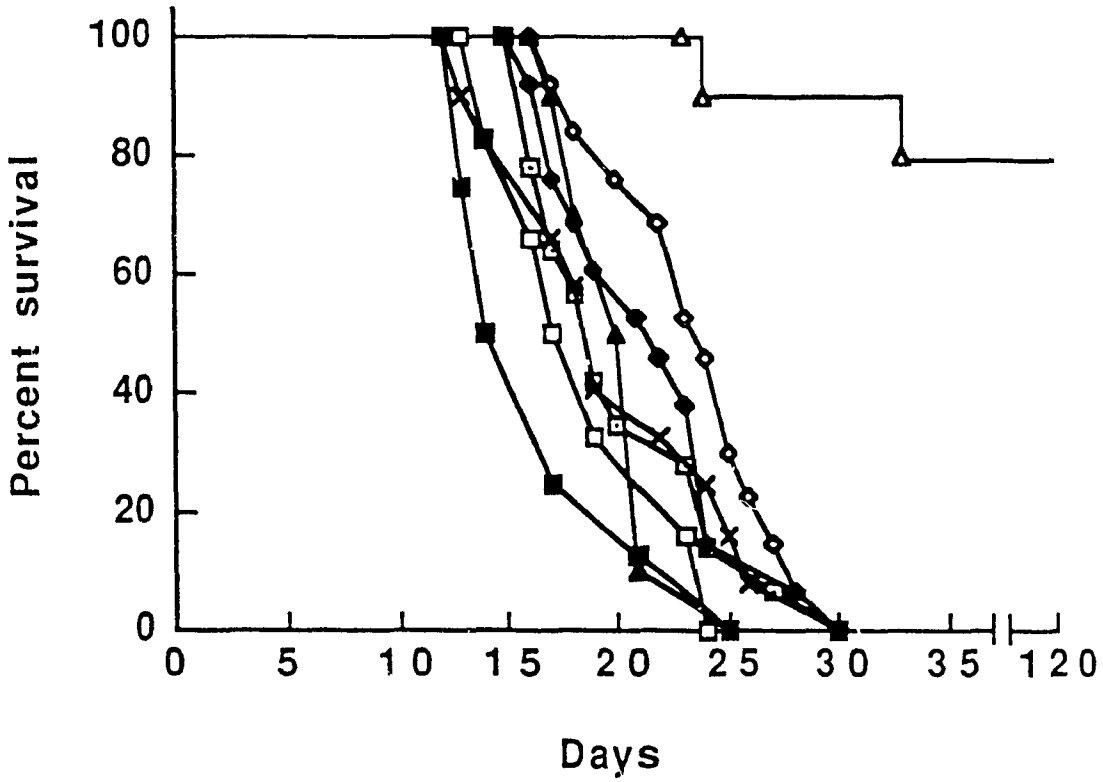

- Control
- Acute copper depletion
- Pair fed
- Steroids after cell implantation
- Penicillamine after cell implantation
- Chronic copper depletion + steroids starting 14 days after implantation
- Chronic copper depletion
- Chronic copper depletion SHAM surgery

Figure 16 Histogram presenting in a different manner the lack of increase of survival time in any of the groups injected with viable tumor cells

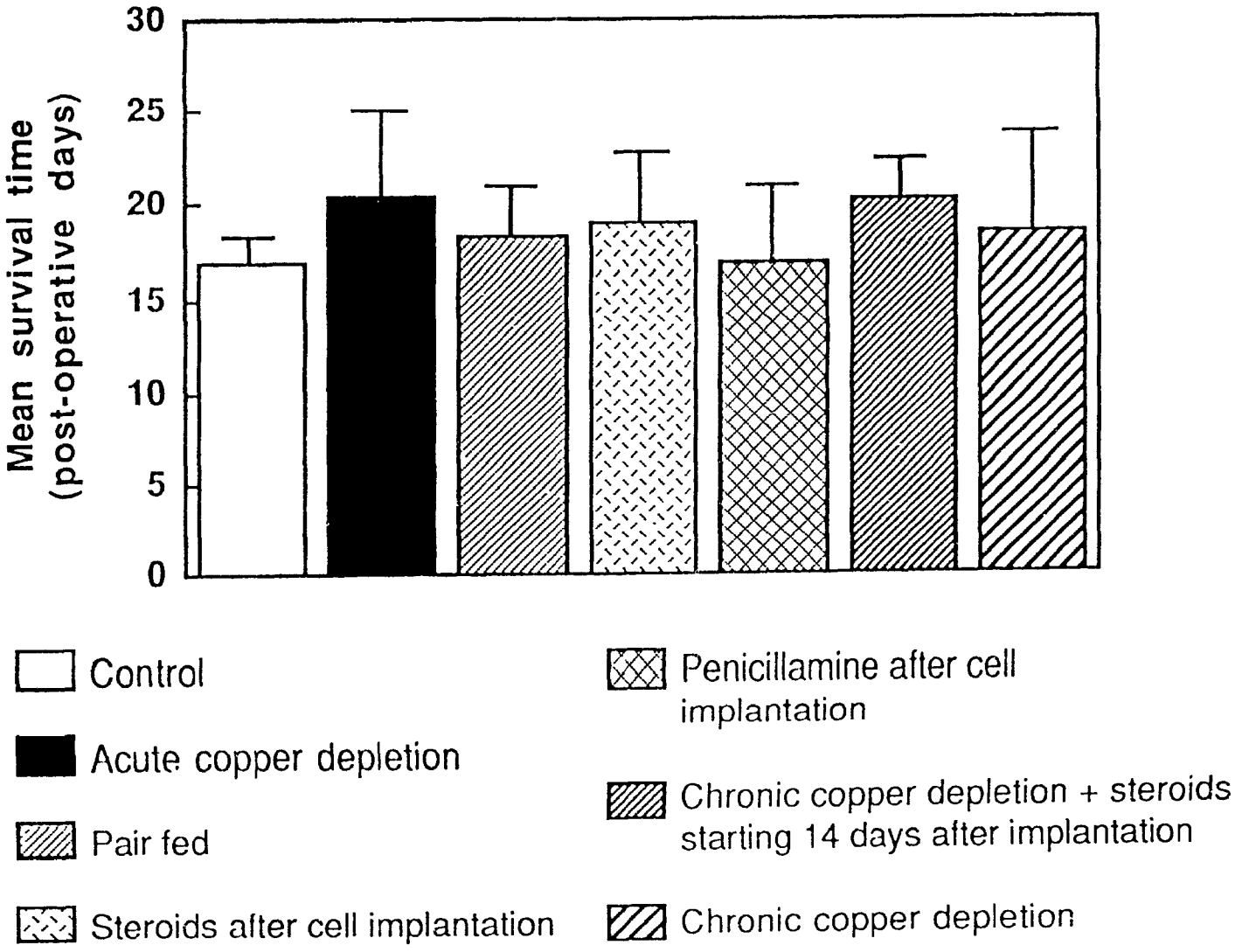
Mean survival time
(post-operative days)
30
25
20
15
10
5
0
Control
Acute copper depletion
Pair fed
Steroids after cell implantation
Penicillamine after cell implantation
Chronic copper depletion + steroids starting 14 days after implantation
Chronic copper depletion

Figure 17 CDPT and CDPT with dexamethasone result in significantly smaller tumors ($p<0.01$). Dexamethasone administration and Penicillamine have an effect on tumor volume ($p<0.05$) as compared to control

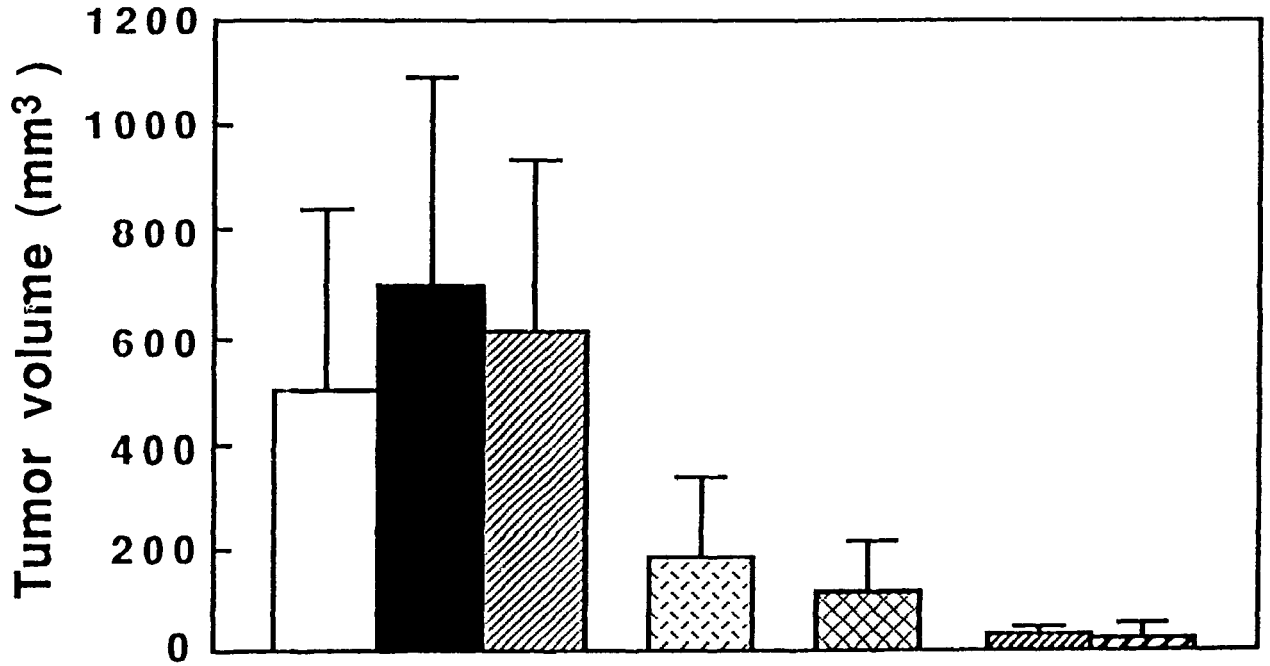

Control

Acute copper depletion

Pair fed

Steroids after cell implantation

Penicillamine after cell implantation

Chronic copper depletion + steroids starting14 days after implantation

Chronic copper depletion

Figure 18 Angiogenesis failed to occur in the two chronic CDPT groups. The effect of Penicillamine is not mediated through an angiogenic inhibitory process

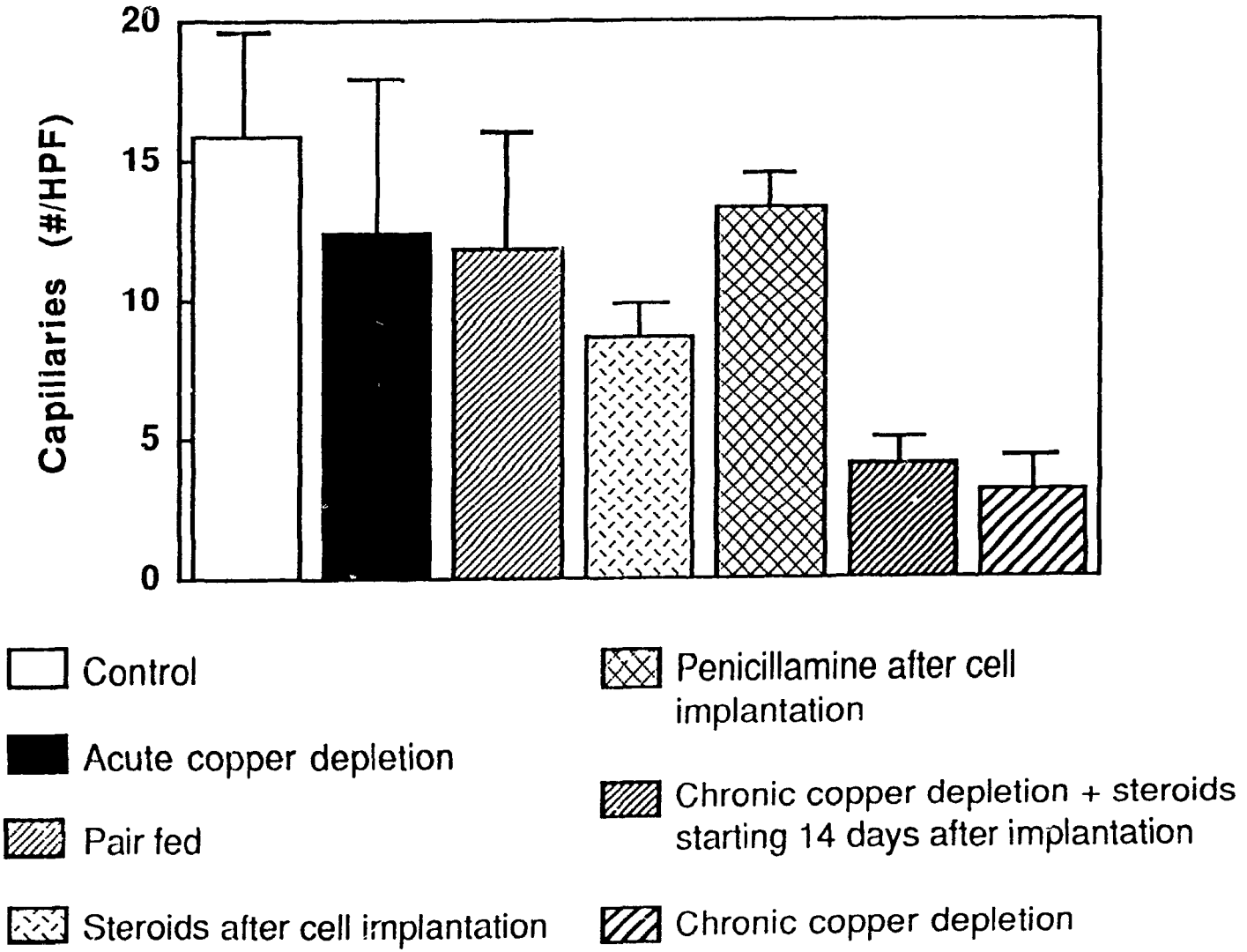
Capillaries (#/HPF)
20
15
10
5
0
Control
Acute copper depletion
Pair fed
Steroids after cell implantation
Penicillamine after cell implantation
Chronic copper depletion + steroids starting 14 days after implantation
Chronic copper depletion

Figure 19 Coronal section in a normocupremic rabbit injected with Evans blue revealing an extravasation of the dye mainly localized to the tumor area

Figure 20 Coronal section in a hypocupremic rabbit injected with Evans blue revealing a diffuse extravasation of the dye in and outside the tumor

TABLE 4: Effects of a Low Copper Diet on the VX2 Carcinoma

Group	Average SCL		Survival	Tumor	Vascular
	Start	Surgery	Sacrifice	Days	Volume (mm^3)	Density
Control	63 ± 17.3	69 ± 15.6	77.3 ± 11.6	16.5 ± 2.3	643.9 ± 383	16.4 ± 4.2
CDPT	72 ± 14.2	32 ± 9.7	38.6 ± 6.1	16 ± 1.3	151 ± 93.1	13.7 ± 5.4

Figure 21 A low copper diet alone results in a significant decrease in tumor volume, $p<0.05$

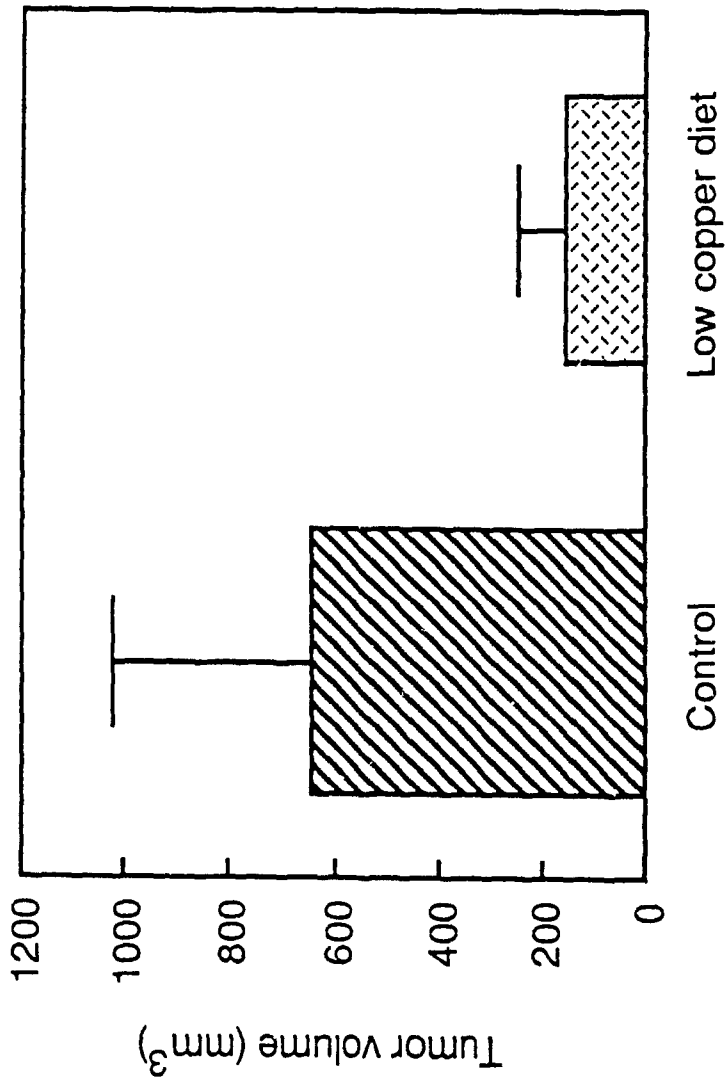
Tumor volume (mm^3)
1200
1000
800
600
400
200
0
Control
Low copper diet

Discussion

This study represents the first inhibition of tumor growth in the brain achieved by angiogenic inhibition. It further supports the concept of close interrelationship between angiogenesis, copper ion, and intracerebral tumor growth. The vascular density in the HC tumors was similar to that of the controlateral hemisphere indicating that angiogenesis failed to occur.

Whatever the mechanisms, this study is consistent with others, pharmacological inhibition of angiogenesis in vivo results in prevention of tumor growth beyond a tiny size (12). To our knowledge this study represents the first example of angiogenic inhibition in the brain. We were able to change the biology of the tumor and to arrest tumor growth by means of copper depletion and penicillamine. In the HC animals, tumor cells appeared viable similar to cells of VX2 carcinoma maintained in the avascular environment of the rabbit vitreous (12).

Despite the dramatic reduction in tumor size and inhibition of angiogenesis, there was no increase in survival time in the HC rabbits. It is likely that the marked degree of peritumoral swelling and midline shift with distortion of the brain stem were responsible for the death of the HC animals. In addition, Evans blue studies revealed broad areas of extravasation in these HC brains indicating a diffuse breakdown of the BBB.

Because of the large peritumoral swelling observed around CDPT tumors (Figure 14), we then tested the effect of steroids on both CDPT and NC tumors, as steroids are known to be potent antiedematous (13)

and antitumor (14) agents. We also wanted to test the effect of penicillamine alone on tumor growth.

The results of the second experiment confirmed the first one. Tumor volume and vascular density were significantly decreased in the hypocupremic as compared to normocupremic groups. Penicillamine inhibited tumor growth without an effect on vascular density suggesting a mechanism not mediated by an angiogenesis inhibition,

In early experiments in our laboratory (6) and in other institutions (15) it was observed that both a low copper diet and penicillamine were necessary for a complete angiogenic inhibition. Our data clearly show that the effect of chronic CDPT on tumor volume is more marked than either low copper diet alone or penicillamine alone. We observed in the second experiment that penicillamine by itself failed to inhibit tumor angiogenesis, in the same manner we observed that a low copper diet by itself does not result in angiogenic inhibition.

The mechanism of action of copper ion in angiogenesis is uncertain (16). Copper ion has been shown to play a role in the growth of hepatoma cells (17) and in healing of wounds (18). The understanding of the different steps of the angiogenic process is important in order to elucidate the possible mechanism of action of copper depletion resulting in angiogenic inhibition. The morphogenesis of a capillary involves a sequence of events. Angiogenesis which mainly originates from sprouting small venules (19), starts with the local degradation of the basement membrane (20), then mobilization of the endothelial cells towards the angiogenic stimulus takes place (19,21,22) resulting in the formation of a solid sprout. Endothelial cell proliferation then

occurs (23-25) followed by the canalization of the solid bud. Finally the periendothelial stroma is formed.

Three major stages exist in the angiogenic process:

- enzymatic degradation of the basement membrane
- endothelial cell locomotion
- endothelial cell proliferation

Which of these components can be altered by copper depletion?

1) Copper depletion, and collagen

The inhibiting effect in tumor angiogenesis may be related to the role of copper as part of the oxidase system of the cupro-protein lysyl-ligase that crosslinks the lysine residues of collagen (26). Type IV collagen, a main component of the basement membrane (27) modulates the growth of endothelial cells (28) and has a key role in endothelial behavior and capillary morphogenesis (29). Copper depletion is known to induce defective collagens (26,30), that might interfere with angiogenesis. Furthermore lysyl-ligase is necessary for migration of endothelial cells and angiogenesis (31) and present in tumor cells and inactivated by chelating agents (32).

2) Copper depletion and fibronectin

The growth of endothelial cells is modulated by fibronectin, (28,29,33) whose synthesis is regulated by copper concentration (34). Copper salts induce the synthesis of fibronectin and low levels of copper blocks its synthesis (34).

3) Copper depletion and fibroblast growth factor (FGF)

The hypothesis that perhaps the affinity of the angiogenic factor

FGF for heparin is copper-dependent (18) was further supported by recent findings that FGF can be extracted by its copper affinity (35).

4) Copper depletion and tumor necrosis factor (TNF)

It has been recently shown that macrophage-induced angiogenesis is mediated by TNF-α (36) that most probably contain a metal-binding site for copper (37). It was shown that sodium azide, a strong chelator for copper is able to inhibit the action of TNF (38), due to its chelating abilities (37). It is conceivable that either copper depletion and/or penicillamine administration result in the inactivation of TNF.

5) The effects of Penicillamine

We observed that penicillamine alone had an effect on tumor growth without obvious evidence of angiogenic inhibition. Penicillamine has both an action on collagen synthesis, able to induce a defective collagen by prevention of collagen cross linking (39,40) and interfere with collagen degradation by collagenase inhibition (41).

In addition to its effects on collagen (39-41), D-penicillamine inhibits mitogen-induced human lymphocyte proliferation (42). This proliferation inhibitory effect is synergistic with copper salts (42). Copper combines with penicillamine forming copper penicillaminate and prevents the oxidation of penicillamine to penicillamine disulfide that is an inactive compound (43). This property of copper might explain the lack of effect observed in the Acute CDPT animals. Penicillamine inhibits the growth of the S-91 mouse melanoma (44) and was used in the treatment of human melanomas (45). Because tyrosinase, a vital respiratory enzyme present in greatly elevated levels in melanomas (46) is a copper dependent-enzyme (26) and depend upon its copper moiety for

reduction-oxidation changes (45), the action of penicillamine might be related to its copper chelating effect.

Whatever the mechanisms underlying the observations reported here, the previous findings link copper with angiogenesis. Clearly much remains to be done to further elucidate and delineate the roles played by copper and copper depletion in angiogenesis and tumor growth.

Les précédentes experimentations révélent et démontrent clairement qu'une diète pauvre en cuivre et une chélation par la D-penicillamine (DCTP), resultant en une dépletion cuprique chez les animaux, est en mesure de prévenir l'angiogenèse tumorale et du même coup la croissance tumorale. Chacune des deux composantes du protocole DCTP a separement un effet sur la croissance tumorale mais pas d'effet inhibiteur sur l'angiogenèse tumorale. Ensemble elles ont un effet net sur l'angiogenèse et la croissance tumorales.

Une importante question persiste: l'effet observé sur le carcinome VX2, est-il egalement retrouvé dans une autre tumeur cerebrale experimentale? Nous avons choisi le gliosarcome 9L qui constitue l'equivalent d'une tumeur primitive du système nerveux central à l'opposé du carcinome VX2 qui pourrait etre rapproché d'un modèle métastatique cérébral. Nous allons donc maintenant présenter les résultats obtenus chez des rats Fisher injectés avec des cellules malignes de la lignée cellulaire tumorale gliosarcomateuse 9L.

CHAPTER IV

Copper Depletion Prevents Tumor Growth and Invasiveness of the 9L Gliosarcoma

Abstract

We implanted the 9L gliosarcoma in 86 Fisher rats. In the first experiment we showed a significant decrease in tumor size achieved by the CDPT protocol. In the second experiment we observed at the ultrastructure level that the invasive growth of the 9L gliosarcoma was entirely blocked in rats depleted of copper. In animals made hypocupremic by diet and chelation with penicillamine, the brains contained tumors sharply demarcated from the adjacent neuropil. Electron microscopy revealed the absence of cytoplasmic extensions. In normocupremic animals we observed cytoplasmic extensions associated with a marked degree of peritumoral invasiveness.

To test the effect of copper depletion on another experimental tumor we repeated the above experiments using the 9L rat glioma. The need for the use of a 9L glioma line was obvious for many reasons: 1) to know if the effect observed with the carcinoma line would be again observed with the glioma line indicating that angiogenic inhibition achieved by copper depletion is independent of the tumor histiotype, 2) in the hierarchy of malignant histiotypes, gliomas are among the most vascular (1) and potent source of endothelial growth factors (2); 3) the capillary systems of the 9L gliosarcoma is similar to that of human tumors (3).

Materials and Methods

First Experiment

Cells of the 9L glioma, originally induced by N-nitrosomethylurea (4) were stored in liquid nitrogen, and passaged twice before implantation. The cells were cultured in 2ml of incubation medium (MEM Alpha Medium, enriched with 10% fetal calf serum, supplemented with 10ug/ml gentamycin), kept in a humidified incubator at 30 C, and the medium replaced twice a week. Confluent cultures were split at a ratio of 1:500, subconfluent cells harvested, and the medium removed. The cells were washed with phosphate buffer solution (PBS), trypsinized, and detached from the dish. The trypsin was inactivated by re-exposure to the medium. After centrifugation at 1000 rpm for ten minutes, the pellet was resuspended in PBS to a concentration of 10^7 cells per ml. The cells were implanted into 70 adult, 240-255gm, male, Fisher 344 rats.

After anesthesia was induced (intraperitoneal pentobarbital, 3.25mg/100gm) with the cranium secured in a stereotaxic frame, we made a 2cm incision along the midline of the scalp over the vertex of the skull, and a 1.3mm hole drilled, 3mm to the right of the saggital suture and 6mm anterior to the frontal zero plane. (5)

With a 26-gauge Hamilton syringe, 10 µl, $1x10^5$ cells, were injected slowly, 1.5mm into the fronto-parietal lobe. The opening in the skull was sealed with bone wax, to prevent reflux of cells, the edges of the scalp were closed with surgical staples. We divided these 70 rats into 7 groups of 10 animals each. 1) Control; rats fed a standard diet (Ralston Purina #5001) ad libitum 2) acute CDPT; rats under a normal standard diet up until tumor implantation and then receiving a low copper diet (Ralston Purina #5890) and D-Penicillamine injected daily, subcutaneously, 1mg/gm, mixed in 3 ml of saline, started after the implantation. Penicillamine was prepared fresh, passed through a 0.2 u millipore filter. 3) Pair-fed; rats receiving the same standard diet but in a restricted way in order to match the weight of the copper depleted animals and rule out the effect of caloric nutrition on tumor growth (6) 4) Steroids; dexamethasone 0.75mg/kg/day injected intramuscularly (IM) from day of tumor implantation up until sacrifice and under a normal standard diet. 5) Penicillamine; started after tumor implantation in the same dosage as group 2, up until sacrifice. 6) Chronic CDPT; low copper diet for six weeks before the implantation and up until sacrifice and penicillamine for six days before and after tumor implantation in the same manner as group 2 and 5. 7) Chronic

CDPT ± Steroids; Diet and Penicillamine regimen identicaql to group 6 and dexamethazone 0.75 mg/kg/day IM, started on day 14 after tumor implantation. When the animal presented neurological deterioration the animal was sacrificed with an overdose of pentobarbital, the skull removed, and the brain placed in phosphate buffered saline for 10 days. The brain was then cut coronally with slices of 1.5mm thickness and embedded in paraffin. In each group 2 animals were injected with 2% Evans blue in the femoral vein one hour before sacrifice. 8) Ten additional sham rats fed a low copper diet and receiving D-Penicillamine in the same manner as group 6 were injected with $1x10^5$ heat-killed cells contained in 10 μl.

Second Experiment

We operated on 16 Fisher rats and implanted tumor cells as previously described. The animals were divided in two groups 1) Control and 2) CDPT animals. Each group was subdivided into 2 subgroups, 4 animals were sacrificed on day 10 and on day 15 after tumor implantation.

At time of sacrifice after pentobarbital anesthesia, each rat underwent a craniectomy. The tumor with the surrounding brain was removed en bloc, yielding a 2x5x8mm cylinder which was recut to 1mm cubes, immersed for one hour in 3% glutaraldehyde in 0.1M cacodylate buffer. The tissues were post-fixed in 1% osmium tetroxide, dehydrated, and embedded in Epon. Thin sections were stained with uranyl acetate and lead citrate and examined with a Phillips 301 transmission electron microscope (EM).

In both experiments at the start, the implantation and sacrifice we took 1 ml of venous blood from the tail, measured the serum level of copper with a Perkins-Elmer 403 atomic absorption spectrophotometer (7) avoiding contamination (8). Statistical analysis was performed by analysis of variance and Tukey Test (9) a p value less than 0.05 was the chosen level for significance.

Results

First Experiment

The results are summarized in Table 1. Neurological deterioration was similar to that presented by rabbits.

Group 1-4 were normocupremic throughout the experiment. (Table 2) Group 5 was normocupremic at time of tumor implantation but became hypocupremic at time of sacrifice. Group 6 and 7 were hypocupremic at time of surgery and at the time of sacrifice as well.

Survival time (Table 1, Figures 1 and 2)

Group 4 (dexamethasone) and group 7 (CDPT + dexamethasone) had a significantly longer survival time ($p<0.01$)

Cortical Surface

The tumor was apparent on the cortical surface in all the rats in groups 1,2,3,5 (Figure 3) and was seen in 1, 3 and 2 animals in group 4,6 and 7 respectively. Evans blue studies (Figures 4 and 5) and coronal sections (Figures 6 and 7) revealed marked differences between NC and HC animals.

Tumor volume (Figure 8)

Chronic CDPT group was significantly different from control, acute CDPT and pair-fed groups ($p<0.01$) and from penicillamine group

TABLE 1: Copper Depletion Prevents the Groowth of the 9L Gliosarcoma

Experimental Group	N	Diet	Penicillamine (mg/day)	Survival _Days ($\bar{X} \pm SD$)	Tumor Size _Volume ($\bar{X} \pm SD, mm^3$)
1) Control	9	Normal	0	13.7 ± 1.6	117.9 ± 56.8
2) CDPT, acute post-implantation	10	Normal, then low copper	1mg/1gm	14.7 ± 2.2	118.1 ± 49.0
3) Pair-fed	8	Restricted	0	14.8 ± 1.7	114.2 ± 41.9
4) Dexamethasone .75mg/kg/day	10	Normal	0	27.1 ± 2.0	3.0 ± 2.4
5) Penicillamine	10	Normal	1mg/1gm	17.4 ± 2.6	98.3 ± 42.0
6) CDPT, chronic	10	Low copper	1mg/1gm	17.6 ± 2.6	41.1 ± 20.1
7) CDPT, chronic Dexamethasone .75mg/kg/day	10	Low copper	1mg/1gm	24.8 ± 5.5	10.7 ± 7.9

TABLE 2: Serum Copper Levels ($\bar{X} \pm SD$, μg/dl)

Group	Intial	Implantation	Death
1) Control	105.8 ± 20.1	127.9 ± 30.0	110.8 ± 32.4
2) Acute CDPT	107.5 ± 16.3	113.8 ± 20.9	20.4 ± 7.5
3) Pair-fed	121.3 ± 26.6	123.4 ± 14.6	108.6 ± 30.5
4) Dexamethasone	126.4 ± 27.4	123.6 ± 28.0	136.0 ± 34.8
5) Penicillamine	90.4 ± 24.1	108.9 ± 20.2	10.9 ± 2.8
6) Chronic CDPT	96.3 ± 26.1	29.6 ± 6.3	9.9 ± 3.6
7) Chronic CDPT + dexamthasone	116.0 ± 30.1	29.9 ± 4.7	17.2 ± 9.1

Figure 1 Survival time of the different group of rats. Chronic CDPT coupled to dexamethasone and dexamethasone alone significantly increased the survival time

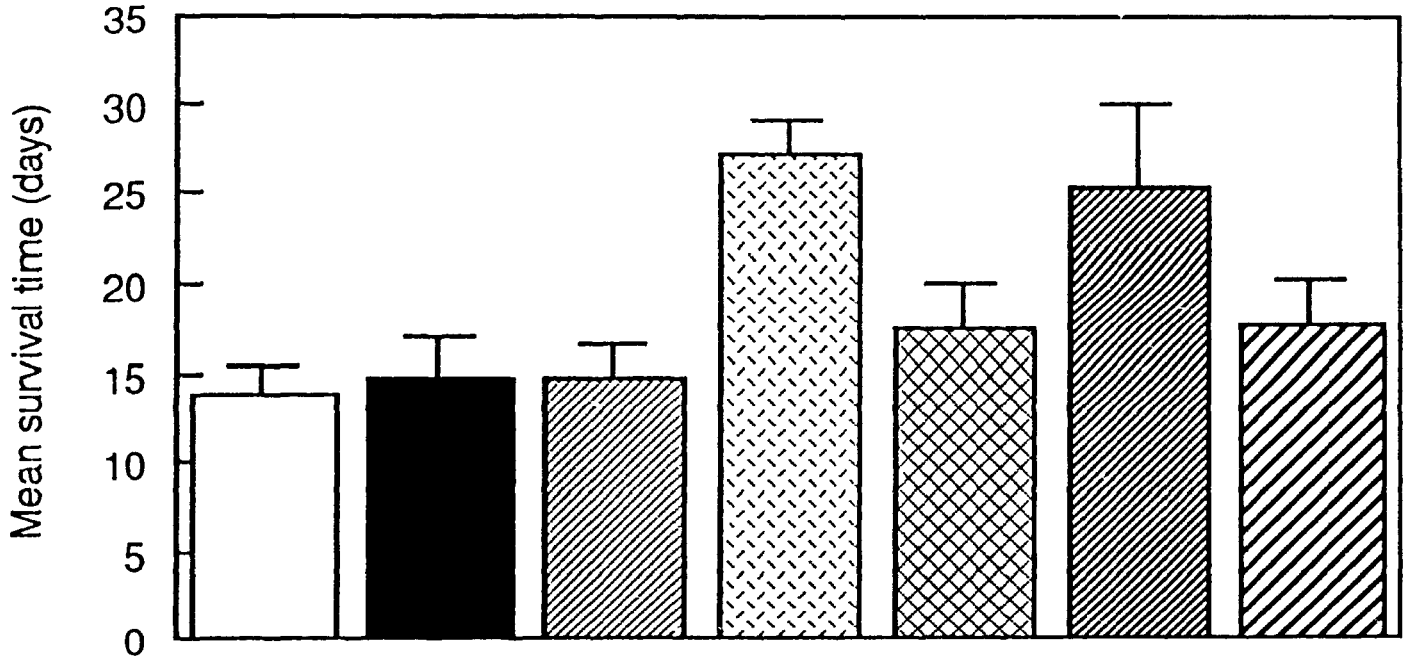

Control

Acute copper depletion

Pair fed

Steroids after cell implantation

Penicillamine after cell implantation

Chronic copper depletion + steroids starting 14 days after implantation

Chronic copper depletion

Figure 2 Survival curves: Chronic CDPT with dexamethasone started 14 days after tumor implantation (-▲-) and dexamethasone started day of surgery (-□-) result in longer survival time. Sham animals (-▲-) live up until sacrifice four months after the beginning of the experiment

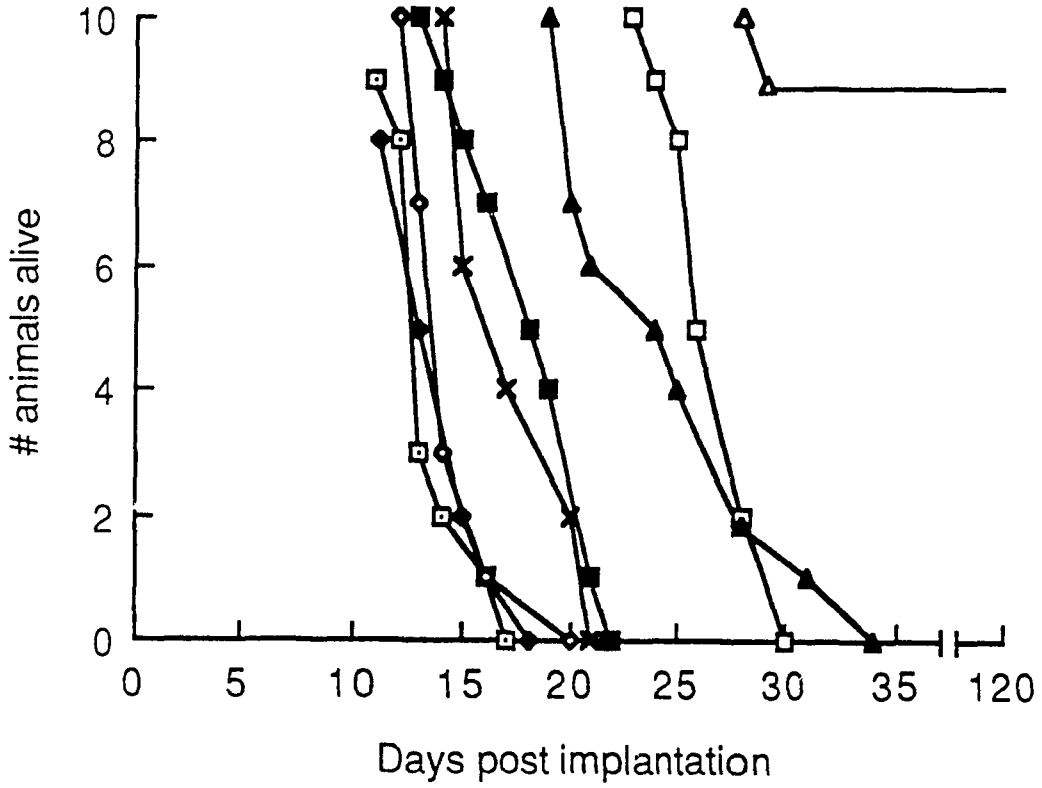

- Control
- Acute copper depletion
- Pair fed
- Steroids after cell implantation
- Penicillamine after cell implantation
- Chronic copper depletion + steroids starting 14 days after implantation
- Chronic copper depletion
- Chronic copper depletion SHAM surgery

Figure 3 In a NC rat the tumor was seen at the level of the cortical surface. The tumor has a large exophytic component. Note the neovascularization (arrows)

Figure 4 In NC rat the Evans blue extravasation is localized to the tumor area

Figure 5 In HC rat the Evans blue extravasation is diffuse, localized in and around the tumor

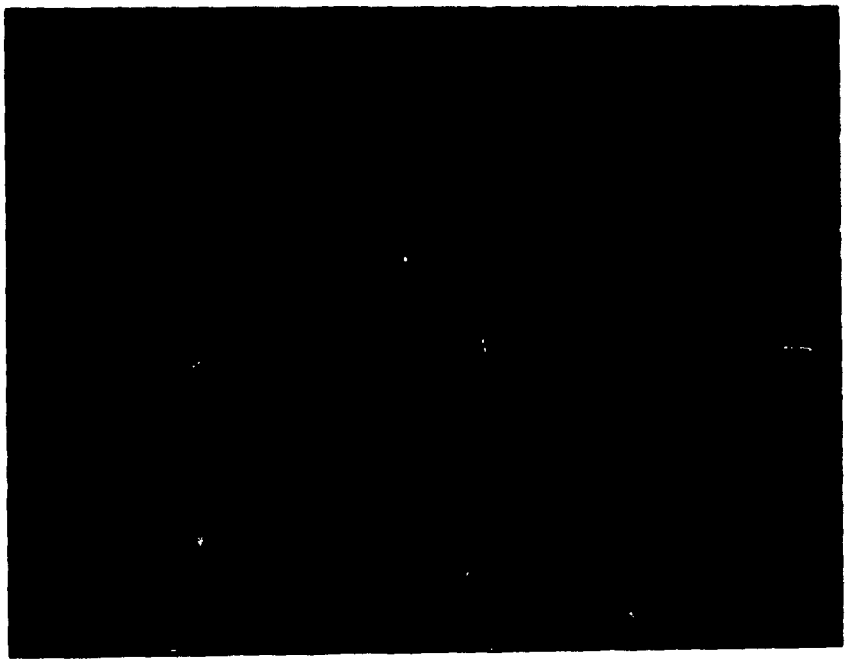

Figure 6 On coronal section the Evans blue extravasation is localized to the tumor area in a NC rat. Note the exophytic growth of the tumor

Figure 7 On coronal section the Evans blue extravasation is found in and around the tumor in a HC rat

Figure 8 Tumor volumes: Chronic CDPT decreases tumor size of the 9L gliosarcoma ($p<0.05$). Dexamethasone and chronic CDPT coupled with dexamethasone started 14 days after tumor implantation have a marked effect on tumor size ($p<0.01$) as compared to control

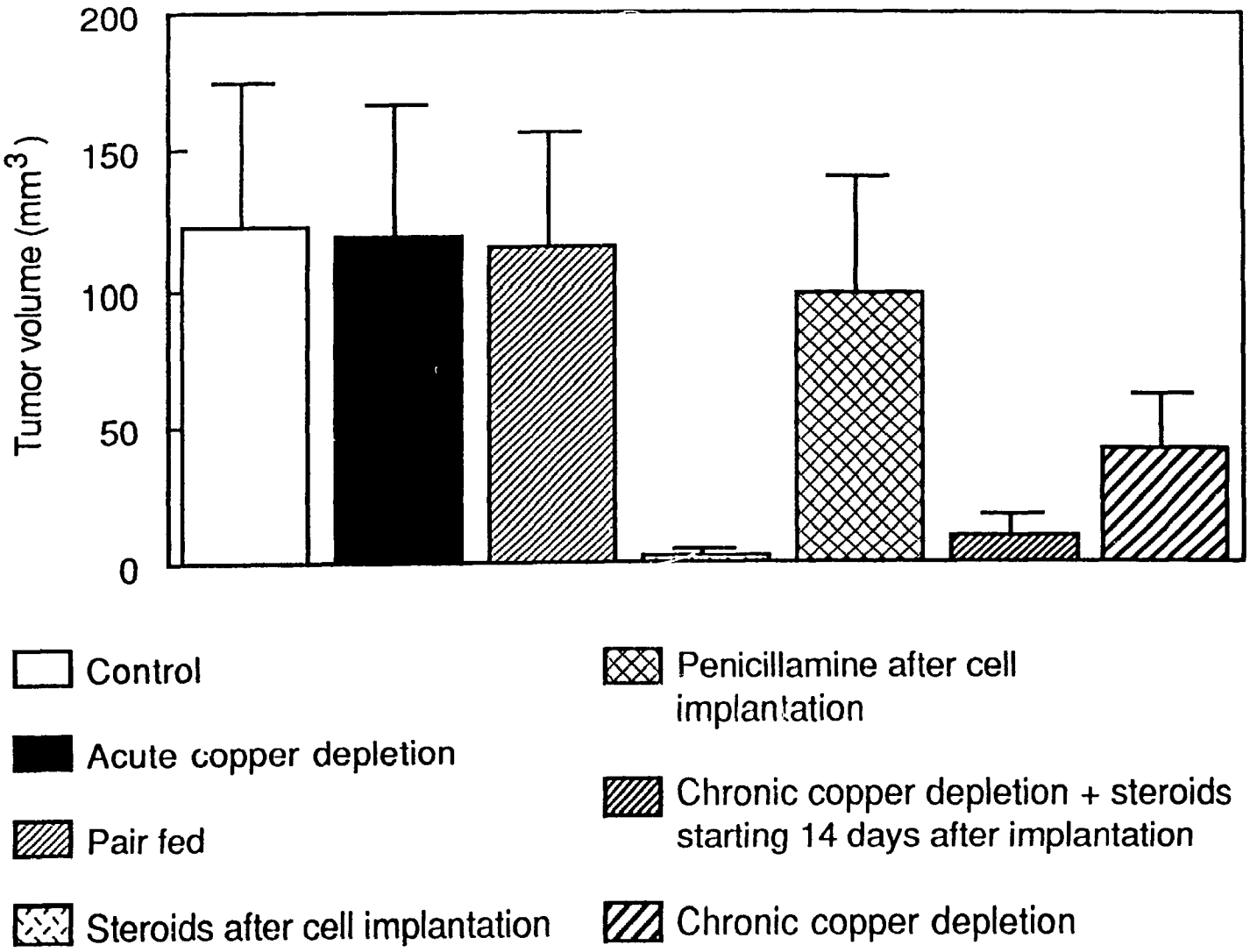
200
150
100
50
0
Tumor volume (mm3)
Control
Acute copper depletion
Pair fed
Steroids after cell implantation
Penicillamine after cell implantation
Chronic copper depletion + steroids starting 14 days after implantation
Chronic copper depletion

($p<0.05$). Steroids and chronic CDPT groups were different from groups 1,2,3,5 ($p<0.01$).

Histology

By means of light microscopy we were unable to establish capillary density because of the tremendous amount of vascular lumens observed in all groups. An obvious difference was observed at the boundaries of the tumors between group 6 and 7 and groups 1,2,3 and 5. In these NC groups there was a clear infiltration by the tumor of the surrounding tissue (Figure 9) By contrast in groups 6 and 7 the border was well demarcated without infiltration (Figure 10).

Second Experiment

Serum copper levels are presented in Table 3.

The ultrastructure of the neoplastic cells was similar in both the NC and CDPT groups. Tumor cells contained large, irregular nuclei with clumps of chromatin apposed to the inner nuclear membranes; bizarre mitotic figures were abundant. The cytoplasm was electron dense due to highly developed rough endoplasmic reticulum and numerous free ribosomes. The mitochondria appeared normal; the Golgi apparatus was poorly developed. Intermediate filaments were rare. Numerous slender interdigitating cell processes or pseudopods were noted, occasionally displaying gap junctions. The extracellular space was enlarged with scanty fine granular material.

There were striking differences, however, between the two groups at the boundary between the tumor and the neuropil. In the NC group, the border was ill-defined. Neoplastic cells penetrated the neuropil

Figure 9 Light microscopy of the 9L gliosarcoma implanted in a NC Fisher rat: There is a marked degree of peritumoral invasiveness. (H & E, X450)

Figure 10 Light microscopy of the 9L gliosarcoma implanted in a hypocupremic Fisher rat: The tumor edge reveals the absence of infiltration in the surrounding neuropil (H & E, X450)

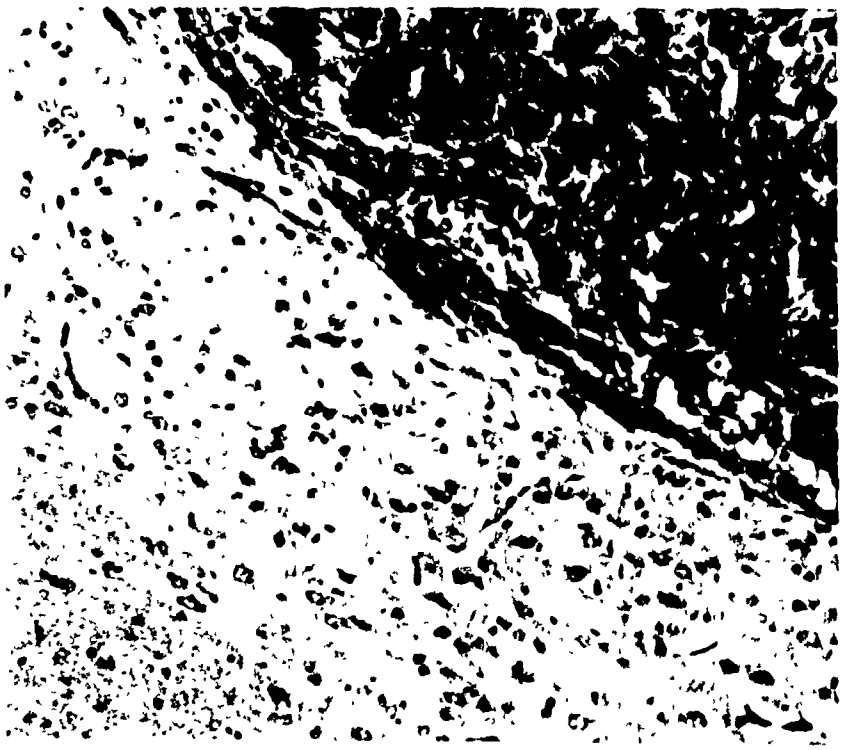

TABLE 3: Serum Copper Levels in Control and Treated Rats (ug/dl)

Stage	Day	N	Control	CDPT
Start	0	8	116.3 ± 14.6	143.8 ± 13.6
Cell Implantation	42	8	119.3 ± 11.2	23.5 ± 15.3
Ten-Day-Old Tumor	53	4	156.0 ± 14.3	6.0 ± 5.3
Fifteen Day-Old Tumor	58	4	167.8 ± 2.1	17.0 ± 3.6

(Figures 11 and 12), infiltrated the matrix between astrocytic feet, axons, glial cell bodies, neurons, and capillaries. By contrast, in the CDPT group, all eight tumors were arranged as tiny nodules, sharply demarcated from the adjacent neuropil. At the tumor edge, there were no cytoplasmic extensions of neoplastic cells, a score of zero by an "invasion index" (14), i.e. there was no invasion into the neuropil (Figure 13).

In both treated and control groups, the capillaries appeared normal, free of injury. Each brain showed peritumoral edema, characterized by enlargement of the astrocytic feet contiguous to the basement membrane of the small blood vessels. The neuropil further than 2 mm from the tumor edge, however, appeared normal. Although the tumors were larger on day 15 than on day 10, there were no differences in ultrastructure.

Discussion

In the first experiment we found a statistical significant decrease in tumor size in CDPT, Dexamethasone and CDPT plus dexamethasone groups. Steroids have a well known effect of glial growth (10). We observed a striking difference at the tumor edge between HC and NC groups. The EM experiment confirmed this difference at the level of the ultrastructure of NC and HC tumors. The use of the 9L gliosarcoma for the study of copper depletion and penicillamine on tumor invasiveness presented a clear challenge: 1) invasiveness is a key feature of malignant glial cells (12) and persists even after transplantation to non-neural tissue (13); 2) Sarcomas are highly invasive (14); 3) Among

Figure 11 Transmission electron micrographs of the tumor edge in normocupremic rats, ten days after implantation. The tumor cell (T) is apposed to the external surface of the basement membrane of a small blood vessel (L-lumen) and sends pseudopods (arrows) between an astrocytic process (A) of the neuropil (N) (x 9000)

Figure 12 The tumor cell (T) embraces a normal blood vessel (L). At the lower left corner, the cytoplasmic extension of the tumor cell entrapping an astrocytic process (A) - an example of invasiveness into the neuropil observed in NC tumor (x13,000)


L
P

Figure 13 In CDPT rats, 15 days after implantation, there is a distinct, well-defined border between the tumor cells (T) and the neuropil (N) (x 17,000)

various experimental brain tumors the 9L gliosarcoma was found to be the most invasive (15).

The absence of invasion in the hypocupremic animals might be explained by the possible interferences of copper depletion and penicillamine with one or more of the three steps required for neoplastic invasion (16).

1) Adhesion of the tumor cell to extracellular matrix (ECM) proteins 2) Enzymatic degradation of the matrix 3) Locomotion of the tumor cells.

Adhesive proteins particularly fibronectin and collagen are abundant in the ECM of malignant glial and non-neural tumors (17). Fibronectin modulates cell locomotion (18), controls extravasation of malignant cells (19) and stimulates the adhesion and spread of carcinoma and sarcoma cells in the extracellular matrix (20). Low copper levels block the synthesis of fibronectin (21) Low levels of copper (22) and Penicillamine (23) induce defective collagen that interferes with attachment of invasive cells (24). The tripeptide GHL, a copper carrier induces adhesion of malignant cells (3) adhesion being a key step for cell locomotion (25).

The previous preliminary findings link the activity of copper with tumor invasiveness, further experiments need to be done to determine the exact role of copper in the invasive growth of malignant tumors.

Les précédentes experimentations conduites chez le rat Fisher avec le gliosarcome 9L, nous ont fait découvrir un autre effet potentiel de la dépletion cuprique sur la biologie tumorale: l'inhibition de l'invasion tumorale. Le volume tumoral des animaux DCTP s'est révéle être significativement plus petit que les animaux controles. Les resultats fournis par la microscopie électronique démontrent clairement l'absence d'invasion tumorale chez les animaux DCTP. Ces résultats sont particulierement significatifs quand on connait le potentiel invasif du gliosarcome 9L avec ses composantes gliale et sarcomateuse.

La similitude des courbes de survie observée chez les animaux normocupremiques et hypocupremiques et les résultats obtenus après injection intraveineuse de bleu d'Evans chez le lapin et le rat nous ont fait soupçonner l'existence d'un édeme peritumoral severe, responsable de la mort des animaux hypocupremiques. Pour tester cette hypothèse nous avons etudié le contenu d'eau present autour des tumeurs cérébrales (carcinome VX2 and gliosarcome 9L). De plus nous avons mesuré le contenu hydrique du parenchyme cérébral chez des animaux normo et hypocupremiques non-porteurs de tumeur cérébrale et nous avons essayé de determiner si la dépletion cuprique avait un role dans la genese de l'édeme cérébral défini comme etant une augmentation du contenu cérébral en eau.

CHAPTER V

Copper Depletion Increases the Peritumoral Brain Edema

Abstract

We measured brain water content in rats and rabbits that had been implanted with viable tumor cells and brain water content of animals that had not been implanted. These experiments had been conducted in normocupremic and hypocupremic rats and rabbits.

We demonstrate that copper depletion, achieved by a low copper diet and penicillamine, increases the cerebral peritumoral water content but fails to increase the brain water content in non-tumor-implanted animals. These findings support the hypothesis that the hypocupremic animals with small tumors had a survival time similar to that of normocupremic animals with large vascularized tumors, because of a severe peritumoral edema leading to brainstem distortion, brain herniation and death.

The endothelial cells of cerebral capillaries compared to those outside the central nervous system are characterized by 1) tight junctions (zona occludens) 2) an increased number of mitochondria 3) sparse pinocytosis 4) lack of fenestrations and 5) the apposition of astrocytic foot processes to the endothelial basement membrane. These properties are responsible for the formation of the blood-brain barrier (BBB) (1-4).

In both the VX2 carcinoma and 9L glioma intracerebral tumor growth we observed in the HC animals the presence of a severe swelling mainly of the right hemisphere where the tumors were located. In order to further elucidate the mechanisms underlying the development of this peritumoral swelling, we measured brain water content (BWC) in the brain of normocupremic and hypocupremic animals, implanted and non implanted with tumor cells.

Materials and Methods

We implanted 10 Fisher rats with the same technique previously described (Chapter IV). These animals were divided in 2 groups of 5 animals each. 1) Control 2) CDPT rats. Ten additional non-tumor-implanted rats were divided in 2 groups. 3) Control brain without tumor implantation. 4) Chronic CDPT rats without tumor implantation. Twenty NZW rabbits were assigned to the same four groups.

One method of measuring water content is to determine the weight of fresh and subsequently dried tissue specimens and express the amount of water as the difference between fresh and dry weight (wt), or:

$$\% \text{ tissue water} = \frac{\text{tissue fresh wt} - \text{tissue dry wt}}{\text{tissue fresh wt}} \times 100(5)$$

To insure accuracy we dried the tissue for 96 hours since tissue drying time may extend beyond 24 hours (6)

The tumor implanted animals were sacrificed when they developed neurological signs. The non tumor implanted animals were sacrificed 8 weeks after the beginning of the experiment. At time of sacrifice a cube of (4x4x4mm in the rats and 6x6x6mm in the rabbits) of the immediate BAT was removed and weighed with an analytical balance (type H16, E Mettler, Zurich, Switzerland). They were then placed in a dessicator (Pyrex, Corning 3118 Fisher Scientific, Montreal, Quebec). The samples were weighed again after 96 hours of dessication.

Results

Serum copper levels are presented in Tables 1 and 2

In the tumor implanted animals we found a greater BWC in the CDPT group ($p < 0.05$) (Figures 1 and 3). In the non implanted animals there was no difference in the BWC (Figure 2 and 4).

Discussion

Brain edema is defined as an increase in cerebral tissue water content leading to an enlargement of tissue mass and volume (7) Our findings demonstrate that CDPT increases the peritumoral BWC of the 9L gliosarcoma and the VX2 carcinoma, but fails to increase BWC of CDPT non-tumor-implanted brains.

What are the possible explanations of the increased brain water content around CDPT tumors as compared to control tumors.

TABLE 1: A - Serum Copper Levels in Tumor-Implanted Rats

Group	Start	Day of Surgery	Sacrifice
Control	131 ± 6.5	126.3 ± 16.2	132 ± 16
CDPT	131.6 ± 21.6	20.0 ± 7.9	6.6 ± 1.5

B - Serum Copper Levels in Non-Tumor-Implanted Rats

Group	Start	Sacrifice
Control	136.7 ± 29.4	142.2 ± 19.67
CDPT	129.8 ± 8.7	38.2 ± 4.65

TABLE 2: A - Serum Copper Levels in Tumor-Implanted Rabbits

Group	Start	Day of Surgery	Sacrifice
Control	69 ± 24.5	74 ± 7.6	68 ± 12.3
CDPT	71 ± 17.3	20.3 ± 4.2	22 ± 5.9

B - Serum Copper Levels in Non-Tumor-Implanted Rabbits

	Start	Sacrifice
Control	72 ± 16.2	69 ± 17.4
CDPT	81 ± 27.3	21.5 ± 7.9

Figure 1 In Fisher rats implanted with 9L gliosarcoma the peritumoral water content was increased in chronic CDPT animals as compared to control ($p < 0.01$)

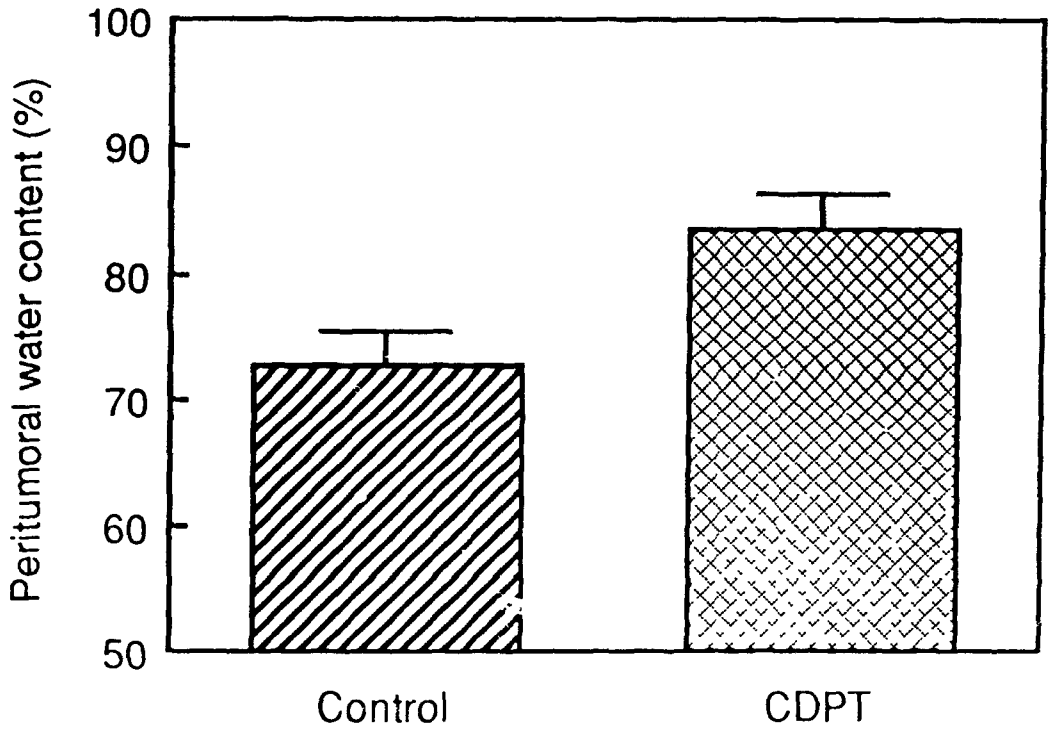
Peritumoral water content (%)
100
90
80
70
60
50
Control
CDPT

Figure 2: There is no difference in the brain water content in control and chronic CDPT Fischer rats that have not been implanted with tumor cells

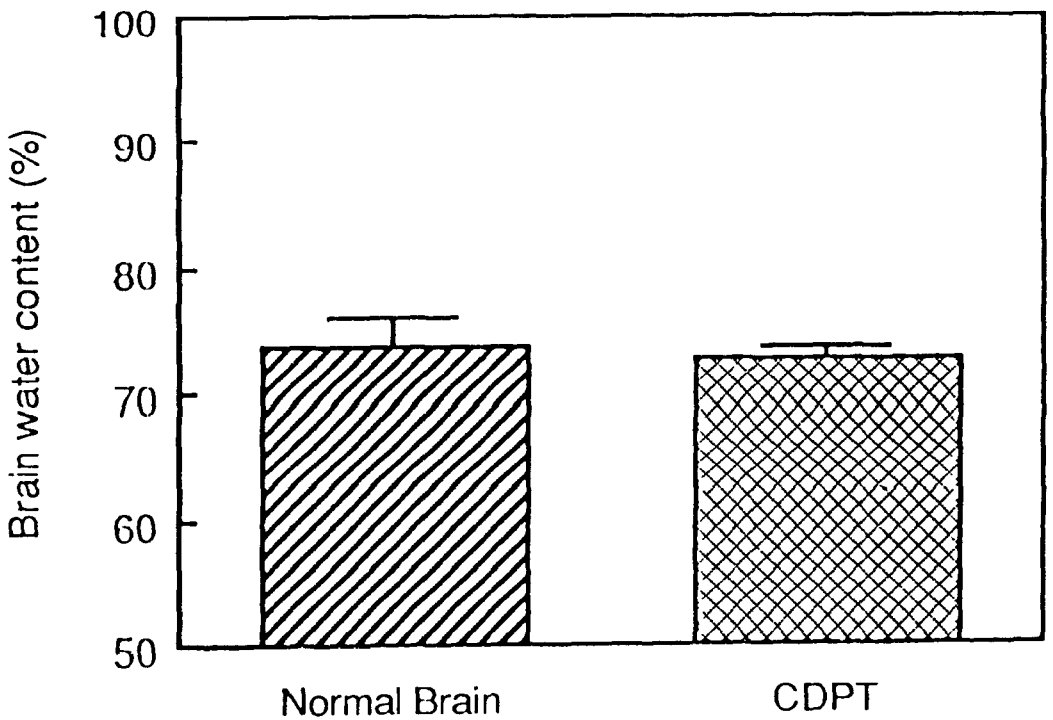
100
90
80
70
60
50
Brain water content (%)
Normal Brain
CDPT

Figure 3 In NZW rabbits implanted with the VX2 carcinoma the peritumoral water content was increased in chronic CDPT animals as compared to control ($p<0.01$)

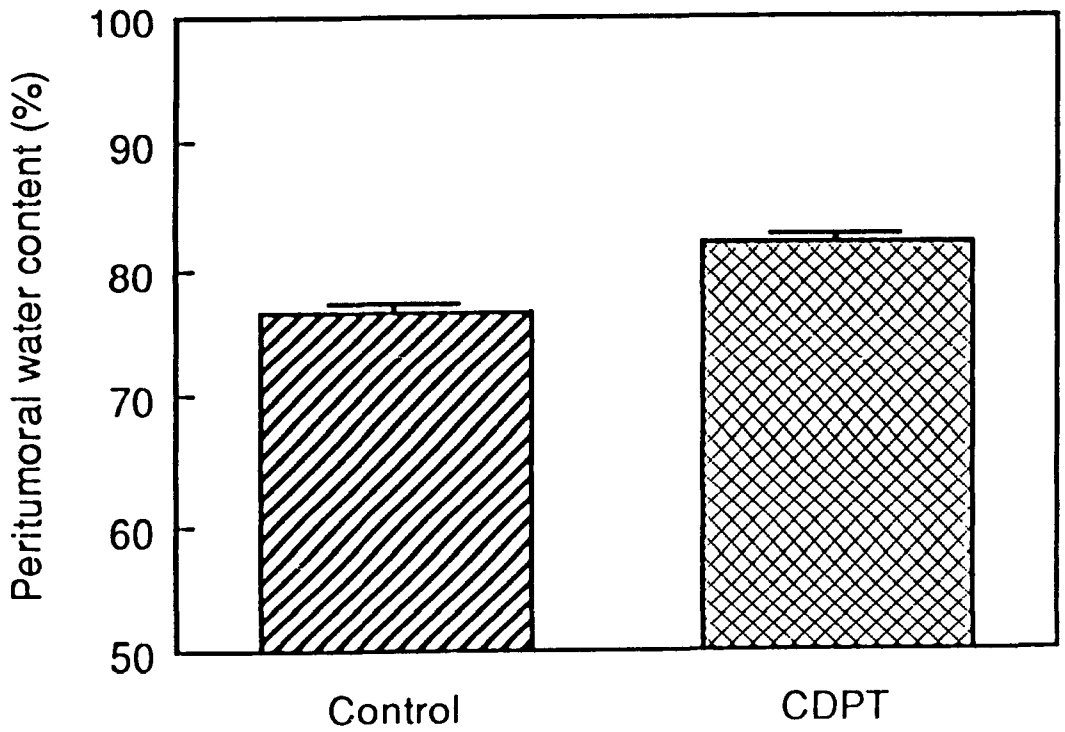
Peritumoral water content (%)
100
90
80
70
60
50
Control
CDPT

Figure 4 There is no difference in the brain water content in control and chronic CDPT rabbits that have not been implanted with tumor cells

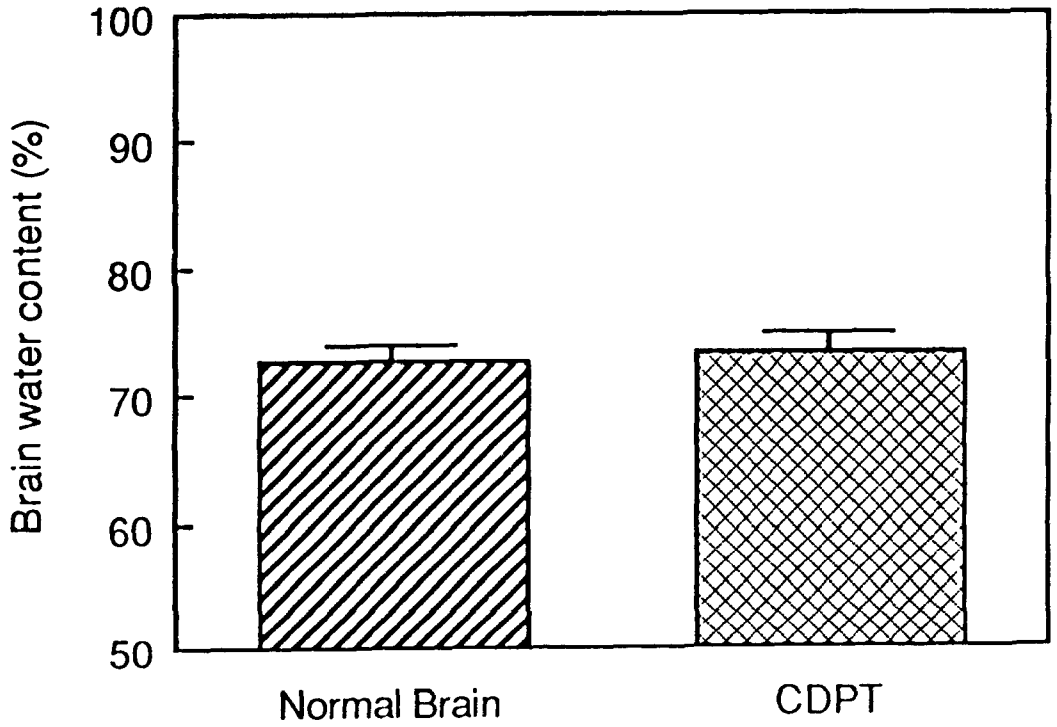
100
90
80
70
60
50
Brain water content (%)
Normal Brain
CDPT

1) It was recently demonstrated that cranial irradiation resulting in a suppression of macrophage-mediated angiogenesis induced a higher water content around a cold lesion as compared to control without irradiation (8). Neovascularization might have a role in reabsorption of extravascular fluid ("sink theory").

2) Superoxide dismutase (SOD) scavenges oxygen-derived free radicals (9). SOD catalyses the decomposition of the superoxide anion as follows: $2H^+ + 2O_2^- \rightarrow H^2O^2 + 0^2$. SOD is a key enzymatic (Figure 5) free-radical-scavenging system in the brain (10). In Eukaryotes this reaction is catalyzed by a copper-zinc protein which is present both in the cytosol and in the mitochondrial intermembranous space and also by a manganese enzyme which is found in the mitochondrial matrix (9,11,12). Oxygen-derived free radicals cause cerebral edema (13). Copper depletion results in a decrease of the SOD activity (14) with a rise of the oxygen-derived free radicals able to induce cerebral edema (13). It is concievable that in our experiment the severe copper depletion led to an increase peritumoral edema via this mechanism.

3) Horseradish peroxidase injections in the lateral cerebral ventricles or in the subarachnoid space of cats revealed that a fluid circulation through the central nervous system occur via paravascular pathways (15). Because of the lack of vascular proliferation observed in the hypocupremic tumors, the paravascular fluid circulation might be decreased as compared to hypervascular normocupremic tumors leading to an increased cerebral edema.

Capillary permeability in the brain adjacent to tumors (9L gliosarcoma and Walker 256 carcinosarcoma) is reduced (16). This

Figure 5 Superoxide dismutase is an important free-radical-scavenging system in the brain, from (9)

1. Enzymatic systems

$$O_2 \cdot^- \xrightarrow{\text{Superoxide dismutase}} O_2 + H_2O_2$$

$$H_2O_2 \xrightarrow[\text{Glutathione peroxidase (other peroxidases)}]{\text{Catalase}} H_2O + O_2$$

2. Nonenzymatic systems

Vitamin E (tocopherol)
Vitamin C (ascorbate)
Glutathione
Selenium
β-Carotene

Enzymatic and nonenzymatic free-radical-scavenging systems in brain. $O_2 \cdot^-$, superoxide radical; H_2O_2, hydrogen peroxide.

reduction could be detrimental to the delivery of water-soluble and rapidly binding drugs (16). BBB modification increases therapeutic efficacy of chemotherapy for brain tumors (17). CDPT interferes with the capillary permeability around brain tumors that could possibly lead to more effective chemotherapy.

The exact mechanisms by which copper depletion increased peritumoral edema are not known, these findings, however, will spur onward new interests in understanding the relationship between copper depletion, breakdown of the BBB and peritumoral cerebral edema.

Après avoir démontré l'existence d'une augmentation du contenu en eau autour des tumeurs chez les animaux CDPT nous avons entrepris l'étude du problème de l'apparition du renforcement de contraste au cours des examens tomodensitometriques. En effet il existe dans la littérature neuroradiologique un débat à ce sujet. Certains affirment que le renforcement de contraste est principalement dû à la rupture de la barrière hemato-encephalique (BHE) alors que d'autres prônent que la néovascularisation tumorale est le principal élément déterminant le renforcement de contraste.

L'existence d'une rupture de la BHE dans les tumeurs hypervasculaires (normocupremiques) et les tumeurs avasculaires (hypocupremiques) nous a permis d'étudier les mechanismes liés à l'apparition du renforcement de contraste au cours des examens tomodensitometriques.

CHAPTER VI

Angiogenesis and Breakdown of the Blood-Brain Barrier Modulate Computerized Tomography Contrast Enhancement of a Rabbit brain tumor

Abstract

Because of the crucial role played by tumor neovascularization in contrast enhancement, we studied the CT imaging of a transplantable rabbit brain tumor, the VX2 carcinoma that induces angiogenesis and breakdown of blood-brain barrier associated with contrast enhancement. Tumor detection by contrast enhancement follows the peak of angiogenesis. Inhibition of angiogenesis, by copper depletion and penicillamine, leads to avascular tumors that lack contrast enhancement. Furthermore, there was no contrast enhancement in brain adjacent to the tumor of normocupremic rabbits or within the hypocupremic tumor, despite the breakdown of the blood-brain barrier, without the concomitant presence of angiogenesis. We conclude that contrast enhancement of intracranial tumor is dependent primarily upon the proliferation of the microvasculature.

Contrast enhancement (CE) is one of the main radiological manifestations of central nervous system tumors; it is not observed, however, in all tumors (1). The mechanisms that cause the CE of brain tumors are not entirely known but remain important to the interpretation of CT scans. These mechanisms relate to breakdown of the blood-brain barrier (BBB) (2-5) and to tumor neovascularization i.e. angiogenesis (6-12).

The rabbit VX2 carcinoma, has been useful for radiological research (13-15). It allowed us to study tumor angiogenesis and breakdown of the BBB (Chapter II). We compare the serial CT images, extravasation of Evans blue (EBE), and histology of normocupremic (NC) and hypocupremic (HC) tumors.

Materials and Methods

We implanted 5 x 10^5 cells of the VX2 carcinoma into the right parietal lobe of 36, 3kg, male New Zealand White rabbits, according to the technique previously described in Chapter II. We divided the rabbits into six groups of six animals each: four for CT imaging, and two for study of the BBB. Tumor size and histology were determined in each of the six animals. Groups 1,2,3,4,5: Control animals and group 6: CDPT animals. CT studies were performed on an Elscint Exel 2002, with the following settings: circle diameter, 140mm; x-ray current, 40mA; voltage, 140KV; scan time, 10.5 sec; slice width, 3mm; and an image matrix, 340/340. The brains of the rabbits were imaged in the coronal and axial planes before and after intravenous administration of 3ml/kg of iothalamate meglumine (Conray 60, Mallinckrodt Laboratories, Ontario Canada).

Group 1 was scanned six days post-implantation, and immediately sacrificed. Groups 2-5 were likewise studied on days 10, 14, 18, 22, respectively. In group 6, a CT scan was performed only when the animals developed neurological deterioration (gait disturbances, decreased level of consciousness). The brains were removed and fixed in 10% phosphate buffered formalin for six days. The specimens were sectioned coronally at 1.5mm intervals and correlated to the CT coronal scans.

Evans blue injections, measurement of tumor volumes, and determination of vascular density were performed as previously described in Chapter II.

Blood samples were taken in all the animals at the beginning of the experiment, at time of surgery, and at time of sacrifice for serum copper determinations (16).

Statistical analysis was perfomed by analysis of variance and Tukey test, a $p < .05$ was considered significant (17).

Results

1) Serum copper levels are shown in Table 1. Groups 1 to 5 were NC throughout the experiment, whereas group 6 was HC at the time of the tumor cell implantation and sacrifice.

2) The mean survival time (MST) in group 6 was 19 + 1.8 days.

3) CT findings: In the NC animals, there was no tumor detection at any time without contrast infusion. Even with contrast infusion, there was still no visualization of the tumor on days 6 and 10.

Starting at day 14 the tumor first showed a dense round homogeneous well defined enhancement (Figure 1A,B). As the tumor enlarged, it became more oval (day 18: Figure 2A,B). Finally, on day 22, patchy

TABLE 1: Average Serum Copper Levels[a]

Group	Day of Sacrifice	No. of Rabbits	Start	Day of tumor implantation	Day of Sacrifice
1	6	6	73.3 ± 10.3	62.4 ± 9.9	62.07 ± 9.42
2	10	6	70.0 ± 10.2	61.1 ± 9.5	60.62 ± 8.93
3	14	6	57.0 ± 10.6	62.9 ± 8.2	59.2 ± 9.83
4	18	6	62.2 ± 11.5	64.6 ± 3.9	63.82 ± 15.20
5	22	5[b]	61.8 ± 8.8	61.3 ± 4.2	61.65 ± 9.28
6	19 ± 1.8	6	69.5 ± 12.8	11.9 ± 3.6	7.4 ± 4.43

[a]Data expressed in μg/dl

[b]Sixth animal excluded because of death prior to scheduled day of CT

Figure 1 Coronal (A) and axial (B) cuts on day 14. The tumor appears as an enhancing nodule of the right high convexity (arrowheads)


A


B

Figure 2 Coronal (A) and axial (B) cuts on day 18. The tumor appears as a large homogenous enhancing mass on the right


A


B

areas of decreased attentuation appeared within the center of the tumor (Figure 3A,B). The lesion itself remained very well defined at all times. A CT scan was not performed on one animal of group 5 due to death before day 22. The tumor was visualized with CT in all the other NC rabbits studied on day 14,18,22.

The CT in the HC animals appeared normal even after injection of contrast material. In both NC and HC groups we failed to observe peritumoral edema.

4) Histological findings:

In NC tumors, a slight capillary proliferation first appeared on day 6. The vascular density increased progressively until day 14 when neovascularization was prominent (Figure 4).

By day 22, large vascularized tumors accompanied by central necrosis were present in all NC rabbits . The cortical surface revealed many enlarged tortuous peritumoral vessels.

The tumors in the HC groups were tiny, pale, laminar plaques with 91% less volume compared to the controls ($p<0.01$). The cortical surface of HC rabbits showed a normal vascular pattern. Microscopically, the tumor cells retained malignant features and appeared viable, but the capillary density was close to that of a normal brain indicating that angiogenesis failed to occur.

5) Evans Blue Studies:

In NC animals (group 1-5) EBE appeared in the tumor area by day 6 and by day 14 around the tumor. By day 18, EBE was prominent (2+) in the tumor and brain adjacent to tumor (BAT) and finally by day 22 we observed a severe (3+) EBE in the tumor present at a lesser extent

Figure 3 Coronal (A) and axial (B) cuts on day 22. The tumor appears as an inhomogenous mass with areas of decreased attenuation in the center related to tumor necrosis. Note the ring enhancement (arrow)


A


B

Figure 4 Progression of vascular density in NC animals. CT tumor visualization correlates with peak tumoral angiogenesis

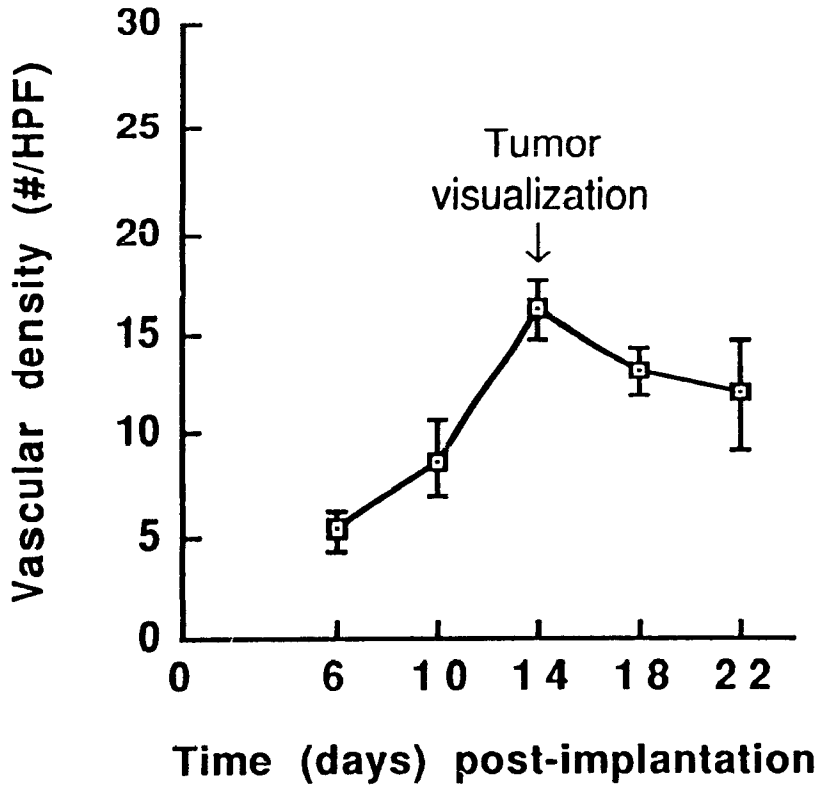
Vascular density (#/HPF)
30
25
20
15
10
5
0
Tumor
visualization
0
6
10
14
18
22
Time (days) post-implantation

around the tumor. The HC animals in group 6 revealed marked EBE both in and around the tumor.

In summary, (Table 2) in NC rabbits, tumor CE, allowing tumor detection was possible only when tumor angiogenesis was prominent by day 14. In the HC rabbits, even though the tumor volume at time of sacrifice was larger ($46.8 \pm 26.6mm^3$) than the tumor volume on day 14 ($13.2 \pm 2.2mm^3$) in NC rabbits, no tumor was visualized on CT, even after contrast material injection. EBE was observed at all stages on the NC tumors and on day 14 around them in HC tumors EBE was noted in and around the tumor.

In NC animals, necrosis was observed on CT on day 22 when it was grossly apparent. On day 18, we observed necrosis and punctate hemorrhages with light microscopy, but not by CT scanning.

Discussion

Currently, two interrelated mechanisms explain the CE of tumors on CT: 1) breakdown of the BBB with passage of iodine across the basement membrane of the capillary bed into the tumor (2-5); 2) Tumor neovascularization leading to increased intravascular levels of iodine (6-12) i.e. "computed angiotomography" (6) with positive correlation between CE and the degree of vascularity (7). Because of the newly discovered ability to pharmacologically suppress capillary growth induced by experimental brain tumors by means of copper depletion we could test the relative contribution of BBB breakdown compared with angiogenesis.

CE appeared on day 14 in NC tumors and failed to appear in larger HC tumors (Table 2) excluding size alone as a main determinant

TABLE 2: Tumor Vascularity, Size, Breakdown of the Blood-Brain Barrier and Contrast Enhancement

Group	Day of CT and Sacrifice	No. of Rabbits	Tumor Vascularity[a]	Tumor Size[b]	Breakdown of the BBB[c]		Contrast Enhancement[d]	
					Tumor	B.A.T.	Tumor	B.A.T.
Normocupremic								
1	6	6	5.2 ± 1.0	0.2 ± 0.04	+	0	No	No
2	10	6	8.7 ± 1.5	0.7 ± 0.2	+	0	No	No
3	14	6	16.5 ± 1.6	13.2 ± 2.2	++	+	Yes	No
4	18	6	13.7 ± 1.4	70.0 ± 17.5	++	++	Yes	No
5	22	5[e]	12.4 ± 1.5	513.5 ± 128.0	+++	++	Yes	No
Hypocupremic								
6	19.5 ± 1.8	6	4.2 ± 0.8	46.8 ± 26.6	+++	++	No	No

All data expressed represent mean ± standard deviation

[a]Number of microvessels per field (X200)

[b]Data expressed in mm^3

[c]Breakdown of the blood-brain barrier (BBB) detected by extravasation of Evans blue:0=none;+=slight;++=moderate;+++severe

[d]B.A.T. = Brain adjacent to tumor

[e]Sixth animal excluded from the study because of death due to tumor growth prior to scheduled day of CT

of CE. In the HC group, the EBE demonstrates the breakdown of BBB both within the tumor and the peritumoral area. CT scans of these HC animals, however, failed to reveal enhancement after iothalamate meglumine injection. In HC tumors, angiogenic inhibition likely prevented CE. On the other hand CE appears in NC malignant tumors that contain numerous new blood vessels.

The permeability of newly formed capillary sprouts compared to that of mature capillaries is increased (18). Normal capillaries of the brain maintain the integrity of the BBB (19) but the blood vessels of experimental (20) and human (21) brain tumors are structurally altered and have an increased capillary permeability. In these NC rabbits the combined effect of tumor angiogenesis and breakdown of the BBB is linked to the appearance of CE.

Evans blue binds to albumin and has a molecular weight (MW) of 68,500 Daltons (22) whereas the iothalamate meglumine that we have used has a MW of 800. Comparison of MW does not explain the passage of Evans blue across the open BBB whereas contrast material does not cross. To explain the paradox between the appearance of EBE and the absence of CE we suggest that active metabolic uptake of albumin-bound compounds is a function of intracerebral tumors (23) and that the appearance of iothalamate depends largely on other mechanisms, e.g. neovascularization.

We conclude from our data (Table 2-3) that in our brain tumor model, angiogenesis is the key determinant for the appearance of CE.

TABLE 3: Angiogenesis and Breakdown of the Blood-Brain Barrier cause Contrast Enhancement

Group	Angiogenesis	Breakdown of the Blood-Brain Barrier[1]	Contrast Enhancement
Normocupremic			
Tumor	+	+	+
B.A.T.[2]	-	+	-
Hypocupremic			
Tumor	-	+	-
B.A.T.[2]	-	+	-

[1] Breakdown of the Blood-brain barrier detected by Evans Blue extravasation

[2] B.A.T. = Brain adjacent to tumor

Nous avons donc demontré que dans notre modèle tumoral cérébral utilisant le carcinome VX2 chez le lapin, la néovascularisation tumorale était l'élément déterminant et principal dans l'apparition du renforcement de contraste au cours des examens tomodensitometriques.

Nous nous sommes ensuite posé la question à savoir si le même protocole DCTP utilisé dans les experimentations cérébrales avait un effet sur la croissance extracerebrale dans le muscle et sur le development des metastases pulmonaires du carcinome VX2.

CHAPTER VII

The Effects of Copper Depletion on Extracerebral Tumor Growth and Lung Metastases of the VX2 Carcinoma

Abstract

We observed that the same protocol CDPT that could inhibit tumor growth in the brain had no effect on the growth of the VX2 carcinoma in the thigh. In the same manner lung metastases were not prevented. The importance of the milieu where a malignant tumor grows and the difference between brain and muscle are discussed.

We addressed the question: would the same protocol treatment CDPT be equally or more effective to block the growth of extracerebral tumors e.g. growth of the VX2 carcinoma in the thigh and would copper depletion prevent metastases by inhibition of tumor neovascularization.

Materials and Methods

We injected 5 x 10^5 viable cells of the VX2 carcinoma in the lateral thigh of 72 NZW rabbits, 5 cm proximal to the knee at a depth of 1 cm, in the vastus lateralis muscle on the right side; care was taken not to inject intravascularly. The rabbits were divided in two groups of 36 animals each: Control and CDPT. Four animals in each group were sacrificed 4,8,12,20,24,28,32 and 36 days after the tumor implantation. At time of sacrifice the tumor of the thigh and the lungs were removed. We measured the maximal diameters of the tumor in three planes, trans- verse (d1), dorsoventral (d2) and caudorostral (d3). Tumor volume was calculated with the formula d1 x d2 x d3 x π /6 (1). The outer surface of the lungs were examined to detect and count metastatic like foci. After fixation in 10% phosphate buffered formalin for 6 days we sectioned a 1 mm thickness slice of the right upper lobe, 5 mm apical to the main right pulmonary fissure. The slices were embedded in paraffin, sectioned and stained with hematoxylin and eosin. We then counted the number of metastases foci in each slide.

Results

Copper levels at time of sacrifice are shown in Table 1.

No significant differences was found between the two groups (Table 1) in the thigh (Figure 1) or lungs (Figures 2 and 3).

TABLE 1: Serum Copper Levels, Tumor Growth in the Thigh, and Lung Metastases

Day of Sacrifice	Serum Copper Levels		Tumor Growth in the Thigh (cm^3)		No. of Lung Metastases	
	Control	CDPT	Control	CDPT	Control	CDPT
4	72.2 ± 11.6	18.2 ± 13	0.2 ± 0.3	0.3 ± 06	0	0
8	86.5 ± 17.6	23.7 ± 5	1.8 ± 1.7	2.5 ± 1.7	1.0 ± 0.8	0.8 ± 0.9
12	91.0 ± 25.8	19.0 ± 8	8.3 ± 5.9	3.7 ± 1.9	5.2 ± 4.6	7.3 ± 4.6
16	83.2 ± 16.7	19.5 ± 5	17.8 ± 8.1	12.7 ± 5.2	7.0 ± 4.8	15.2 ± 8.5
20	65.7 ± 16.5	23.6 ± 7.5	34.9 ± 11	12.4 ± 2.7	8.5 ± 8.3	23.3 ± 23.2
24	78.0 ± 39.4	25.2 ± 4.5	40.4 ± 5.2	19.5 ± 12.7	73 ± 2.1	12.2 ± 10.7
28	92.7 ± 37.9	24.2 ± 2.5	47.4 ± 17	23.6 ± 16.2	12.7 ± 4.9	10.0 ± 6.2
32	84.5 ± 31.4	18.3 ± 2.8	68.6 ± 13	52 ± 3.7	32.5 ± 31.4	12.0 ± 8.0
34	78.2 ± 19.3	11.6 ± 10	109.2 ± 53	111 ± 58	152.3 ± 37.6	61.7 ± 57.5

Figure 1 There was no significant difference in the progression of tumor volume in the thigh between control and CDPT groups

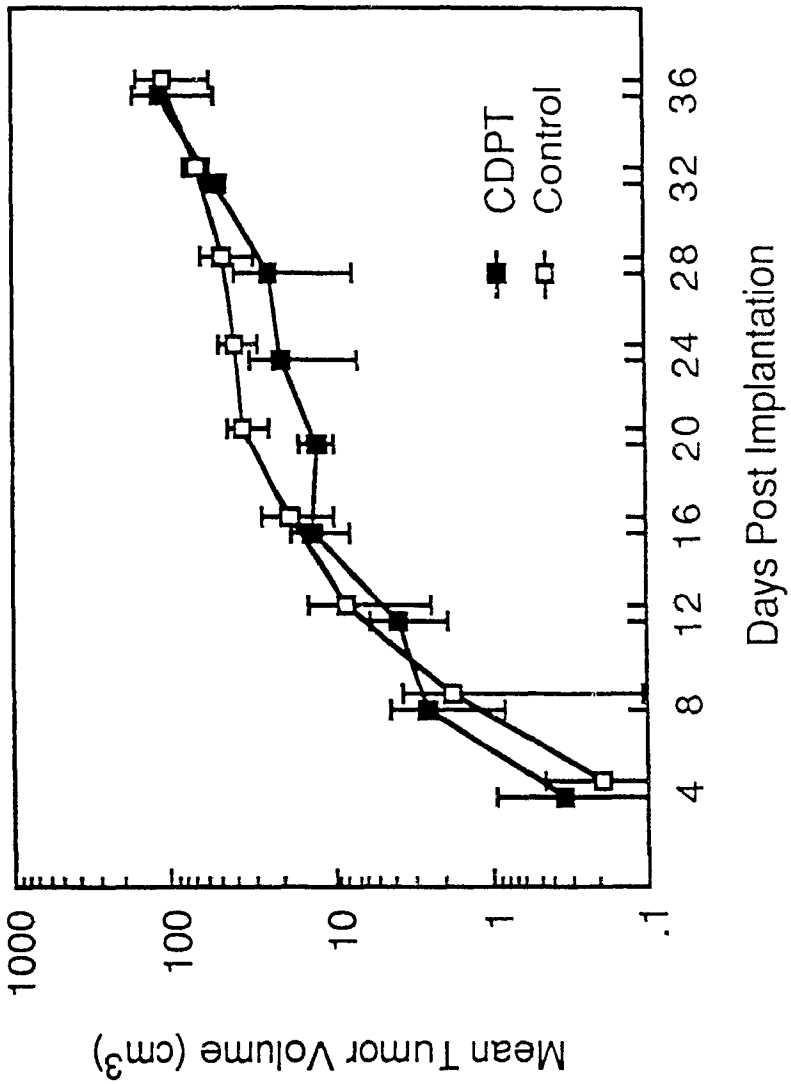
Mean Tumor Volume (cm^3)
1000
100
10
1
.1
4
8
12
16
20
24
28
32
36
Days Post Implantation
CDPT
Control

Figure 2 There was no significant difference in the development of lung metastases in control and CDPT groups

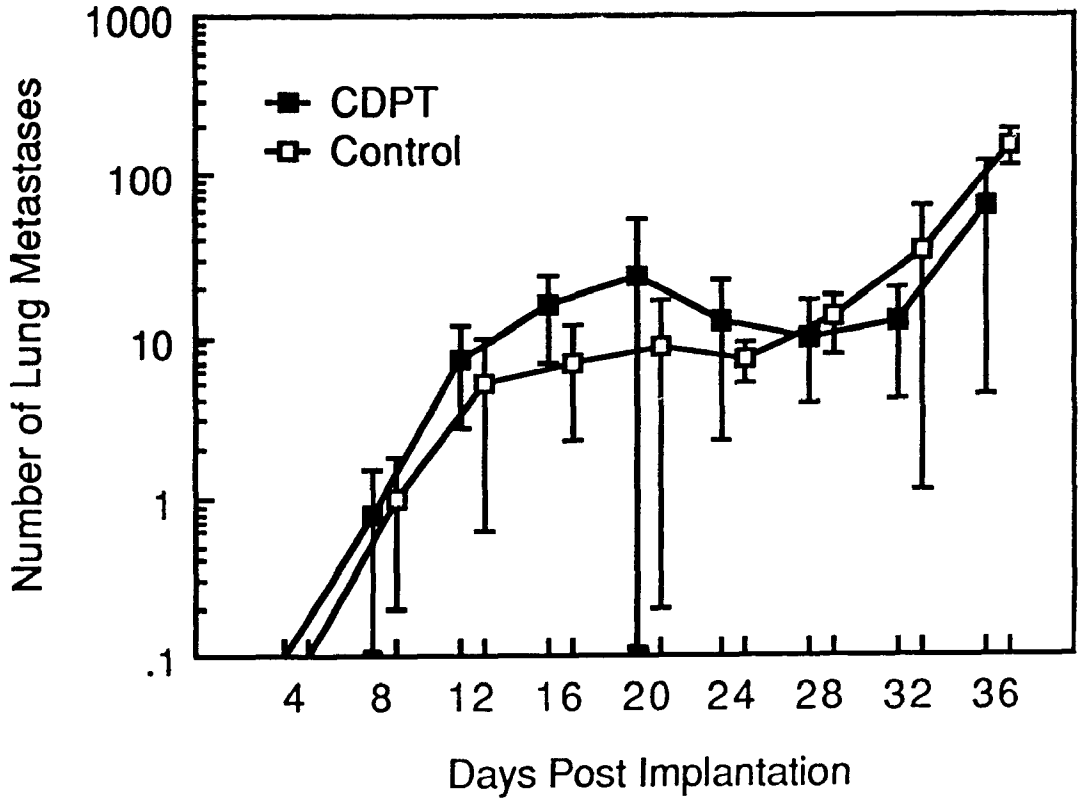
1000
100
10
1
.1
Number of Lung Metastases
CDPT
Control
4
8
12
16
20
24
28
32
36
Days Post Implantation

Figure 3 Multiple metastases could be seen on the outer surface of the lung in both groups on day 36

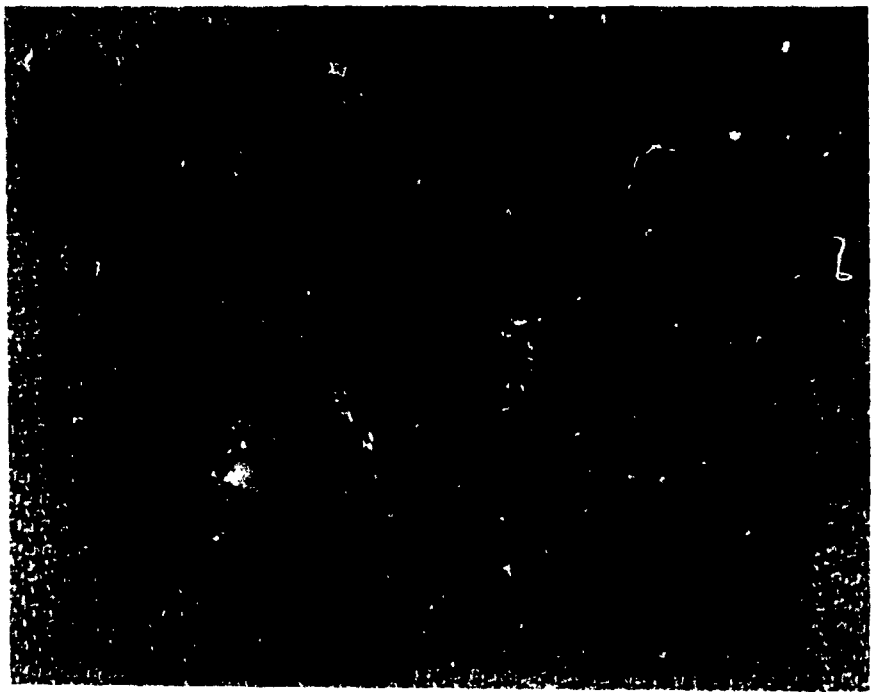

Discussion

The same protocol CDPT that had an inhibitory effect on the intracerebral growth of the VX2 carcinoma had no effect on its growth in the thigh nor on the development of lung metastases. The milieu where a malignant tumor grows has a critical importance. The morphology of the C6 astrocytoma implanted in the brain or in the illiacus muscle of the rat was found to be entirely dictated by the tumor environment (2). Vessels of lymphoma were also found to be different whether they were located in the retroperitoneal cavity or in the brain (3)

Cerebral capillaries are different from those outside the central nervous system (CNS), tight junctions, increased number of mitochondria, lack of pinocytosis and fenestrations. With the apposition of the astrocytic foot processes to the basement membrane of the endothelial cells the blood-brain barrier is formed (4-7). The tissue uptake of copper from ^{67}Cu-labelled ceruloplasmin after intravenous administration to normal and tumor-bearing rats was found to be very low in the brain (8). Copper content is very high in the muscle (44%) as compared to 11% for the brain (9). It is conceivable that despite the general copper depletion of the CDPT animals some copper was still available in the muscle. It is possible that a more severe copper depletion (achieved i.e. by a different schedule in penicillamine administration) would succeed to inhibit tumor growth in the muscle of the thigh.

These experiments add a new dimension to the differences between CNS and the remainder of the organism.

CHAPTER VIII

Conclusions

We showed that copper depletion, achieved by a low copper diet and D-penicillamine, was able to inhibit intracerebral tumor growth of two experimental tumors the VX2 Carcinoma and the 9L Gliosarcoma. We described a model of intracerebral tumor growth allowing the study of tumor angiogenesis and breakdown of the blood-brain barrier. Copper depletion prevents tumor angiogenesis and growth of the VX2 carcinoma implanted in the rabbit brain. Despite the dramatic reduction in tumor size there was no increase in the survival time in the hypocupremic rabbits. We found a diffuse breakdown of the blood-brain barrier in these animals (detected by extravasation of Evans blue) and an increase in the peritumoral water content indicating an increase in the peritumoral brain edema as compared to control normocupremic animals, this severe brain edema causing brain herniation leading to the death of the animals. Low copper diet and penicillamine are both necessary to achieve angiogenic inhibition.

Copper depletion inhibits the invasive growth of the 9L gliosarcoma in the Fisher rat brain. In the same manner as in the rabbit VX2 carcinoma there was no increase in survival time in the hypocupremic rats. Evans blue injections revealed a diffuse breakdown of the blood-brain-barrier in hypocupremic animals as opposed to dye extravasation mainly located at the tumor area in normocupremic rats. The peritumoral edema was significantly increased in hypocupremic rat as compared to normocupremic rats. Copper depletion by itself in non tumor-implanted animals has no effect on brain water content.

Tumor angiogenesis is the key parameter for the appearance of contrast enhancement in computerized tomography scans. The CDPT

protocol described here has no effect on tumor growth of the VX2 carcinoma in the thigh or on the lung metastases.

The findings described here link copper ion activity to neoplastic and vascular growth. It was suggested that angiogenesis is but one example of the more general biological phenomenon of tissue invasion (1) and the three steps of neoplastic invasion - adhesion, matrix degradation and migration - are also the basic components of the angiogenic cascade (2,3,4). Our findings further support this concept.

These results indicate that pharmacological suppression of angiogenesis, by copper depletion halts the growth of experimental tumors in the brain. Angiosuppression as a "biological modifier", could represent an important, new strategy for the treatment of human brain tumors.

CONTRIBUTION ORIGINALE[1]

Nous avons developpé un modèle tumoral cérébral utilisant le carcinome VX2 permettant l'étude experimentale de l'angiogènese tumorale et la rupture de la barrière hemato-encephalique in vivo dans le cerveau du lapin. Ce modèle reproductible, démontre qu'au niveau du cerveau aussi, la croissance tumorale est essentiellement dépendente de l'angiogenese.

Nous avons demontré que la dépletion cuprique obtenue à la fois par une diète pauvre en cuivre et par la D-penicillamine, était en mesure d'inhiber l'angiogenèse et la croissance tumorales du Carcinome VX2 implanté dans le cerveau du lapin. La diète pauvre en cuivre d'une part et la penicillamine d'autre part sont toutes deux necessaires pour inhiber l'angiogenèse.

Nous avons observé que la dépletion cuprique était capable de freiner l'invasion et la croissance du Gliosarcome 9L.

Nous avons établi que la dépletion cuprique entrainait une augmentation de l'édeme cérébral péritumoral.

Nous avons determiné que l'angiogenèse tumorale était l'element capital pour l'apparition du renforcement de contraste au cours des examens tomodensitometriques.

Nous avons observé que le même protocole capable d'inhiber la croissance du carcinome VX2 dans le cerveau n'avait pas d'effet sur la croissance du carcinome dans le muscle de la cuisse, renforcant l'importance du milieu où les tumeurs malignes se developpent et ajoutant une nouvelle dimension aux differences entre système nerveux central et autres organes. Enfin ce même protocole DCTP n'a pas empêché le

developpementdes metastases pulmonaires chez les animaux porteurs du Carcinome VX2 au niveau du muscle de la cuisse.

[1]This section is a mandatory requirement of Ph.D. Theses submitted to the Faculty of Graduate Studies and Research, McGill University, Montreal.

BIBLIOGRAPHY

Chapter I

1. Marin-Padilla M: Early vascularization of the embryonic cerebral cortex: Golgi and electron microscopic studies. J Comp Neurol 1985, 241:237-249
2. Brem SS, Jensen HM, Gullino PM: Angiogenesis as a marker of preneoplastic lesions of the human breast. Cancer 1978, 41:239-244
3. Folkman J: Tumor Angiogenesis. Adv Cancer Res 1985, 43:175-203
4. Patz A, Brem S, Finkelstein D, Chen CH, Lutty G, Bennett A, Coughlin WR, Gardner J: A new approach to the problem of retinal neovascularization. Ophthal 1978, 85:626-637
5. Barger AC, Beeuwkes R 3d, Lainey LL, Silverman KJ: Hypothesis: vasa vasorum and neovascularization of human coronary arteries. A possible role in the pathophysiology of atherosclerosis. N Engl J Med 1984, 310:175-177
6. Folkman J, Klagsbrun M: Angiogenic factors. Science 1987, 235:442-447
7. Goldman E: The growth of malignant disease in man and the lower animals, with special reference to the vascular system. Lancet ii 1907, 1236-1240
8. Hardman J: Angioarchitecture of Gliomata. Brain 1940, 63:91-118
9. Folkman J: Tumor angiogenesis. Adv cancer Res 1974, 19:331-358
10. Folkman J: Tumor angiogenesis: Therapeutic implications. N Engl J Med 1971, 285:1182-1186

11. Gullino PM: Angiogenesis and neoplasia. N Engl J Med 1981, 305:884-885

12. Kumar S: Angiogenesis and antiangeogenesis. J Natl Cancer Inst 1980,64:683-687

13. Folkman J: Tumor angiogenesis a possible control point in tumor growth. Ann Int Med 1975, 82:96-100

14. Gimbrone MA Jr, Leepman SB, Cotran RS, Folkman J: Tumor dormancy in vivo by prevention of neovascularization. J Exp Med 1972, 136:261-276

15. Brem S. Brem H, Folkman J, Finkelstein D, Patz A: Prolonged tumor dormancy by prevention of neovascularization in the vitreous. Cancer Res 1976, 36:2807-2812

16. Greene HSN, Arnold H: Homologous and heterologous transplantation of brain and brain tumors. J Neurosurg 1945, 2:315-331

17. Yamada K, Hayakawa T, Ushio Y, Arita N, Kato A, Mogami H: Regional blood flow and capillary permeability in the ethyl nitrosourea-induced rat glioma. J neurosurg 1981, 59:922-928

18. Annegers JF, Schoenberg BS, Okazi H, Kurland LT: Epidemiologic study of primary intracranial neoplasms. Arch Neurol 1981, 38:217-219

19. Weiss JB, Brown RA, Kumar S, Phillips P: An angiogenic factor isolated from tumours: A potent low-molecular-weight compound. Br J Cancer 1979, 40:493-496

20. Brem S: The role of vascular proliferation in the growth of brain tumors. Clin. Neurosurg 1976, 23:440-453

21. Deane BR, Lantos PL: The vasculature of experimental brain tumors. Part 1: A sequential light and electron microscope study of angiogenesis. J Neurol Sci 1981, 49:55-66

22. Fugita T: Vascularization in infantile brain tumors induced by human adenovirus type 12 in rats. Acta Pathol Jpn 1984, 34:1343-1354

23. Salcman M: The morbidity and mortality of brain tumors. Neurol clin 1985, 3:229-257

24. Lieberman A, Ransohoff J: Treatment of primary brain tumors. Med Clin N Amer 1979, 63:835-848

25. Levin VA, Patlak CS, Landahl HD: Heuristic modeling of drug delivery to malignant brain tumors. J Pharmaco Bio Pharm 1980, 8:257-296

26. Kornblith PL: Malignant gliomas. In current therapy in Neurological Surgery CV Mosby Publisher, Toronto, 1985:25-27

27. Folkman J: Anti-angiogenesis. New concept for therapy of solid tumors. Ann Surg 1972, 175:409-416

28. Brem S. Preis I, Langer R, Brem H, Folkman J, Patz A: Inhibition of neovascularization by an extract derived from vitreous. Am J Ophthalmol 1977, 84:323-328

29. Brem H, Folkman J: Inhibition of tumor angiogenesis mediated by cartilage. J Exp Med 1975, 141:427-439

30. Taylor S, Folkman J: Protamine is an inhibitor of angiogenesis. Nature 1982, 297:307-312

31. Folkman J, Langer R, Linhardt RJ, Haudenschild C, Taylor S: Angiogenesis inhibition and tumor regression caused by heparin of a heparin fragment in the presence of cortisone. Science 1983, 221:719-725

32. Challa VR, Moody DM, Marshall RB, Kelly DL: The vascular component in meningiomas associated with severe cerebral edema. Neurosurg 1980, 7:363-368

33. Hobson B, Denekamp J: Endothelial proliferation in tumours and normal times: Continuous labelling studies. Br J Cancer 1984, 49:405-413

34. Suddith RL, Kelly PS, Hutchison HT, Munsy EA, Haber B: In vitro demonstration of an endothelial proliferative factor produced by neural cell lines. Science 1975, 190:682-684

35. Klagsbrun M, Knighton D, Folkman J: Tumor angeogenesis activity in cells grown in tissue culture. Cancer Res 1976, 36:110-114

36. Burger PC, Dubois PJ, Schold SC, Smith KR, Odom GL, Crafts DC, Giangaspero F: Computerized tomographic and pathological studies of the untreated, quiescent, and recurrent glioblastoma multiforme. J Neurosurg 1983, 58:159-169

37. Drake CG, McGee D: Apoplexy associated with brain tumours. Can Med Ass J 1961, 84:303-305

38. Feigin IH, Gross SW: Sarcoma arising in glioblastoma of the brain. Am J Pathol 1955, 31:633-653

39. Willis RA: The direct spread of tumours. Pathology of tumours. third edition, Washington DC. Buttersworths and Co., Ltd. 19[illegible], 148-166

40. Nicosia RF, Tchao R, Leighton J: Angiogenesis dependent tumor spread in reinforced fibrin clot culture. Cancer res 1983, 43:2159-2166

41. McAuslan BR, Reilly W: Endothelial cell phagokinesis in response to specific metal ions. Exp Cell Res 1980, 130:147-157

42. Folkman J, Moscona A: Role of cell shape in growth control. Nature 1978, 273:345-349

43. Pickart L, Thaler MM: Growth modulating tripeptide (glycyl Histidyl lysine): association with copper and iron in plasma and stimulation of adhesiveness and growth of hepatoma cells in culture by tripeptide-metal ion complexes. J Cell Physiol 1980, 102:129-139

44. Kramer RH, Nicolson GL: Interactions of tumor cells with vascular endothelial cell monolayers: A model for metastatic invasion. Proc Natl Acad Sci 1979, 76:5704-5708

45. Ziche M, Jones J, Gullino PM: Role of prostaglandin E1 and copper in angiogenesis. J Natl Cancer Inst 1982, 69:475-482

46. McAuslan BR, Reilly WG, Hannan GN, Gole GA: Angiogenic factors and their assay: Activity of [illegible]myl, methionyl phenylalanine, adenosine diphosphate, heparin, copper and bovine endothelium stimulating factor. Microvasc Res 1983, 26:323-338

47. Parke A, Bhattacherjee P, Palmer RMJ, Lazarus NR: Characterization and quantification of copper sulfate-induced vascularization of the rabbit cornea. Am J Pathol 1988, 130:173-178

48. Raju KS, Alessandri G, Ziche M, Gullino PM: Ceruloplasmin, copper ions and angiogenesis. J Natl Cancer Inst 1982, 69:1183-1188

49. Alpern-Elran H, Brem S: Angiogenesis in human brain tumors: Inhibition by copper depletion. Surg forum 1985, 36:498-500

50. Pagliardi E, Giangrande E: Clinical significance of the blood copper in Hodgkin's disease. Acta Haemat 1960, 24:201-212

51. Jensen KB, Thorling EB, Anderson CJ: Serum copper in Hodgkin's disease. Scand J Haemat 1966, 1:63-74

52. Roguljic A, Roth A, Kolaric K, Maricic Z: Iron, copper and zinc liver tissue levels in patients with malignant lymphomas. Cancer 1980, 46:565-569

53. Hrgovcic M, Tessmer CF, Minckler TM, Mosure B, Taylor G: Serum copper levels in lymphoma and leukemia. Special reference to Hodgkin's disease. Cancer 1968, 21:743-755

54. Martazani SH, Bani-Hashemi A, Mozafari M, Raffi A: Values of serum copper measurement in lymphomas and several other malignancies. Cancer 1972, 29:1193-1198

55. Hrgovcic M, Tessmer CF, Thomas FB, Fuller LM, Gamble JF, Shullenberger CC: Significance of serum levels in adults patients with Hodgkin's disease. Cancer 1973, 31:1337-45

56. Hrgovcic M, Tessmer CF, Thomas FB, Ony PS, Gamble JF, Shullenberger CC: Serum copper observations in patients with malignant lymphoma. Cancer 1973, 32:1512-1524

57. Tessmer CF, Hrgovcic M, Wilbur J: Serum copper in Hodgkins disease in children. Cancer 1974, 31:303-315

58. Fisher GL, Byers VS, Shifrine M, Levin AS: Copper and zinc level in serum from human patients with sarcomas. Cancer 1976, 37:356-363

59. Kolaric K, Roguljic A, Fuss V: Serum copper levels in patients with solid tumors. Tumori 1975, 61:173-177

60. Margalioth EJ, Schenker JG, Chevion M: Copper and zinc levels in normal and malignant tissues. Cancer 1983, 52:868-872

61. Linder MC, Moor JR, Wright K: Ceruloplasmin assays in diagnosis and treatment of human lung, breast, and gastrointestinal cancers. J Natl Canc Inst 1981, 67:263-275

62. Tessmer CF, Hrgovcic M, Thomas FB, Fuller LM, Castro JR: Serum Copper as an index of tumor response to radiotherapy. Radiology 1973, 106:635-639

63. Thorling EB, Thorling K: The clinical usefulness of serum copper determinations in Hodgkin's disease. Cancer 1976, 38:225-231

64. Christian GD, Purdy WC: A polygraphic study of copper complexes with some cancer chemotherapeutic agents. Biochem, Biophysics Acta 1961, 54:587-588

65. Canelas HM, De Jorje FB, Pereira WC, Sallum J: Biochemistry of cerebral tumours: sodium, potassium, calcium, phosphorus, magnesium, copper and sulfur contents of astrocytomata, medulloblastomata and glioblastomata multiforme. J Neurochem 1968, 15:1455-1461

66. Turecky L, Kalina P, Uhlikova EV, Namerova S, Krizko J: Serum ceruloplasmin and copper levels in patients with primary brain tumor. Klin Wochenschr 1984, 62:187-189

67. Kaizer J, Gullotta F: Estimation of copper content of astrocytoma and glioblastoma by the cupran method. Neurochirurgia (Stuttgart) 1980, 23:20-23

68. El Yazigi A, Alsaker I, Almefty O: Concentration of Ag, Al, Alc, Bi, Cd, Cu, Pb, Sb and Se in cerebro-spinal fluid in patients with cerebral neoplasm. Clin Chem 1984, 30:1338-1360

69. Ungar-Waron H, Gluckman A, Spira E, Waron M, Trainin Z: Ceruloplasmin as a marker of neoplastic activity in rabbits bearing the VX2 carcinoma. Cancer Res 1978, 38:1296-1299

70. Miatto O, Casaril M, Gabrielli GB, Nicoli N, Bellisola G, Corrocher R: Diagnostic and pronostic value of serum copper and plasma fibrinogen in hepatic carcinoma. Cancer 1985, 55:774-778

Chapter II

1. Gimbrone MA Jr, Cotran RS, Leapman SB, Folkman J: Tumor growth and neovascularization: An experimental model using the rabbit cornea. J Natl Cancer Inst 1974, 52: 413-427

2. Muthukkaruppan V, Auerbach R: Angiogenesis in the mouse cornea. Science 1979, 205: 1416-1418

3. Fournier GA, Lutty GA, Watt S, Fenselau A, Patz A: A corneal micropocket assay for angiogenesis in the rat eye. Invest Ophthalmol Vis Sci 1981, 21: 351-354

4. Ausprunk DH, Knighton DR, Folkman J: Vascularization of normal and neoplastic tissues grafted to the chick chorioallantois. Role of host and prexisting graft blood vessels. Am J Pathol 1975, 79: 597-618

5. Schreiber AB, Winkler ME, Derynck R: Transforming growth factor - alpha: a more potent angiogenic mediator than epidermal growth factor. Science 1986, 232: 1250-1253

6. Kidd JG, Rous P: A transplantable rabbit carcinoma originating in a virus-induced papilloma and containing the virus in masked or altered form. J Exp Med 1940, 71: 813-838

7. Morgan DF, Silberman AW, Bubbers JE, Rand RW, Storm FK, Morton DL: An experimental brain tumor model in rabbits. J Surg Oncol 1982, 20: 218-220

8. Carson BS, Anderson JH, Grossman SA, Hilton J, White CL 3d, Colvin OM, Clark AW, Grochow LB, Kahn A, Murray KJ: Improved rabbit brain tumor model amenable to diagnostic radiographic procedures. Neurosurg 1982, 11: 603-608

9. Cochran ST, Higashida RT, Holburt E, Winter J, Iwamoto K, Norman A: Development of rabbit brain tumor model for radiologic research. Invest Radiol 1985, 20: 928-932

10. Kumar AJ, Hassenbusch S, Rosenbaum AE, Beck TJ, Hadfield R, Ahn HS, Anderson J: Sequential computed tomographic imaging of a transplantable rabbit brain tumor. Neuradiology 1986, 28: 81-86

11. Shek JW, Wen GY, Wisniewski HM: Atlas of the rabbit brain and spinal cord. Karger, New York, 1986, pp 26-29

12. Klatzo I: Neuropathological aspects of brain edema. J Neuropath Exp Neurol 1967, 26: 1-14

13. Auerback R, Morrissey LW, Sidky YA: Regional differences in the incidence and growth of mouse tumors following intradermal or subcutaneous inoculation. Cancer Res 1978, 38: 1739-1744

14. Brem S, Cotran R, Folkman J: Tumor angiogenesis: a quantitative method for histologic grading. J Natl Cancer Inst 1972, 48: 347-356

15. Sokal RR, Rohlf FJ: Biometry. The principles and practice of statistics in biological research. Second edition. San Francisco, WH Freeman and Co., 1981, pp 454-477

16. Chou SN: Experimental brain tumors in rabbits and associated cerebral edema. J Lancet 1961, 81: 78-82

17. Feigin I, Popoff N: Neuropathological observations on cerebral edema. The acute phase. Arch Neurol 1962, 6: 151-160

18. Brem S, Brem H, Folkman J, Finkelstein D, and Patz A: Prolonged tumor dormancy by prevention of neovascularization in the vitreous. Cancer Res 1976, 36: 2807-2812

19. Brem H, Folkman J: Inhibition of tumor angiogenesis mediated by cartilage. J Exp Med 1975, 141: 427-439

20. Hobson B, Denekamp J: Endothelial proliferation in tumours and normal tissues. Continuous labelling studies. Br J Cancer 1984, 49:405-413

21. Nystrom S: Pathological changes in blood vessels of human glioblastoma multiforme. Comparative studies using plastic casting, angiography, light microscopy and electron microscopy, and with reference to some other brain tumours. Acta Path Microbiol Scand 1960, 49 (Suppl 137): 1-83

22. Deane BR, Lantos PL: The vasculature of experimental brain tumours. Part 1. A sequential light and electron microscope study of angiogenesis. J Neurol Sci 1981, 49: 55-66

23. Craigie EH: On the relative vascularity of various parts of the central nervous system of the albino rat. J Comp Neurol 1919 31 429-464

24. Vick NA, Bigner DD: Microvascular abnormalities in virally-induced canine brain tumors. Structural bases for altered blood-brain barrier function. J Neurol Sci 1972, 17: 29-39

25. Abell RG: The permeability of blood capillary sprouts and newly formed blood capillaries as compared to that of older blood capillaries. Am J Physiol 1946, 147: 237-241

26. Nishio S, Ohta M, Abe M, Kitamura K: Microvascular abnormalities in ethylnitrosurea (ENU) - induced rat brain tumors: structural basis for altered blood-brain barrier function. Acta Neuropathol (Berl) 1983, 59: 1-10

27. Long DM: Capillary ultrastructure and the blood-brain barrier in human malignant brain tumors. J Neurosurg 1970, 32: 127-144

28. Folkman J: Tumor angiogenesis. Adv Cancer Res 1985, 43:175-203

29. Tannock IF: The relationship between cell proliferation and the vascular system in a transplanted mouse mammary tumour. Br J Cancer 1968, 22: 258-273

30. Tannock IF: Population kinetics of carcinoma cells, capillary endothelial cells, and fibroblasts in a transplanted mouse mammary tumor. Cancer Res 1970, 30: 2470-2476

31. Nicosia RF, Tchao R, Leighton J: Angiogenesis-dependent tumor spread in reinforced fibrin clot culture. Cancer Res 1983, 43: 2159-2166

32. Willis RA: The direct spread of tumours, Pathology of Tumours. Third edition. Washington DC, Butterworths and Co., Ltd., 1960, pp. 148-166

Chapter III

1. McAuslan BR, Reilly W: Endothelial cell phagokinesis in response to specific metal ion. Exp Cell Res 1980, 130:147-157
2. Ziche M, Jones J, Gullino PM: Role of prostaglandin E1 and copper in angiogenesis. J Natl Cancer Inst 1982, 69:475-482
3. McAuslan BR, Reilly WG, Hannan GN, Gole CA: Angiogenic factors and their assay: Activity of formyl methionyl phenylalanine, adenosine diphosphate, heparin, copper and bovine endothelium stimulating factor. Microvasc Res 1983, 26:323-338
4. Raju KS, Alessandri G, Ziche M, Gullino PM: Ceruloplasmin, copper ions, and angiogenesis. J Natl Cancer Inst 1982, 69:1183-1188
5. Alpern-Elran H, Brem S: Angiogenesis in human brain tumors: Inhibition by copper depletion. Surg Forum 1985, 36:498-500
6. Brem S, Alpern-Elran H, O'Donnell A et al: Copper deficiency and penicillamine suppress angiogenesis induced by human brain tumors. Submitted for publication
7. Tannenbaum A: The initiation and growth of tumors. II. Effects of caloric restriction per se. Cancer Res 1942, 2:460-467
8. White FR: The relationship between underfeeding and tumor formation, transplantation, and growth in rats and mice. Cancer Res 1961, 21:281-290
9. Meret S, Henkin RI: Simultaneous direct estimation by atomic absorption spectrophotometry of copper and zinc in serum, urine and cerebrospinal fluid. Clin Chem 1971, 17:369-373
10. Iyengar V: Presampling factors in the elemental composition of biological systems. Anal Chem 1982, 54:554-558

11. Sokal RR, Rohlf FJ: Biometry, the principles and practice of statistics in biological research. Second edition, San Francisco, WH Freeman and Co. 1981, pp 400-453

12. Brem S, Brem H, Folkman J, Finkelstein D, Patz A: Prolonged tumor dormancy by prevention of neovascularization in the vitreous. Cancer Res 1976, 36:2807-2812

13. Blinderman EE, Graff CJ, Fitzpatrick T: Basic studies in cerebral edema: Its control by a corticosteroid (solu-medrol). J Neurosurg 1962, 19:319-324

14. Wilson CB, Barker M, Hoshino T, Oliver A, Downie R: Steroid-induced inhibition of growth in glial tumors: a kinetic analysis, in Reulen HJ, Schurman K (editors): Steroids and brain Edema. New York:Springer-Verlag, 1972, pp 95-100

15. Gullino PM: Personal communication, 1986

16. Folkman J, Klagsbrun M: Angiogenic factors. Science 1987, 235:442-447

17. Pickart L, Thaler MM: Growth-modulating tripeptide (glycylhistidillysine): association with copper and iron in plasma, and stimulation of adhesiveness and growth of hepatoma cells in culture by tripeptide-metal ion complexes. J Cell Physiol 1980, 102:129-139

18. Downey D, Larrabee WF, Voci V, Pickart L: Acceleration of wound healing using glycylhistidyllysil Cu(11). Surg Forum 1986, 36:573-575

19. Ausprunk DH, Folkman J: Migration and proliferation of endothelial cells in preformed and newly formed blood vessels during tumor angiogenesis. Microvasc Res 1977, 14:53-65.

20. Gross JL, Moscatelli D, Rifkin DB: Increased capillary endothelial cell protease activity in response to angiogenic stimuli in vitro. Proc Natl Acad Sci USA 1983, 80:2623-2627

21. Zetter BR: Migration of capillary endothelial cells is stimulated by tumor derived growth factors. Nature (London) 1980, 285:41-43

22. Azizkhan RG, Azizkhan JC, Zetter BR, Folkman J: Mast cell heparin stimulates migration of capillary endothelial cells in vitro. J Exp Med 1980, 152:931-944

23. Gospodarowicz D, Moran J, Braun D, Birdwell C: Clonal growth of bovine vascular endothelial cells: fibroblast growth factor as a survival agent. Proc Natl Acad Sci USA 1976, 73:4120-4124

24. Birdwell CR, Gospodarowicz D, Nicolson GL: Factors from 3T3 cells stimulate proliferation of cultured vascular endothelial cells. Nature (London) 1977, 268:528-531

25. Folkman J, Haudenschild CC, Zetter BR: Long-term culture of capillary endothelial cells. Proc Natl Acad Sci USA 1979, 76:5217-5221

26. O'Dell BL: Biochemistry of copper. Med Clin N Amer 1976, 60:687-703

27. Mayne R: Collagenous proteins of blood vessels. Arteriosclerosis 1986, 6:585-593

28. Form DH, Pratt BM, Madri JA: Endothelial cell proliferation during angiogenesis. In vitro modulation by basement membrane components. Lab Invest 1986, 55:521-530

29. Nicosia RF, Madri JA: The microvascular extracellular matrix: Developmental changes during angiogenesis in the aortic ring-plasma clot model. Am J Pathol 1987, 128:78-90

30. O'Dell BL, Hardwick BC, Reynolds G: Connective tissue defect resulting from copper deficiency. Proc Soc Exper Biol Med 1961, 108:402-405

31. Kumar S: Angiogenesis and antiangiogenesis. J Natl Cancer Inst 1980, 64:683-687

32. Roguljic A, Roth A, Kolaric K, Maricic Z: Iron, copper, and zinc liver tissue levels in patients with malignant lymphomas. Cancer 1980, 46:565-569

33. McAuslan BR, Gole GA: Cellular and molecular mechanisms in angiogenesis. Trans Ophthalmol Soc UK 1980, 100:354-358

34. Hannan GN, McAuslan BR: Modulation of synthesis of specific proteins in endothelial cells by copper, cadmium, and disulfiram: an early response to an angiogenic inducer of cell migration. J Cell Physiol 1982, 111:207-212

35. Shing Y: Heparin-copper bi-affinity chromatography of fibroblast growth factors. J Cell Biol 1987, 105:110 (Abst)

36. Leibovich SJ, Polverini PJ, Shepard HM, Wiseman DM, Shively V, Nuseir N: Macrophage-induced angiogenesis is mediated by tumour necrosis factor -α. Science 1987, 329:630-632

37. Ruff MR, Gifford GE: Tumor necrosis factor. in Lymphokine Reports 1985, 2:135-272

38 Matthews N, Watkins JF: Tumour-necrosis factor from the rabbit. I. Mode of action, specificity and physicochemical properties. Br J Cancer 1978, 38:302-309

39. Nimni ME, Bavetta LA: Collagen defect induced by penicillamine. Science 1965, 150:905-907

40. Siegel RC: Collagen cross-linking. Effects on D-penicillamine on cross-linking in vitro. J Biol chem 1977, 252:254

41. Francois J, Cambie E, Feher J: Collagenase inhibition with penicillamine. Ophthalmologica 1973, 166:222-225

42. Lipsky PE, Ziff M: The effect of D-penicillamine on mitogen-induced human lymphocyte proliferation: synergistic inhibition by D-penicillamine and copper salts. J Immunol 1978, 120:1006-1013

43. Scheinberg IH: Copper Penicillaminate for rheumatoid arthritis? J Rheumatol 1981, (Suppl 7) 8:178-179

44. Hourani BT, Demopoulos HB: Inhibition of S-91 mouse melanoma metastases and growth by D-Penicillamine. Lab Invest 1969, 21:434-438

45. Demopoulos HB: Effects of reducing the phenylalanine tyrosine intake of patients with advanced malignant melanoma. Cancer 1966, 19:657-664

46. Fitzpatrick TB, Kukita A: Tyrosinase activity in vertebrate melanocytes. In pigmented cell biology 1959, New York, Academic Press, p 489

Chapter IV

1. Brem S, Cotran R, Folkman J: Tumor angiogenesis a quantitative method for histologic grading. J Natl Cancer Inst 1972, 48:347-356

2. Suddith RL, Kelly PJ, Hutchison HT, et al: In vitro demonstration of an endothelial proliferative factor produced by neural cell lines. Science 1975, 190:682-684

3. Boggan JE, Walter R, Edwards MS et al: Distribution of hematoporphyrin derivative in the rat 9L gliosarcoma brain tumor analyzed by digital video fluorescence microscopy. J Neurosurg 1984, 61:1113-1119

4. Barker M. Hoshino T, Gurcay O et al: Development of an animal brain tumor model and its response to therapy with 1.3-bis(2-chloroethyl)-1-nitrosurea. Cancer Res 1973, 33:976-986

5. Konig JFR, Klippel RA: The rat brain: A sterotaxic atlas of the forebrain and lower parts of the brainstem (Williams and Willkins, Baltimore) 1963.

6. Tannenbaum A, Silverstone H: The influence of the degree of caloric restriction on the formation of skin tumors and hepatomas in mice. Cancer Res 1949, 9:724-727

7. Meret S, Henkin RI: Simultaneous direct estimation by atomic absorption spectrophotometry of copper and zinc in serum, urine and cerebrospinal fluid. Clin Chem 1971, 17:369-373

8. Iyengar V: Presampling factors in the elemental composition of biological systems. Analyt chem 1982, 54:554-558

9. Sokal RR, Rohlf FJ: Biometry. The principles and practice of statistics in biological research. Second Edition, San Francisco, W.H. Freeman and Co., 1981, pp 454-477

10. Gurcay O, Wilson C, Barker M, Eliason J: Corticosteroid effect on transplantable rat glioma. Arch Neurol 1971, 24:266-269

11. Mealey J, Chen TT, Schanz GP: Effects of dexamethasone and methylprednisolone on cell cultures of human glioblastomas. J Neurosurg 1971, 34:324-334

12. Kornblith PL: Malignant gliomas in: Current therapy in Neurological Surgery, CV Mosby, Toronto 1985, pp 25-27

13. Mork S, De Ridder L, Laerum DD: Invasive pattern and phenotypic properties of malignant neurogenic rats cells in vivo and in vitro. Anticancer Res. 1982, 2:1-9

14. Abercrombie M: Contact inhibition and malignancy. Nature (London) 1979, 281:259-262

15. Groothuis DR, Fischer JM, Lapin, G, Bigner DD, Vick NA: Permeability of different experimental brain tumor models to horseradish peroxidase. J Neuropath Exp Neurol 1982, 41:164-185

16. Liotta LA, Rao CN, Barsky SH: Tumor invasion and the extracellular matrix. Lab Invest 1983, 49:636-649

17. Rutka JJ, Myatt CA, Giblin JR, Davis RL, Rosenblum ML: Distribution of extracellular matrix proteins in primary human brain tumors: An immunohistochemical analysis. Can J Neurol Sci 1987, 14:25-30

18. Schor SL, Schor AM, Bazill GW: The effets of fibronectin on the migration of human foreskin fibroblasts and Syrian hamster melanoma into three-dimensional gels of native collagen fibres. J Cell Sci 1981, 48:301-314

19. Kramer RH, Gonzalez R, Nicolson GL: Metatstatic tumor cells adhere preferentially to the extracellular matrix underlying vascular endothelial cells. Int J Cancer 1980, 26:639-645

20. Vlodavsky I, Gospodarowicz D: Respective roles of laminin and fibronectin in adhesion of human carcinoma and sarcoma cells. Nature (London) 1981, 289:304-306

21. Hannan GN, McAuslan BR: Modulation of synthesis of specific proteins in endothelial cells by copper, cadmium, and disulfiram: An early response to an angiogenic inducer of cell migration. J Cell Physiol 1982, 111:207-212

22. Keiser HR, Henkin RI, Kare M: Reversal by copper of the lathyrogenic action of D-penicillamine. Proc Soc Exp Biol Med 1968, 129:516-522

23. Nimni ME, Bawetta LA: Collagen defect induced penicillamine. Science 1965, 150:905-907.

24. Newman SA, Frenz DA, Tomasek JJ, Rabuzzi DD: Matrix-driven translocation of cells and nonliving particles. Science 1985, 228:885-88

25. Kramer RH, Nicolson GL: Interactions of tumor cells with vascular endothelial cell monolayers: A model for metastatic invasion. Proc Natl Acad Sci 1979, 76:5704-5708

Chapter V

1. Reese TS, Karnovsky MJ: Fine structural localization of a blood-brain barrier to exogenous peroxidase. J Cell Biol 1967, 34:207-217

2. Westergaard E, Brightman MW: Transport of proteins across normal cerebral arterioles. J Comp Neurol 1973, 152:17-44

3. Oldendorf WH, Brown WJ: Greater number of capillary endothelial cell mitochondria in brain than in muscle. Proc Soc Exp Biol Med 1975, 149:736-738

4. Goldstein GW, Betz AL: Recent advances in understanding brain capillary function. Ann Neurol 1983, 14:389-395

5. Ferzt R, Hahm H, Cervos-Navarro J: Measurement of the specific gravity of the brain as a tool in brain edema research. Adv Neurol 1980, 28:15-26

6. Marmarou A, Tanaka K, Shulman K: Cerebral edema. J Neurosurg 1982, 56:246-253

7. Papius HM: Fundamental aspects of brain edema. In: Vinken PJ, Bruyn GW: Handb clin Neurol., Volume 16, Part I: Tumors of the brain and skull. New York, North Holland Publ., Amsterdam American Elsevier 1974, pp 167-185

8. Olson JJ, Beck DW, Warner DS, Coester H: The role of new vessels and macrophages in the development and resolution of edema following a cortical freeze lesion in the mouse. J Neuropath Exp Neurol 1987, 46:682-694

9. McCord JM, Fridovich I: Superoxide dismutase. An enzymic function for erythrocuprein (hemocuprein). J Biol Chem 1969, 244:6049-6055

10. Chan PH, Fishman RA: Brain edema from Handb Neurochem, Volume 10, Edited by Abel Lajtha, Plenum Publishing Corporation, 1985, pp 153-174

11. Weisiger RA, Fridovich I: Mitochondrial superoxide dismutase. Site of synthesis and intramitochondrial localization. J Biol Chem 1973, 248:4793-4796

12. Keele BB, McCord JM, Fridovich I: Superoxide dismutase from Escherichia coli B. A new manganese-containing enzyme. J Biol Chem 1970, 245:6176-6181

13. Chan PH, Schmidley JW, Fishman RA, Kibgar SM: Brain injury, edema, and vascular permeability changes induced by oxygen-derived free radicals. Neurology 1984, 34:315-320

14. Williams DM, Lynch RE, Lee GR, Cartwright GE: Superoxide dismutase activity in copper deficient swine. Proc Soc Exp Biol Med 1975, 149:534-536

15. Rennels ML, Gregory TF, Blaumanis OR, Fujimoto K, Grady PA: Evidence for a 'parvascular" fluid circulation in the mammalian central nervous system, provided by the rapid distribution of tracer protein throughout the brain from the subarachnoid space. Brain Res 1985, 326:47-63

16. Levin VA, Freeman-Dove M, Landahl HD: Permeability characteristics of brain adjacent to tumors in rats. Arch Neurol 1975, 35:785-791

17. Neuwelt EA, Howieson J, Frenkel EP et al: Therapeutic efficacy of multiagent chemotherapy with drug delivery enhancement by blood-brain barrier modification in glioblastoma. Neurosurg 1986, 19:573-582

Chapter VI

1. Ambrose J, Gooding MR, Richardson AE: Sodium iothalamate as an aid to diagnosis of intracranial lesions by computerized transverse axial acanning. Lancet 1975, 2:669-674
2. Ambrose J: Computerized transverse axial scanning (tomography) Part 2. Clinical application. Br J Radiol 1973, 46:1023-1047
3. Gado MH, Phelps ME, Coleman E: An extravascular component of contrast enhancement in cranial computed tomography. Part I: the tissue blood ratio of contrast enhancement Part II: Contrast enhancement and the blood tissue barrier. Radiology 1976, 117: 589-593, 595-597
4. Kormano M, Dean PB: Extravascular contrast material: The major component of contrast enhancement. Radiology 1976, 121:379-382
5. Britt RH, Lyons BE, Enzmannd R, Saxer EL, Bigner SH, Bigner DD: Correlation of neuropathological findings, computerized tomographic and high resolution ultrasound scans of canine avian sarcoma virus-induced brain tumors. J Neuro-Oncol 1987, 4:243-268
6. Ethier R, Sherwin A, Taylor S et al: Computerized angiotomography. The use of 100cc of hypaque -60%, clinical and experimenta results. Paper presented at the first symposium on computerized axial tomography. Montreal, Quebec Canada May 31-June 1, 1974

7. Taveras JM, Wood EH: Computerized x-ray tomography (CT brain scan): use of contrast agents. in Diagnostic Neuroradiology Vol 2, second edition 1976, p 1000

8. Messina AV, Potts G, Rottenberg D, Patterson RH: Computed tomography: Demonstration of contrast medium within cystic tumors. Radiol 1976, 120:345-347

9. Butler AR, Horii SC, Kricheff II, Shannon MB, Budzilovich GN: Computed tomography in astrocytomas. A statistical analysis of the parameters of malignancy and the positive contrast-enhanced CT scan. Neuroradiology 1978, 129:433-439

10. Daumas-Duport C, Meder JF, Monsaingeon V, Missir O, Aubin ML, Szikla G: Cerebral gliomas: Malignancy, limits and spatial configuration. Comparative data from serial stereotaxic biopsies and computed tomography. J Neuroradiol 1983, 10:51-80

11. Zimmerman HM: The pathology of primary brain tumors. Seminars in Roentgenology 1984, 29:129-138

12. Kelly PJ, Daumas-Duport C, Kispert DB, Kall BA, Scheithauer Illig JJ: Imaging based steriotaxic serial biopsies in untreated intracranial glial neoplasms. J Neurosurg 1987, 66:865-874

13. Carson BJ, Anderson JH, Grossman JA et al: Improved rabbit brain tumor model amenable to diagnostic radiographic procedures. Neurosurg 1982, 11:603-608

14. Cochran ST, Hyashida RT, Holburt E, Winter J, Iwamoto K, Norman A: Development of rabbit brain tumor model for radiologic research. Invest Radiol 1985, 20:938-939

15. Kumar AJ, Hassenbusch S, Rosenbaum AE et al: Sequential computed tomographic imaging of a transplantable rabbit brain tumor. Neurorad 1986, 28:81-86

16. Yasuda K, Koizumi H, Ohishi K, Noda T: Zemman effect atomic absorption. Prog Anal Atomic Spectroscopy 1980, 3:299-368

17. Sokal RR, Rohlf FJ: Biometry. The principles and practice of statistics in biological research. Second edition. San Francisco, WH Freeman and Co., 1981, pp 454-477

18. Abell RG: The permeability of blood capillary sprouts and newly formed blood capillaries as compared to that of older blood capillaries. Amer J Physiol 1946, 147:237-241

19. Goldstein GW, Betz AL: Recent advances in understanding brain capillary function. Ann Neurol 1983, 14:389-395

20. Nishio S, Ohta M, Abe M et al: Microvascular abnormalities in ethylnitrosourea (ENU) - induced rat brain tumor: structural basis for altered blood brain barrier function. Acta Neuropathol 1983, 59:1-10

21. Long DM: Capillary ultrastructure an the blood brain barrier in human malignant brain tumors. J Neurosurg 1970, 32: 127-144

22. Neuwelt EA, Rapoport SI: Modification of the blood-brain barrier in the chemotherapy of malignant brain tumors. Federation Proc 1984, 43: 214-219

23. Tator CH, Morley TP, Olszewski J: A study of the factors responsible for the accumulation of radioactive iodinated human serum albumin (RIHSA) by intracranial tumors and other lesions. J Neurosurg 1965, 22:60-76

Chapter VII

1. Auerbach R, Morrisey LW, Sidky YA: Regional differences in the incidence and growth of mouse tumors following intradermal or subcutaneous inoculation. Cancer Res 1978, 38:1739-1744.
2. Comber BL, Stewart PA, Hayakawa EM, Farrell CL, DelMaestro RF: A quantitative assessment of microvessel ultrastructure in C6 astrocytoma spheroids transplanted to brain and to muscle. J Neuropath Exp Neurol 1988, 47:29-40
3. Hirano A, Ghatak UR, Becker NH, Zimmerman HM: A comparison of the fine structure of small blood vessels in intracranial and retroperitoneal malignant lymphomas. Acta Neuropathol (Berl) 1974, 27:93-104
4. Reese TS, Karnovsky MJ: Fine structural localization of a blood-brain barrier to exogenous peroxidase. J Cell Biol 1967, 34:207-217
5. Westergaard E, Brightman MW: Transport of proteins across normal cerebral arterioles. J Comp Neurol 1973, 152:17-44
6. Oldendorf WH, Brown WJ: Greater number of capillary endothelial cell mitochondria in brain than in muscle. Proc Soc Exp Biol Med 1975, 149:736-738
7. Goldstein GW, Betz AL: Recent advances in understanding brain capillary function. Ann Neurol 1983, 14:389-395
8. Campbell GH, Brown R, Linder MC: Circulating ceruloplasmin is an important source of copper for normal and malignant cells. Biochim Biophys Acta 1981, 628:27-38

9. Linder MC: Changes in the distribution and metabolism of copper in cancer: A review. J of Nutr Grow Cancer 1983, 1:27-38

Chapter VIII

1. Eisenstein R, Sorgente N, Soble LW, Miller A, Kuettner KE: The resistance of certain tissues to invasion: penetrability of explanted tissues by vascularized mesenchyme. Am J Pathol 1973, 73:765-774

2. Ausprunk DH, Folkman J: Migration and proliferation of endothelial cells in preformed and newly formed blood vessels during tumor angiogenesis. Microvasc Res 1977, 14:53-65

3. Schor AM, Schor SL, Kumar S: Importance of a collagen substratum for stimulation of capillary endothelial cell proliferation by tumour angiogenesis. Int J Cancer 1979, 24:225-235

4. Furcht LT: Critical factors controlling angiogenesis: cell products, cell matrix, and growth factors. Lab Invest 1986, 55:505-509